

https://dspace.org/

The development of an oral copolymeric carbon dot drug delivery platform for application in Parkinson's disease

Cohen, Eemaan Natashah

2022
https://hdl.handle.net/10539/34259

Downloaded from a DSpace repository. https://dspace.org/

THE DEVELOPMENT OF AN ORAL COPOLYMERIC CARBON DOT DRUG DELIVERY PLATFORM FOR APPLICATION IN PARKINSON'S DISEASE

EEMAAN NATASHAH COHEN

A Dissertation Submitted to the Faculty of Health Science, University of the Witwatersrand, Johannesburg, in Fulfilment of the Requirements for the Degree of Master of Pharmacy.



Supervisors:

Prof. Yahya E. Choonara
Department of Pharmacy and Pharmacology, University of the Witwatersrand, South Africa

Prof. Pierre P. D. Kondiah
Department of Pharmacy and Pharmacology, University of the Witwatersrand, South Africa

Prof. Lisa C. du Toit
Department of Pharmacy and Pharmacology, University of the Witwatersrand, South Africa

Johannesburg, 2022

DECLARATION

I, Eemaan Natashah Cohen, declare that this dissertation is my own, unaided work. It is being submitted for the degree of Master of Pharmacy in the Faculty of Health Sciences at the University of the Witwatersrand, Johannesburg. It has not been submitted before for any degree or examination at this or any other University.



_____ (Signature of candidate)

___21____day of___June_____2022_____in_____

ABSTRACT

The burden of Parkinson's disease is global, ranking second to Alzheimer's disease among neurodegenerative diseases with approximately 10 million new diagnoses made per annum. Parkinson's is neurodegenerative in nature, which ultimately results in effects ranging from paraesthesias to paralysis and cognitive impairments in middle-aged to elderly patients. The golden standard for Parkinson's disease treatment at the moment is dopamine. These current treatment options are not as effective in treating Parkinson's as they have less capability of crossing the Blood-Brain Barrier (BBB).

The BBB is a selectively permeable barrier that controls the exchange and transport of substances between the blood and the brain and in comparison, to other vascular endothelial cells found in the body, the BBB has highly expressed tight junction proteins, which function to primarily inhibit the random diffusion of substances between the blood and the brain. This provides an intensely strict regulation of para- and transcellular traversal of molecules (having a reported size of approximately 4 nm) across the BBB. Hence, there is a dire need for the development of nanomedicines for the effective delivery of neurological drugs across the BBB.

To provide a targeted approach for the above limitations, we have proposed the development of a carbon dot technology, loaded with a site-specific therapeutic, dopamine. This research will entail the development of a non-toxic, water soluble, drug-loaded carbon dot system for the delivery of dopamine across the BBB. Carbon dots are zero-dimensional spherical allotropes of carbon and may be the ideal nanocarriers for neurological drugs as they have noteworthy properties, low toxicity, favourable photostability, easily functionalized surfaces, high specific surface area, high quantum yield, high biocompatibility, high thermal stability and being chemically inert; resulting in optimal neuro-availability of drugs. The carbon dots will be synthesized from sodium citrate and urea. This allows for a shorter reaction time, no need for expensive reagents or costly production methods and the resultant carbon dots do not need further surface functionalization. Dopamine is required in the treatment of Parkinson's disease, hereby providing the platform for the challenging of conventional treatment for Parkinson's disease. The dopamine-loaded carbon dots would be loaded in a chitosan-alginate nanogel, allowing for the delivery of dopamine across the BBB via the intranasal route. The copolymeric nanogel allows for the

complete protection of the dopamine-loaded carbon dots in the gastric environment, enabling delivery and absorption through nasal mucosa only. This results in higher bio- and neuro-availability of dopamine at dopamine receptors in the brain. The physicochemical properties of the loaded and unloaded system were analyzed utilizing Fourier Transform Infrared Spectroscopy (FTIR), X-ray Diffraction (XRD), Differential Scanning Calorimetry (DSC), Zeta size and Zeta Potential analysis. The morphological characteristics of the system was analyzed employing Transmission Electron Microscopy (TEM). The viscoelastic properties of the nanogel was determined by rheological analysis. *In vitro* drug release studies were undertaken and the toxicity of the system was determined by performing cytotoxicity studies on a PC12 cell line. A Box-Benkhen design was utilized for generation of an optimized formulation. FTIR analysis proved the synthesis of the carbon dots and the surface passivation of dopamine to the carbon dot surface. Zeta potential results also confirmed the surface passivation of dopamine due to the zeta potential becoming more positive. DSC analysis verified the synthesis of the carbon dot and also surface passivation of dopamine to the surface of the carbon dots due to shifts in the transition temperatures. The diffractogram generated from XRD demonstrated the crystalline nature of the carbon dots. TEM images showed the morphology of the carbon dots, which presented distinctive outlines around the circular core. The carbon dots were ~10nm in size, corroborated by zeta size analysis and TEM microscopy. *In vitro* drug entrapment efficiency was 98.67%. The drug release curves illustrated a controlled and sustained release pattern. *In vitro* cell studies confirmed that the unloaded carbon dots and the loaded carbon dots were minimally toxic to the neurological cells. Further, cell proliferation was enabled by the unloaded and loaded carbon dots.

This study proved the vast potential for carbon dot usage in drug delivery, specifically for Parkinson’s Disease as highlighted in this specific project. The carbon dots were simplistic cost-effective and not time-consuming to synthesize. The loading of dopamine to the carbon dots was also non-complex and the carbon dots loading capacity was very high. This delivery system could potentially reduce the side effect profiles suffered by the patients drastically as the dosage administered can be reduced and the drug levels could be maintained for an extended period. This would potentially enhance patient outcomes and dramatically increase patient compliance.

ACKNOWLEDGEMENTS

The author would like to express her heartfelt and endless gratitude to every individual that supported, encouraged, motivated and assisted her during this process. The author would like to sincerely gives thanks:

First and foremost, to God without whom none of this would be possible.

To my father, for always supporting me, motivating me and believing in me when I didn't even believe in myself.

To my mother, for your endless love and comfort through trials and tribulations. For raising me to be the woman I am today.

To my sister, for always supporting me, being my role model and inspiring me to be better.

To my husband, for your ceaseless support, love and patience. For picking me up every time I fell.

To my beautiful baby in heaven, for the honour of being your mother and for being a means of unlocking colossal strength I didn't know I had.

To my uncle Najmudeen, for standing by me, encouraging me and going above and beyond to assist me in every possible way.

To my aunty Fatima, for your pearls of wisdom, angelic love and infinite support through the good times and the bad.

To my uncle Noor and cousin Saabirah, for you undying support, love and prayers.

To all my colleagues who became family, I don't even know where to begin to thank you. It was such a privilege and honour working with such kind-hearted individuals who guided me through rough patches. You all helped me through the toughest of times, celebrated my smallest achievements and carved such deep and precious memories into my heart. I would not have survived this degree without your perpetual and overflowing support, love, encouragement and motivation. I am so grateful for the honour of meeting each and every one you. You all have been my pillar of strength, source of comfort and encouragement, shoulder to cry on and fountains of knowledge. Your kind and selfless characters have touched my heart. You all radiate happiness,

perseverance, purity and humility. You all are an inspiration to me and deserve only the best of this world and the hereafter. I owe so much to you all, I am so blessed to have you all in my life and I pray that God grants you His choicest blessings always.

To my supervisor Professor Yahya E Choonara, for your assistance and vast scientific knowledge.

To my supervisor Professor Lisa C du Toit, for your kind heart, support and assistance over the course of my project.

To my Professor Pradeep Kumar, for your limitless motivation, assistance and guidance throughout my project. For your immense knowledge and selfless drive to help every student.

To my supervisor Professor Pierre P. D. Kondiah, for your selfless assistance and motivation in every aspect of my project. You have really proven to be such an inspiration and true example of what a WADDP supervisor should be. You were a means of making my journey so much smoother and I am so deeply grateful for the honour of working with you. Thank you for your undying support, understanding and impeccable scientific knowledge.

To Dr Philemon, thank you so much for your patient nature and desire to help us in every way you can. Thank you for making cell work such a pleasure to carry out. It was so refreshing to actually look forward to doing this part of my project. I utterly enjoyed it and it is majorly because of you.

To Dr Hillary Ndhlovu, for your tireless efforts to make our experience better every day. You are appreciated.

To Mr Kleinbooi Mohlabi, for your thoughtful nature, boundless assistance and jokes that made every day brighter. You are appreciated.

To Mr Bafana Temba, for your diligent efforts to aid each student, for your hours of dedication and jovial nature. You are appreciated.

To Mr Sello Ramarumo and Ms Tshidi Mosete, for your assiduous efforts in assisting all of us in ordering chemicals and tending to any request.

To the National Research foundation for your financial assistance which is immensely appreciated.

To everyone who contributed in any way to bringing this project into fruition, I am profoundly thankful.

"And my success is only by Allah"

The Holy Qur-aan; Surah Huud [11:88]

DEDICATION

This work is dedicated to my father, the light of my heart, the one I draw inspiration and hope from and my greatest gift. I love you.

RESEARCH OUPUTS

Eemaan N. Cohen, Pierre P.D. Kondiah, Yahya E. Choonara, Lisa C. du Toit1 and Viness Pillay, Carbon Dots as Nanotherapeutics for Biomedical Application. Current Pharmaceutical design (2020), Volume 26, Issue 19, 1-15 [Review Article]. IF: 3.052

1.CHAPTER 1: INTRODUCTION AND MOTIVATION FOR THIS STUDY. (1-7)

1.1. Background for this research 1-2

1.2. Rationale and motivation for this research 2-3

1.3. Aims and objectives 3-4

1.4. Graphical abstract 4

1.5. Overview of the dissertation 5

1.6. References 6-7

2. CHAPTER 2: A LITERATURE REVIEW OF CARBON

DOTS AS NANOTHERAPEUTICS FOR BIOMEDICAL APPLICATION. (8-54)

2.1. Introduction 8-10

2.2. Various methods to synthesize carbon dots. 10-21

2.2.1. Synthesis of carbon dots utilising the Bottom-Up approach. 11-18

2.2.1.1. Carbonization 11-12

2.2.1.2. Plasma treatment 12-13

2.2.1.3. Microwave synthesis 13-14

2.2.1.4. Solvothermal treatment 15

2.2.1.5. Hydrothermal treatment 15-18

2.2.2. Synthesis of carbon dots utilising the Top-Down approach. 18-21

2.2.2.1. Arc discharge 18

2.2.2.2. Laser Ablation 18-19

2.2.2.3. Chemical Ablation/Oxidation 19-20

2.2.2.4. Electrochemical Oxidation 20-21

2.3. Carbon dots and Green chemistry – Feasibility in terms of synthesis 21-24

2.4. The difference between Nano-Carbon/Carbon Nanotubes (CNTs)

and Carbon dots 24

3. Surface functionalization of Carbon dots for biomedical application 25-26

3.1. Surface modification 26

4. Carbon dots in theranostic biomedical applications 26-29

4.1. Carbon dots in Bio-Sensing and Bio-Imaging 27

4.2. Selective detection of Nucleic Acids 27

4.3. Carbon dots and Chemo-sensing 27-28

4.4. Heavy metal cation detection by carbon dot fluorescent detection 28

4.5. Bio-active molecule detection by fluorescent sensing 28-29

5. Carbon dots for targeted drug delivery 30-38

5.1. Carbon dots traversing the Blood-Brain Barrier. 30-31

5.2. Carbon dots and their application in CNS drug delivery. 31-32

5.3. Carbon dots in Chemo-therapeutic applications. 33-34

5.4. Carbon dots in Gene therapy 34-36

5.5. Carbon dots in Antimicrobial therapy. 36-38

6. Conclusion 38

7. References 39-54

3. CHAPTER 3: CRITICAL EVALUATION OF THE PYSICOCHEMICAL AND PHYSICOOMECHANICAL PROPERTIES OF A NOVEL LOADED AND UNLOADED CARBON DOT SYSTEM (55-90)

3.1. Introduction 55-56

3.2. Methods and materials 56-64

3.2.1. Materials 56

3.2.2. Synthesis of carbon dots 56

3.2.3 Surface passivation of carbon dots by attachment of dopamine to the carbon dot surface 57
3.2.4. Nanogel synthesis 57
3.2.5. Box Benkhen design for optimised carbon dot formulation 57-60
3.2.6. Fourier Transform Infrared Spectroscopy (FTIR) 60
3.2.7. Thermal properties of the prestine reagents, pure drug, loaded and unloaded carbon dot systems using Differential Scanning Calorimetry (DSC) analysis 60-61
3.2.8. X-Ray Diffraction (XRD) analysis of the carbon dot 61
3.2.9. Rheological analysis of the nanogel 61-62
3.2.10. Particle size and zeta potential analysis of carbon dot formulations 62
3.2.11. Morphological characteristics of the system using Transmission electron microscopy (TEM) 62
3.2.12. Drug loading and drug release analysis 63
3.2.13. Cytotoxicity studies 63-64
3.3. Results and Discussion 64-87
3.3.1. Evaluation of the unloaded- and dopamine-loaded carbon dot systems. 64-87
3.3.1.1. Evaluation of Box-Benkhen optimization 64-68
3.3.1.2. Particle size and zeta potential analysis of the unloaded- and dopamine-loaded carbon dot formulations. 68-71
3.3.1.3. FTIR Spectroscopy 71-73
3.3.1.4. Thermal evaluation utilizing Differential Scanning Calorimetry

(DSC) analysis 74-75

3.3.1.5. X-Ray Diffraction (XRD) analysis 76

3.3.1.6. Morphological characteristics of the optimized loaded carbon dot system using Transmission electron microscopy (TEM) 77-78

3.3.1.7. Rheological evaluation of nanogel 78-80

3.3.1.8 Drug loading and drug release 80-83

3.3.1.8a. Encapsulation of dopamine in both the unloaded- and loaded carbon dot systems. 80

3.3.1.8b. *In vitro* drug release study 81-83

3.3.1.9. Cytotoxicity studies 83-87

3.3.1.10. Concluding remarks 87

3.4. References 88-90

4. CHAPTER 4: CONCLUSION (91-92)

4.1. Conclusion 91-92

4.2. Future recommendations 92

Appendix 93

LIST OF FIGURES

Figure 1: Graphical abstract demonstrating the manner in which the Dopamine-loaded carbon dot system will function in body from synthesis to targeted delivery to the brain.

Figure 2: Image describing the structure, advantageous characterizations, synthesis methods, size and applications of carbon dots.

Figure 3: Schematic depicting carbon dot design with various functional groups on the carbon dot surface.

Figure 4: Schematic illustrating some biodegradable polymers which can be utilized to synthesize carbon dots.

Figure 5: Schematic depicting both bottom-up and top-down approaches utilized for the synthesis of carbon dots.

Figure 6: Schematic depicting various applications for carbon dots.

Figure 7: Schematic demonstrating the chemotherapeutic drug-loading of carbon dots as well as the mechanism of action within tumour cells.

Figure 8: Schematic portraying mode of action of carbon dots in gene therapy.

Figure 9: Box-Benkhen design depicting the optimization plot for predicted values for the optimized formulation.

Figure 10: Zeta size analysis of the unloaded carbon dot optimized formulation illustrating particle size.

Figure 11: Zeta size analysis of the dopamine-loaded carbon dot optimized formulation depicting the particle size.

Figure 12: Graph depicting the zeta potential analysis of the unloaded carbon dot optimized formulation.

Figure 13: Graph illustrating the zeta potential analysis of the dopamine-loaded carbon dot optimized formulation.

Figure 14 A: FTIR spectrum of Urea.

Figure 14 B: FTIR spectrum of Sodium Citrate.

Figure 14 C: FTIR spectrum of the Unloaded carbon dot system.

Figure 14 D: FTIR spectrum of Dopamine.

Figure 14 E: FTIR spectrum of the Dopamine-loaded carbon dot system.

Figure 14 F: FTIR spectrum of Chitosan.

Figure 14 G: FTIR spectrum of Sodium Alginate.

Figure 14 H: FTIR spectrum of the Chitosan-Alginate Nanogel.

Figure 15 A: Thermogram depicting Urea.

Figure 15 B: Thermogram depicting Sodium citrate.

Figure 15 C: Thermogram depicting the Unloaded carbon dot system.

Figure 15 D: Thermogram depicting Dopamine.

Figure 15 E: Thermogram depicting the Dopamine-loaded carbon dot system.

Figure 16: The diffractogram depicting the unloaded carbon dot system.

Figures 17 A: TEM images of carbon dots.

Figures 17 B: TEM images of carbon dots.

Figures 17 C: TEM images of carbon dots.

Figure 18: Graph depicting the viscosity of the nanogel.

Figure 19: Graph demonstrating the temperature ramp of the nanogel.

Figure 20 A: Graph illustrating the drug release curve for the dopamine-loaded carbon dot without the nanogel at pH 7.4.

Figure 20 B: Graph illustrating the drug release curve for the dopamine-loaded carbon dot in the nanogel at pH 7.4.

Figure 20 C: Graph illustrating the drug release curve for the dopamine-loaded carbon dot without the nanogel at pH 5.5.

Figure 20 D: Graph illustrating the drug release curve for the dopamine-loaded carbon dot in the nanogel at pH 5.5.

Figure 21: Graph depicting the MTT Assay after 48 hours.

Figure 22: Graph depicting the MTT Assay after 72 hours.

Figure 23 A: Image of PC12 cells treated with CDots at 48 hours.

Figure 23 B: Images of PC12 cells treated with CDots at 72 hours.

Figure 23 C: Images of PC12 cells treated with CDopa at 48 hours.

Figure 23 D: Images of PC12 cells treated with CDopa at 72 hours.

Figure 23 E: Images of PC12 cells treated with Dopamine at 48 hours.

Figure 23 F: Image of PC12 cells treated with Dopamine at 72 hours.

Figure 23 G: Image of Negatvive control at 48 hours.

Figure 23 H: Image of Negative control at 72 hours.

Figure 23 I: Image of Positive control at 48 hours.

Figure 23 J: Image of Positive control at 72 hours.

LIST OF TABLES

Table 1: Comparison of “Top-down” and “Bottom-up” approaches for the synthesis of carbon dots.

Table 2: The independent and dependant variables generated by the experimental design.

Table 3: Formulations generated by the experimental design.

Table 4: Parameters set for FTIR analysis.

Table 5: Parameters set for Rheological analysis of CHT-ALG nanogel.

Table 6: Zeta size and potential results for Box-Benkhen generated formulations.

Table 7: Optimized formulation generated by Box-Benkhen design.

Table 8: Multipurpose prediction table illustrating the optimal variables generated by the Box-Benkhen design.

Table 9: Manners in which drug release was tested

LIST OF EQUATIONS

Equation 1: Equation for calculating the %entrapment efficiency of the carbon dots.

Equation 2: Equation used to calculate the %cell viability during in vitro cytotoxicity studies.

Equation 3: Equation demonstrating Brigg's law which is what XRD analysis is based on.

1. CHAPTER 1: INTRODUCTION AND MOTIVATION FOR THIS STUDY

1.1. Background for this research

The burden of Parkinson's disease is global, ranking second to Alzheimer's disease among neurodegenerative diseases with approximately 10 million new diagnoses made per annum [1]. Parkinson's is neurodegenerative in nature, which ultimately results in effects ranging from paraesthesias to paralysis and cognitive impairments in middle-aged and elderly patients. Current treatment options are not as effective in treating Parkinson's as they have less capability of crossing the Blood-Brain Barrier (BBB), resulting in higher concentrations of drug required for treatment. Additionally, a longer period of treatment is implemented to increase the biocirculation time of drugs in the CNS and bioadhesion at the endothelial cells and/or receptors at the BBB. Higher concentrations of drugs administered also results in a higher frequency of side effects experienced by patients [1].

Furthermore, conventional neuro-therapy exudes a therapeutic effect after a prolonged period of time which decreases patient compliance. The suboptimal delivery of neuro-actives is due to the BBB and neurotransmitters such as dopamine are unable to cross the BBB (by itself) as it has a high H-bonding potential, undergoes complete ionization at physiological pH and is extensively metabolized by the liver when administered orally [2]. The BBB is a selectively permeable barrier that controls the exchange and transport of substances between the blood and the brain and is primarily composed of astrocytes, endothelial cells and pericytes [3].

The BBB, in comparison to other vascular endothelial cells found in the body, have highly expressed tight junction proteins, which function to specifically inhibit the random diffusion of substances between the blood and the brain [3]. This provides an intensely strict regulation of para- and transcellular traversal of molecules (having a reported size of approximately 4 nm) across the BBB [4]. Hence, there is a dire need for the development of nanomedicines for the effective delivery of neurological drugs across the BBB. In order to circumvent the weak capability of conventional neuro-therapy for crossing the BBB, this study proposes to focus on the development of a carbon dot loaded with dopamine, for the potential treatment of Parkinson's disease. Carbon dots (C-Dots) have an excellent ability for crossing the BBB [5].

C-Dots are revolutionizing the field of drug delivery due their ability to cross the BBB, if synthesized from a BBB-suitable precursor [5]. C-Dots are zero-dimensional spherical allotropes of carbon and may be ideal nanocarriers for neurological drugs as they have noteworthy properties [6], low toxicity, favourable photostability, easily functionalised surfaces, high specific surface area, high quantum yield, high biocompatibility, high thermal stability and being chemically inert [7]. The functionalization of neuro-specific precursors or ligands to the surface of carbon dots allows for increased permeation across the BBB, via the specific neuro-transporters targeted by the precursor or ligand selected [8]. This eliminates the need for drugs to conjugate at neuroreceptors, yielding low neuro-availability. In addition, C-Dots have intrinsic photo-luminesce, which can be enhanced using precursors with strong photo-luminescent properties. This allows carbon dots to be ideal for bio-imaging and bio-sensing [9]. The high specific surface area of the carbon dots allows for the efficient drug-loading of neuro-drugs.

1.2. Rationale and motivation for this research

The incidence of Parkinson's disease, is plaguing this generation more than ever before. One in every 37 people are diagnosed with Parkinson's disease [10]. The dopamine-loaded carbon dot (dopamine-loaded C-Dot) technology to be developed in this study aims to enable more efficient traversal of dopamine across the BBB, enabling higher neuro-availability at dopamine receptors in the brain. This will result in lower dosages of medication required, and also the reduction of side effects experienced by the patient. Reducing neurodegeneration will lead to stability of the disease and enhancing the overall well-being and quality of life of the patient. The C-Dots will be synthesized from sodium citrate and urea.

Sodium citrate and urea are inexpensive reagents and allow for a reduced reaction time, simpler production method and produce water-soluble carbon dots that require no further surface functionalization [11]. The C-Dots have an ability to cross the BBB via adsorptive transcytosis [12]. The chemical structures of sodium citrate and urea will be utilised as the structure template for the carbon dots, rendering it viable to be effectively loaded with dopamine. The biocompatible, controlled release dopamine-loaded C-Dots will be placed in an enteric gel capsule, allowing for the oral delivery of the C-dot system, where it will permeate the small intestinal wall, be absorbed into the

bloodstream, and target the BBB to release dopamine at dopamine receptors in the brain.

Carbon dots have been intravenously administered [13] but an oral formulation may prove safer and much more patient compliant. The enteric gel capsule will enable the protection of the dopamine-loaded C-Dots in the gastric environment, enabling delivery and absorption of the C-dots in the small intestine (SI) only. Due to the decreased absorption in the stomach, a higher bio- and neuro-availability of dopamine will be transported to the brain. The enteric gel capsule will dissolve in the small intestine, the C-Dots will be released and permeate the small intestine mucosa. C-Dots will then be absorbed into the systemic circulation where they will target the BBB and permeate the BBB transcellularly via adsorptive transcytosis and receptor-mediated transcytosis due to the transferrin functionalization on the surface of the C-Dots. Dopamine will then be released from the C-Dots and bond at dopamine receptors in the brain.

1.3. Aims and objectives

The aim of this research was to synthesize carbon dots, loaded with dopamine, formulated in a copolymeric nanogel for utilization as an intranasal delivery system. This system preferentially permeated nasal mucosa as well as the BBB and ensured optimum targeted bioavailability of dopamine for treatment of Parkinson's disease.

The aim of this research was achieved through the following objectives:
1) Carbon dots were synthesized utilizing sodium citrate and urea for inclusion in a nanogel, as an intranasal targeted neurotherapy.
2) Loading of Dopamine onto the carbon dot.
3) The physicochemical properties and degree of cross-linking of the unloaded- and dopamine-loaded carbon dots was determined employing FTIR, XRD and DSC characterization analysis.
4) The morphological properties of the unloaded and dopamine-loaded carbon dots were detected employing Zeta-sizer and TEM analysis to determine the size and uniformity in particle distribution.

5) The stability of the carbon dot formulation was proven employing Zeta Potential analysis.

6) Evaluation of the *in vitro* drug entrapment and drug release kinetics of the dopamine-loaded carbon dot was undertaken by utilizing fluorescence spectroscopy which determined the entrapment efficiency and degree of controlled-release of the dopamine-loaded carbon dots.

7) Biocompatibility and cytotoxicity analysis were performed employing luminescence evaluation utilising PC12 cell lines and evaluation of cellular uptake and the effect of the carbon dots on cell viability was determined.

1.4. Graphical abstract

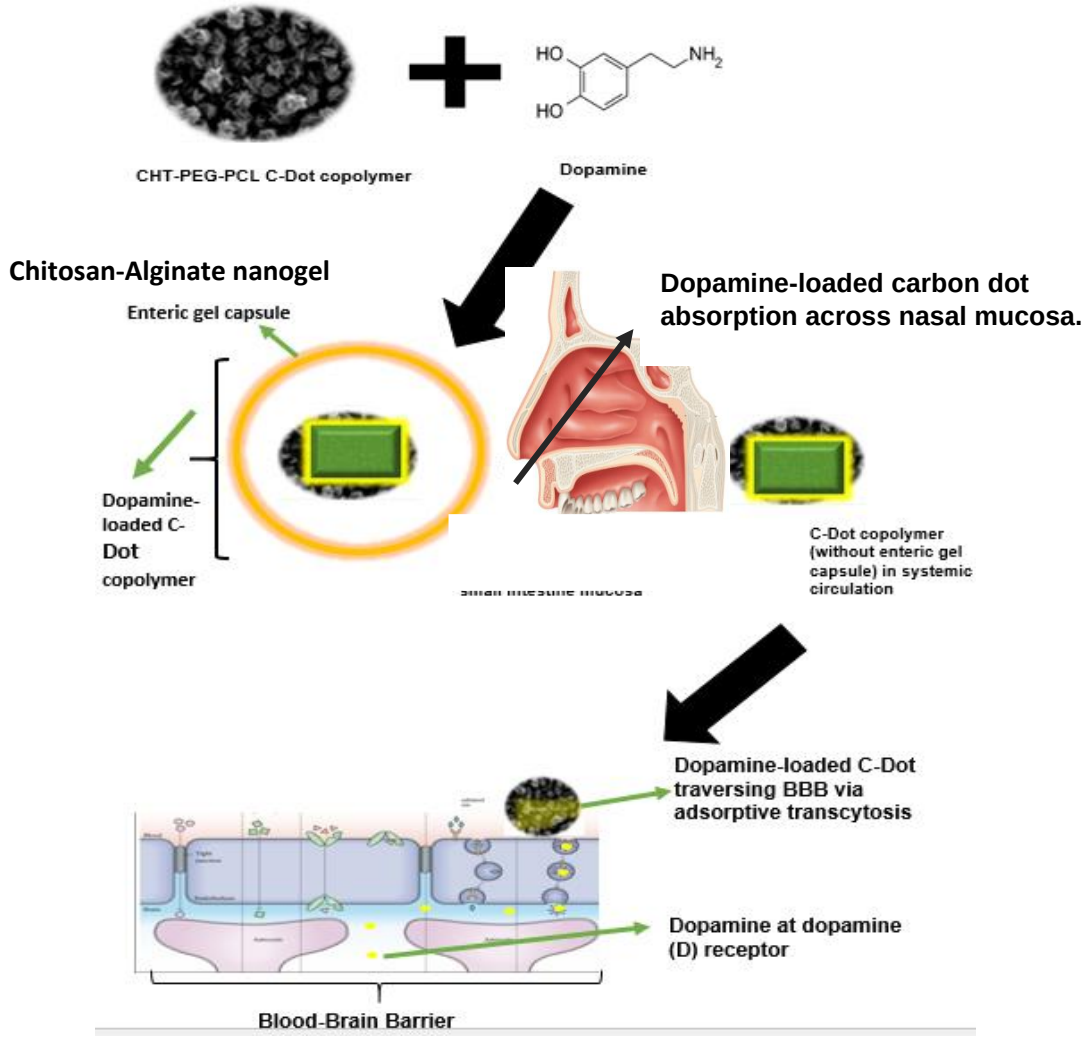


Figure 1: Schematic depicting the synthesis mechanism by which the Dopamine-loaded carbon dot system would function in the body following targeted delivery to the brain.

1.5. Overview of the dissertation

Chapter one is introduction to this study. It highlights the burden of Parkinson's disease (PD) and explains the effects that the disease has on the body. This chapter also illustrates the current treatment options for PD and their limitations. The chapter then goes on to describe and define the Blood-Brain barrier. The chapter then elucidates carbon dots, its advantages and how it will be applied and beneficial in this study. The aims and objectives of this study are explained in this chapter.

Chapter two is a literature review detailing the origin of carbon dots, the recent peaked interest in biomedical application and drug delivery using carbon dots, the synthesis methods and various works from researches who have utilized carbon dots in different fields of drug delivery for various purposes. This review was published in Current Pharmaceutical Design in 2020.

Chapter three details the synthesis of the carbon dot and the dopamine-loaded carbon dot system. In this chapter, FTIR, XRD, DSC, TEM, and Zeta size and potential analysis was undertaken to determine the physicochemical properties of the loaded and unloaded carbon dots. *In vitro* drug entrapment, drug release and cytotoxicity studies were also undertaken and are outlined in this chapter.

Chapter four provides an overall synopsis and conclusion to this dissertation, explaining the outcomes of the study and recommendations for future works due to shortfalls in current research and limitations of the project.

1.6. References

1. Parkinson's News Today. (2019). *Parkinson's disease Statistics - Parkinson's News Today.*
[online] Available at: https://parkinsonsnewstoday.com/parkinsons-disease-statistics/ [Accessed 18 Mar. 2019].

2. Trapani A, Mandracchia D, Tripodo G, Cometa S, Cellamare S., De Giglio E, Klepetsanis P and Antimisiaris S. (2018). Protection of dopamine towards autoxidation reaction by encapsulation into non-coated- or chitosan- or thiolated chitosan-coated liposomes *Colloids and Surfaces 8: Biointerfaces,* 170, pp.11 -19.

3. Kim J, Ahn, S. and Kim Y. (2019). Nanotherapeutics engineered to cross the blood-brain barrier for advanced drug delivery to the central nervous system. *Journal of Industrial and Engineering Chemistry,* 73, pp.8-18.

4. Murphy E (2017). The blood-brain barrier and protein-mediated fatty acid uptake: role of the blood-brain barrier as a *metabolic* barrier. *Journal of Neurochemistry,* 141 (3), pp.324-329.

5. Mintz K, Mercado G, Zhou Y, Ji Y, Hettiarachchi S, Liyanage P, Pandey R, Chusuei C, Dallman J. and Leblanc R. (2019). Tryptophan carbon dots and their ability to cross the blood-brain barrier. *Colloids and Surfaces B: Biointerfaces,* 176, pp.488-493.

6. Zhou A, Song F, Yao W, Han Y, Song F, Wu W, Ming C, Ju D. and Khan A. (2019). Efficient solid-state and dual-mode photoluminescence of carbon-dots/NaluF4 microcrystals for multifunctional applications. *Journal of Alloys and Compounds,* 775, pp.457-465.

7. Zhang S, Zhang L, Huang L, Zheng G, Zhang P, Jin Y, Jiao Z. and Sun X. (2019). Study on the fluorescence properties of carbon dots prepared via combustion process. *Journal of Luminescence* 206, pp 608-612.

8. Perreira J, Pradella Hallinan M. and Alves R. (2017). Secondary to excessive melatonin synthesis, the consumption of tryptophan from outside the blood-brain barrier and melatonin over-signaling in the pars tuberalis may be central to the pathophysiology of winter depression. *Medical Hyptheses.* 98, pp 69-75.

9. Parvin N. and Mandal T. (2017) Dually emissive P,N-co-doped carbon dots for fluorescent and photoacoustic tissue imaging in living mice. *Microchimica Acta,* 184(4) pp.1117-1125.

10. Parkinsons.org.uk. (2019). [online] Available at:

https://www.parkinsons.org.uk/sites/default/files/2018-01/CS2960%201ncidence%20and%20prevalence%20report%20branding%20summary%20report.pdf [Accessed 7 Mar. 2019].

11. Hou Y, Lu Q, Deng J, Li H, Zhang Y. One-pot electrochemical synthesis of functionalized fluorescent carbon dots and their selective sensing for mercury ion. *Analytica Chimica Acta.* 2015; 866:69-74.

12. Malhotra M, Tomaro-Duchesneau C, Saha S, and Prakash S. (2014). Intranasal Delivery of Chitosan-siRNA Nanoparticle Formulation to the Brain. *Methods in Molecular Biology,* pp.233-247

12. Sonali Agrawal P, Singh R, Rajesh C, Singh S, Vijayakumar M, Pandey B, and Muthu M. (2015). Transferrin receptor-targeted vitamin E TPGS micelles for brain cancer therapy: preparation, characterization and brain distribution in rats. *Drug Delivery,* 23(5), pp.1788-1798.

13. Zhang J, and Yu S. (2016). Carbon dots: large-scale synthesis, sensing and bioimaging. *Materials Today*, 19(7), pp.382-393.

2. CHAPTER 2: A Literature Review of Carbon Dots as Nanotherapeutics for Biomedical Applications

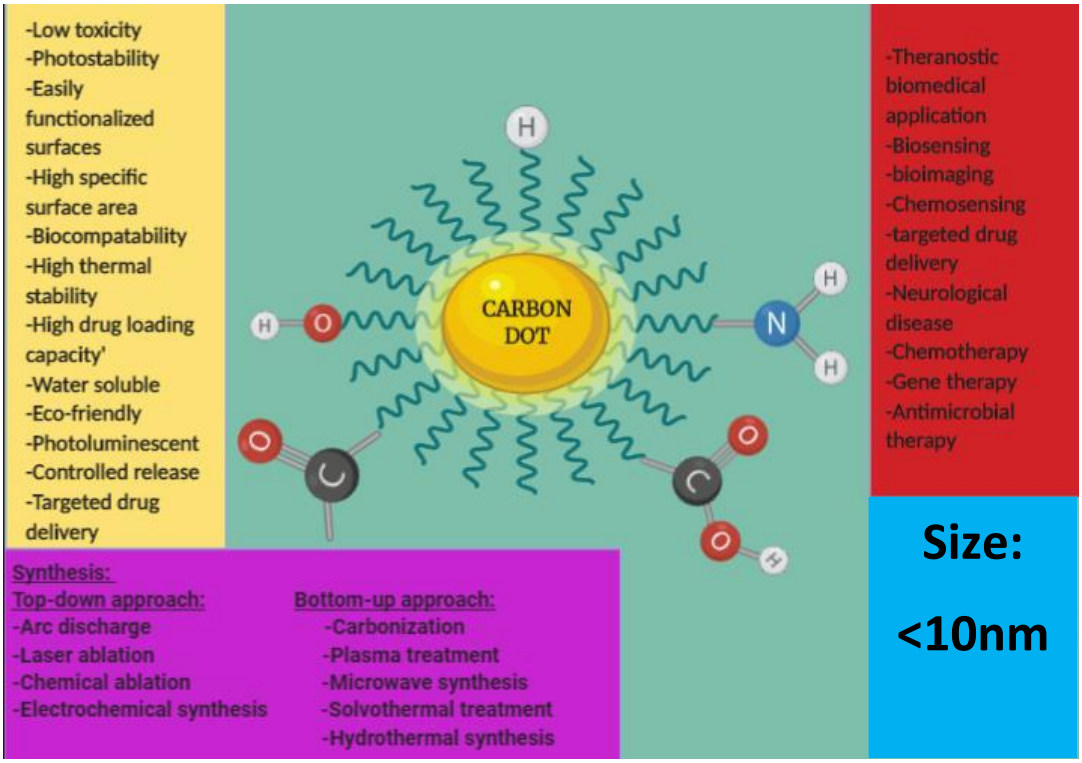


Figure 2: Schematic describing the structure, characterizations, synthesis methods, size and applications of carbon dots.

2.1. INTRODUCTION

Nanomedicine is a vast field explored by many researchers to design novel, biocompatible and non-toxic platforms that can be applied in various biomedical fields. An emergent nanomaterial of great interest is Carbon Dots (CDots) [1]. CDots form a part of an ingenious series of carbonaceous nanomaterials and are zero- dimensional spherical allotropes of carbon [2, 3]. These nanomaterials (10nm in size; ranging from 2-8nm) are environmentally benign clusters of carbon atoms, with traces of oxygen, hydrogen and nitrogen and have a sp^2 hybridized structure, including various functional groups such as carboxyl (-COOH), aldehyde (-CHO) and hydroxyl (-OH) groups [4, 5, 6]. This is depicted in figure 3 below.

CDots are also known as Carbon Nano-Dots, graphene quantum dots or carbon quantum dots. CDots were accidentally discovered in 2004 by Xu *et al.* during the

processing of single-walled carbon nanotubes (SWCNTs) [1, 7], also known as the arc discharge synthesis of carbon nanotubes [5]. CDots obtained their scientific designation as “carbon quantum dots” in 2006 by Su *et al.,* who worked on their surface passivation in order to enhance the intrinsic quality of fluorescence that CDots possess [1, 7]. These fluorescent nanoparticles serve as an alternative to the orthodox semi-conductor quantum dot, which possesses limitations such as high toxicity, due to the addition of heavy metals during their formulation [2, 8]. CDots are documented to have been synthesized from a myriad of different sources. Some of these sources include, but are not limited to carbon fibre, citric acid, graphite and glucose [9].

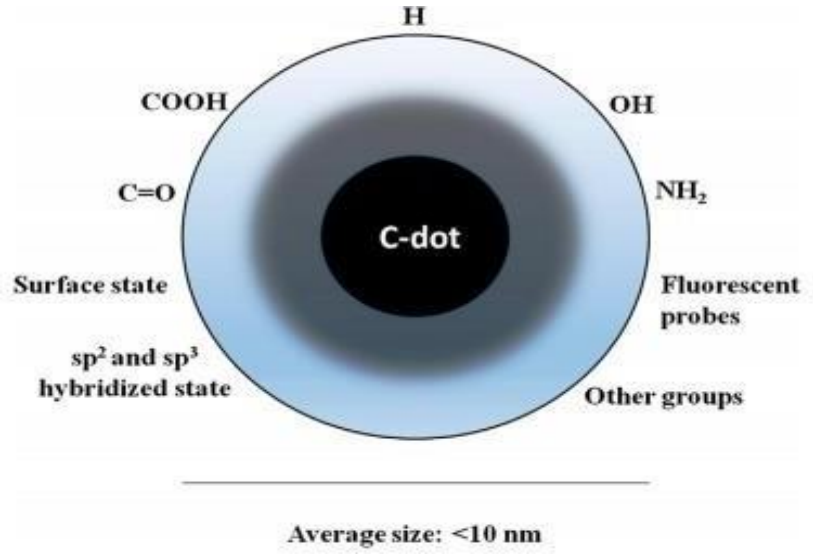


Figure 3: Schematic depicting carbon dot design with various functional groups on the carbon dot surface. Adapted with permission from Ref: 4 [4].

Since the discovery of carbon dots, their properties and chemical nature have been extensively researched and they have been designated as a new class of the smallest, biocompatible, viable nanomaterials [7]. Carbon dots can be crystalline or amorphous in nature [10] and have revolutionized chemical, biomedical and nanomedical fields as they possess noteworthy properties [1]. These include; low toxicity, favourable photostability, easily functionalized surfaces, high specific surface area, high quantum yield, high biocompatibility, high thermal stability and being chemically inert [11]. These are illustrated in figure 2 above. Carbon dots also have a higher drug-loading capacity as opposed to

particles which are larger i.e. quantum dots [4]; they have remarkable water solubility, are eco-friendly, are good conductors and in addition, carbon dots have intrinsic photo-luminesce, which can be enhanced using precursors with strong photo-luminescent properties. This allows carbon dots to be ideal for bio-imaging and bio-sensing [2,12]. Carbon dots have thus been instrumental in the advancement of the selective detection of nucleic acids [13], heavy metal detection by fluorescent detection [14] and bioactive molecule detection by fluorescent sensing [15].

CDots also allow for targeted drug delivery, as this is one of the most prominent properties of the nanomaterial [4]. This is mainly due to the intrinsic photo-luminescence property, which allows for easy and effective *in vivo* tracking of drug delivery platforms. In addition, the easily functionalized surfaces allow the attachment of receptor-specific ligands or precursors, facilitating the specific targeting of drugs to specific sites, which ultimately leads to a decrease in side-effects experienced by patients [15]. This property generated advancements in both chemo- and gene therapy. Unfortunately, conventional chemotherapeutics result in patients' suffering from off-target effects [16]. In order for chemo- and gene therapy to be effective, the chemotherapeutic vehicle or vehicle for the transfection of DNA has to possess an inherent safety and efficient- drug loading capacity.

2.2. Various methods to synthesize carbon dots.

The carbon sources used in the synthesis of CDots determine the morphology of the resultant carbon dots, as they provide the chemical structure template for the carbon dots. Carbon dots can be synthesized employing one of two approaches i.e. bottom-up or top- down approach. The "bottom-up" approach utilizes polymer precursors or organic monomers, whereas, the "top-down" approach utilizes carbon materials such as carbon nanotubes or graphite [17].

Biodegradable polymers are beneficial for drug delivery due to their high biocompatibility and low toxicity [18]. The utilization of biodegradable polymers for the synthesis of carbon dots allows these processes to be cost-efficient and non-toxic. These polymers provide the structure template for the resultant carbon

nanodots. Therefore, the surface functional groups of the carbon dots can be fine-tuned due to the careful selection of a specific biodegradable polymer.

2.2.1. Synthesis of carbon dots utilising the Bottom-Up approach.

Precursors such as polymers, carbohydrates and organic acids have been extensively employed in this potential approach, utilizing an array of methodologies such as carbonization of polymers, plasma treatment, microwave synthesis, solvothermal treatment and hydrothermal treatment [17].

2.2.1.1. Carbonization

This involves the conversion of polymeric precursors into materials of a carbonaceous nature via controlled chemical reactions. These polymers provide the chemical structure for the resultant microstructures [20]. Polymers are preferred to hydrocarbons and biomass as the synthesis from polymers results in carbon nanomaterials with structures which are well-defined [20]. Carbonization is a low-cost method comparable with the hydrothermal and solvothermal processes, which have also been reported to be cost- effective processes. Carbonization is a more cost-effective process in comparison to microwave synthesis, laser ablation and arc discharge [19]. Carbonization results in products with a broad size distribution, which is also the case with chemical oxidation. Carbonization is a process that is easy to perform, and this has been reported for arc discharge as well [19].

On the other hand, processes such as chemical oxidation, electrochemical oxidation and laser ablation are all sophisticated processes and are therefore more challenging to perform [19]. Cai *et al.,* synthesized molybdenum-doped carbon dots via *in situ* carbonizations of glutamic acid and ammonium molybdate in PEG fluid [21]. Polyethylene glycol (PEG) exhibits excellent bio- compatibility and enables carbon dots to circulate in a “stealth mode” in the bloodstream. It allows carbon dots not to be taken up by the reticuloendothelial system (RES), resulting in a prolonged circulation time *in vivo.* PEG also decreases the risk of immunogenicity [22]. Naik *et al.,* demonstrated the rapid and cost-effective synthesis of CDots doped with sulfur via simple acidic carbonization of sucrose to detect Fe3+ ions

in a highly acidic environment [23]. Cheng *et al.,* proved the easy synthesis of carbon dots through the carbonization of walnut shells [24]. Various biodegradable polymers that can be utilized for carbon dot synthesis are illustrated in figure 4 below.

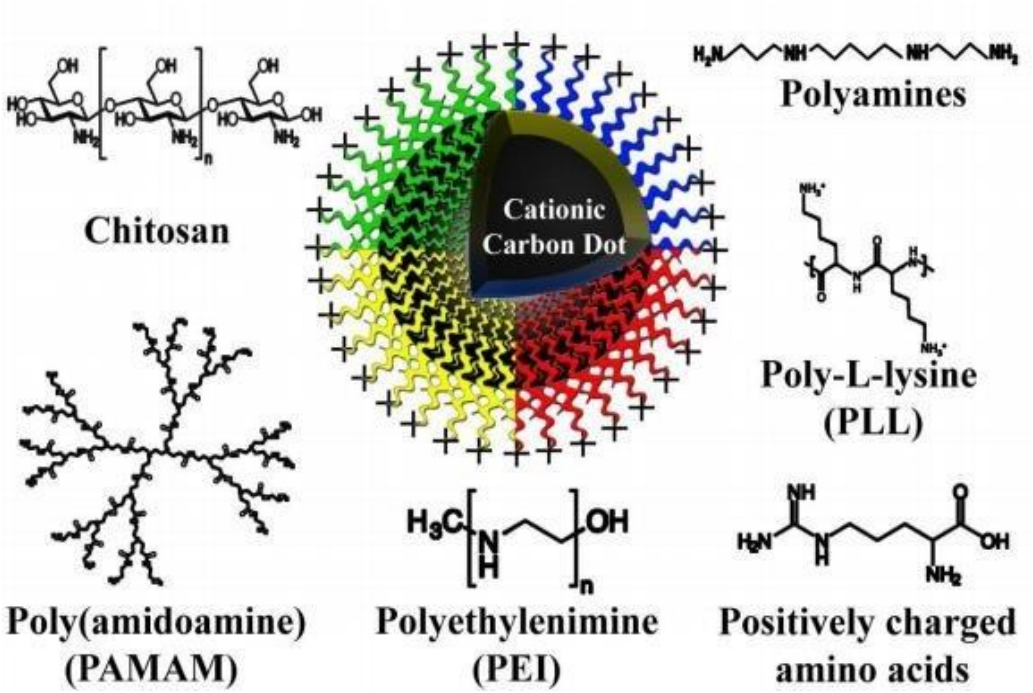


Figure 4: Schematic illustrating some biodegradable polymers which can be utilized to synthesize carbon dots. Adapted with permission from Ref: 19 [19].

2.2.1.2. Plasma treatment

This is comprised of a microwave plasma torch that exudes nitrogen radicals, which are highly activated and are also close to thermodynamic equilibrium in a pure nitrogen plasma. The plasma flame is uninterrupted due to microwave radiation, and stability is induced by a mixture of nitrogen and argon, which is injected in a swirling motion. Turbulence is generated by the injection of the gas directly into the plasma flame, which is stabilized by the swirl of the gas. Carbon atoms then rapidly get mixed with the iron atoms provided by the plasma flame, and this allows for the continuous growth of carbon nanomaterials [25]. Ma *et al.,* demonstrated carbon dot synthesis through micro-plasma technology at atmospheric pressure [26]. Zhou *et al.,* illustrated the plasma-enabled conversion

of ethanol into carbon dots near room temperature without the addition of a catalyst [1].

2.2.1.3. Microwave synthesis

Microwave synthesis has been developed as a means of time- efficient and rapid method of synthesis of carbon nanomaterials. This method employs the assistance of a microwave, which is an electromagnetic spectrum of frequency 300 MHz-300 GHz. This energy source is utilized as a source of heat to the synthesis process. The heat supply has been found to be homogenous, which is advantageous for the resultant carbon nanomaterials produced [27]. The size of the particles generated by this process has been found to be easy to control. This proves true for laser ablation as well as electrochemical oxidation [19]. The particles resulting from microwave synthesis possess a uniform size distribution, which is, contrary to both carbonization and chemical oxidation wherein the particles possess a broad size distribution [19]. Microwave synthesis is a high-cost process to run, which is comparable to laser ablation and arc discharge, which are too expensive processes. Contrary to these high cost processes; hydrothermal treatment, solvothermal treatment, and carbonization are low cost processes of synthesis [19].

Yang *et al.,* proved the microwave-assisted synthesis of CDots for application in the bio-sensing of tetracycline [28]. Choi *et al.,* reported the microwave-assisted synthesis of biocompatible and luminescent lysine-based carbon dots [29]. Hou *et al.,* demonstrated the rapid microwave-assisted synthesis of molecularly imprinted polymers on carbon dots for fluorescent sensing of tetracycline in milk [30].

Liu *et al.,* reported the use of acrylamide/chitosan as a precursor for carbon dots. This polymer also provided a nitrogen source for carbon dots, resulting in amino groups on the carbon dot surface. They were able to develop rapid and high yield synthesis of carbon dots by means of microwave-hydrothermal carbonization. These carbon dots were used for the fluorescent detection of ferrous ions in the body [31]. Liu *et al*., also reported in the same study that current synthetic methods of nitrogen-doped carbon dots are time- consuming (>4 hours) and require high temperatures (>180° C). Additionally, the fluorescence quenching mechanism

induced by metal ions is vague at present [31]. Huang *et al.,* developed chitosan carbon dots as a biosensor for detecting dopamine with a detection limit of 11.2 nm. They further modified these carbon dots with gold to enable a lower detection limit of 1.0 nm. [32, 33]. Sakar *et al.,* reported a vitamin D biosensor with high specificity. This bio- sensor was synthesized from chitosan [34].

Jia *et al.,* utilized HA-based theranostic nanogels for chemo- therapy and tumor diagnosis. They achieved this by cross-linking the folate-terminated PEG-modified HA with carbon dots for the first time. The researchers found that these nanoprobes exhibited extraordinary fluorescence due to the property of the integrated carbon dots. These nanoprobes were able to be loaded with doxorubicin due to the drug-loading ability of HA. The nanoprobes provided non-invasive location tracking of cancer cells and exhibited pH-responsive controlled release behavior in that there was an ideal release of doxorubicin in the weak acidic environment of the tumor cells while restraining the release in neutral media. The cytotoxicity and cellular uptake results of this study clearly proved that most of the doxorubicin released and accumulated in the cancer cell nuclei resulting in the efficacious death of cancer cells owing to the dual receptor-mediated targeting characteristics of these nanoprobes [35]. HA has been documented to exude excellent biocompatibility as it is a natural anionic polysaccharide. It is also a major extracellular matrix of connective tissues [36, 37].

Advancements in research have enabled the microwave-assisted synthesis of CDots to obey green principles. Liu *et al.,* illustrated a one-step microwave-assisted polyol method for the synthesis of green luminescent carbon dots. The source of carbon was sucrose and diethylene glycol was the reaction medium. The carbon dots were synthesized within one minute under microwave irradiation. These carbon dots proved to be luminescent, were able to be taken up by C6 glioma cells and exuded low cytotoxicity, which was suggestive of the potential for future prospects in bio-imaging applications [38].

2.2.1.4. Solvothermal treatment

This includes exfoliation, which is carried out in a solvent that is highly polar in a Teflon-lined autoclave, which is set to 180º C for 12h. The high pressure which is generated within the autoclave stimulates the insertion of molecules of the solvent into the interlayer of the carbon source [38]. Solvothermal treatment refers to chemical reactions occurring in non-aqueous solvents [40]. Yang *et al.,* demonstrated a one-step solvothermal method for the preparation of a novel type of quaternized carbon dot. They utilized glycerol and dimethyloctadecy l[3-(trimethoxysilyl)propy] ammonium chloride (Si-QAC). These carbon dots were able to interact with both gram-negative and positive bacteria, and due to the absorption of the carbon dots, bacterial cell surface destruction was induced in gram-positive bacteria [41]. Liu *et al.,* reported a one-pot solvothermal synthesis of EDTA-derived CDots for the enhanced removal of tetracycline [42].

2.2.1.5. Hydrothermal treatment

This synthesis is defined as the process of crystallization at high pressure (> 1 atm) and above room temperature. This process is conducted in either aqueous or non-aqueous media and via heterogeneous reactions. This synthesis process is typically conducted in a stainless-steel autoclave with a Teflon liner- able to withstand high pressure and temperature that is generated in association with the chemical reactions taking place. The fundamental rationale for employing these conditions is to account for materials that are insoluble and or tough to dissolve. These materials then enter into a solution as complexes due to the co-operation between the solvent, pressure and temperature which generate an effect [40]. Khan *et al.,* illustrated the hydrothermal synthesis of CDots from red lentils for application in Fe3+ sensing [43]. Guo *et al.,* synthesized nitrogen- doped carbon dots through a hydrothermal treatment process for application in biological imaging [44]. Yuan *et al.,* reported the one- pot, easy and cost-effective synthesis of carbon dots, which are water-soluble, by hydrothermal treatment of wheat straw. The CDots were used for application in labelling, bio-imaging and bio-sensing [45].

Ding *et al.,* synthesized Janus-like poly(methyl methacrylate)-b-poly(ethylene

glycol)-folic acid grafted carbon dots via aqueous phase radical polymerization technique. These carbon dots were used as non-invasive location tracking of cancer cells as they were loaded with doxorubicin. These carbon dots were found to exhibit zero premature leakage in physiological media, which resulted in a significant decrease in the toxic side effects of the cancer drug.

Poly(methyl methacrylate) (PMMA) is vastly utilized in the bio- medical synthesis of carbon dots due to its non-toxicity, biocompatibility and biodegradability as drug delivery systems [46]. Ding *et al.,* did however state that the fabrication of a controlled-drug delivery nanocarrier with long blood circulation time, excellent biodegradability and biocompatibility still needs time to be investigated [46]. Hyaluronic acid (HA) is advantageous in the targeted drug delivery of chemotherapeutics due to the overexpression of the HA receptor on tumor cells as well as the ability of the HA to be broken down into smaller molecules by hyaluronidase (HAse) which is abundant in some tumor cells. These advantages prove HA to be an excellent cancer drug delivery system in that it enhances intracellular intake as well as improves the therapeutic efficacy [37].

Jaleel *et al.,* formulated chitosan carbon dots, via hydrothermal synthesis, for the transduction of Tissue Necrosis factor α (TNF-α) into cancer cells. These carbon dots provided targeted delivery of the gene to the tumour sites, as well as efficient *in vivo* bio-imaging due to the fluorescent properties of carbon dots. These carbon nanodots were also able to be functionalized with folate, which is overly expressed on tumors, due to the abundant functional groups present on the surface of the carbon dots [47]. Jaleel *et al.,* also reported that in order for gene therapy to be safe and target-specific, its de- livery to the target site has to be controlled. The transfection efficiency of Polyethylenimine (PEI) is higher than that of chitosan, but PEI is more toxic than chitosan; therefore chitosan was utilized in the study [47].

Huang *et al.,* developed chitosan carbon dots as a biosensor for detecting dopamine with a detection limit of 11.2 nm. They further modified these carbon

dots with gold to enable a lower detection limit of 1.0 nm [32, 33]. Huang *et al*., stated that there are various other biodegradable polymers that are used to modify electrodes to detect dopamine. These include; o-carboxymethylchitosan (OCMCS), graphene (GME), methoxypolyethylene glycol (MPEG), polypyrrole and graphene (PPy/eRGO), hollow nitrogen-doped carbon nanospheres (HNCMS/GC), multi-walled nanotubes (f-MWCNTs), a CU_2O/graphene nanocomposite (CU_2O/graphene), a nanoporous morphology of a gold nanofilm (NPG/ITO), and Au nanoparticle- polyaniline nanocomposite layers (AuNP/ PANI). The researchers have found that although most of these systems have attributed to dopamine detection, these modified biomaterials possessed limitations either regarding the method of synthesis being sophisticated or regarding the sensitivity of the biomaterial [32, 33].

Zhao *et al.,* utilized HA as a precursor for the hydrothermal synthesis of mesoporous silica nanoparticles to pose as targeted drug delivery systems for cancer drugs. The researchers found that due to HA being a big molecule, it was an excellent capping agent for the reduction of premature drug leakage in this study [48]. Yamina *et al.,* developed PEGylated halloysite nanotubes, which can be used as a precursor for carbon dots, and reported that due to the PEGylation, the nanocomposites displayed excellent hydrophilicity, biocompatibility and biodegradability. They also reported that the PEGylation decreased the immunogenicity, toxicity, protein absorption, surface interaction, cell adhesion and undesirable cellular uptake of the nanocomposites at sites other than the cancerous tumor sites [49].

Solvothermal and hydrothermal treatments are distinctive from one another in the light of hydrothermal treatment comprising chemical reactions that occur in both aqueous and non-aqueous solvents, whereas the chemical reactions occurring via solvothermal treatment only occur in non-aqueous solvents. The comparable properties of solvothermal and hydrothermal treatment are thus the same and will be discussed simultaneously as follows. Solvothermal/Hydrothermal treatment is a low-cost synthesis comparable to carbonization. Solvothermal/Hydrothermal treatment is a more cost-effective process compared to arc discharge, laser

ablation and microwave synthesis [19]. Solvothermal treatment/Hydrothermal treatment generates a yield which is of superior quantum efficiency but a low yield, which is contrary to electrochemical oxidation, which generates a high quantum yield [19].

2.2.2. Synthesis of carbon dots utilising the Top-Down approach.

These processes act in accordance with cutting the carbon source (e.g. graphene sheets) into graphene quantum dots (GQD) [50].

2.2.2.1. Arc discharge

This was the initial method utilized for the fabrication of both MWCNTs as well as SWCNTs. This method employs carbon electrodes, which are heated to a high temperature, in the complete absence of oxygen, via electric current. Due to the addition of a catalyst to one of the electrodes, carbon nanotubes can be acquired. The basic mechanism of action of this method is dependent on the energy transfer between the target materials, e.g. graphite, and the external radiation source, bearing in mind that the target materials are maintained close to their melting point [51]. Arc discharge is a process that is easy to perform, similar to carbonization and chemical oxidation, which are also simple to perform [19]. This is contrary to electrochemical oxidation and laser ablation, as these processes are sophisticated and more challenging to perform [19]. Arc discharge is a high-cost process, comparable to microwave synthesis and laser ablation. Arc discharge is distinguished based on cost from carbonization, hydrothermal and solvothermal treatment in that the latter three methods are more cost effective [19].

2.2.2.2. Laser Ablation

Laser ablation is a method in which the primary mechanism is similar to arc discharge. The difference is that the source of energy is now a laser that hits a graphite pellet, which encompasses catalyst materials. The laser has the ability to operate in one of two modes, i.e., pulsed or continuous mode. This laser causes the vaporization of the carbon and metal catalyst. Those vaporized

species are then made to enter a copper-collector, which is cooled by means of water. The vaporized species are directed via the flow of neutral gas, and they then condense. Laser ablation is a high-cost process, similar to arc discharge and microwave synthesis. In terms of cost, this method is contrary to hydrothermal and solvothermal treatment and carbonization as these processes are more cost-effective [19]. Laser ablation is a sophisticated process to perform, similar to electro- chemical oxidation, which is a sophisticated process to perform as well [19]. Processes such as arc discharge, chemical oxidation and carbonization are simple to perform. The size of the particles synthesized via laser ablation is easy to control, similar to that of microwave synthesis and electrochemical oxidation [19].

Calabro *et al.,* demonstrated the synthesis of CDots from carbon nano-onions via a liquid-phase laser ablation method [52]. Sattarahmady *et al.,* synthesized CDots utilizing the laser ablation method for application in bactericidal effects of carbon dots on antibiotic-resistant *Staphylococcus aureus* [53].

2.2.2.3. Chemical Ablation/Oxidation

This method is also called chemical vapor deposition (CVD) which allows for the direct growth of carbon nanotubes on a substrate. This takes place at a lower temperature compared to that of laser ablation and arc discharge. The energy source here is a furnace with either a resistive or inductive heater, infrared lamp or a hot filament, which functions to decompose the precursor gas as well as the heating of the sample. The decomposition of the precursor gases, as well as the catalytic function of the substrate, is dependent on the heat of the furnace [51].

Another such method is referred to as *chemical ablation from graphene*, in which the process proceeds as follows. The graphene oxide sheets are cut into small sheets via controlled oxidation within a mixture of nitric and sulphuric acid under mild ultrasonication. Thereafter the minute, oxidized graphene sheets are placed in a Teflon-lined autoclave and reduced under hydrothermal conditions at an elevated temperature [50].

Chemical ablation/oxidation is a simple process to perform, similar to arc discharge and carbonization. Processes such as electrochemical oxidation and laser ablation are more challenging to perform [19]. Chemical ablation/oxidation accommodates large scale generation, which is similar to carbonization [19]. The particles produced via this method fall into a broad size distribution similar to that of carbonization, but is contrary to microwave synthesis in that the particles generated therefrom are uniformly distributed in size [19].

2.2.2.4. Electrochemical Oxidation

Electrochemical synthesis enables the generation of fluorescent carbon nanoribbons, nanoparticles and graphene from a graphite electrode. This process is enabled due to the ionic liquid (IL)-assisted chemical exfoliation which utilizes an electrolyte (e.g. water-soluble IL 1-butyl-3-methylimidazolium tetrafluoroborate [bmim][BF4]). This electrolyte contains up to 90% water. The exfoliation mechanism occurs due to a complex interaction of anodic oxidation of water and anionic intercalation from the ionic liquid. If an IL with an electrolyte of high-water content (>10% water) is utilized, this results in the generation of water-soluble, oxidized carbon nanomaterials. On the other hand, if an IL of low water content (<10% water) is utilized, the result is IL-functionalized carbon nanomaterials. However, the production of carbon nanoribbons which have a similar structure to graphene carbon dots, can be performed through anionic intercalation and oxidative cleavage of graphite [50].

Electrochemical oxidation produces particles of high purity and high yield. This is contrary to hydrothermal and solvothermal treatments, which produce particles of superior quantum efficiency but low yield [19]. Electrochemical oxidation is a sophisticated process to perform, similar to laser ablation, which is challenging to perform as well. Processes such as hydrothermal and solvothermal treatment, chemical ablation/oxidation and carbonization are simpler to perform [19]. The particle size generated by this process is able to be easily controlled, similar to the particle produced by laser ablation and microwave synthesis [19]. A summary

of the synthetic processes of carbon dots is depicted in figure 5 below.

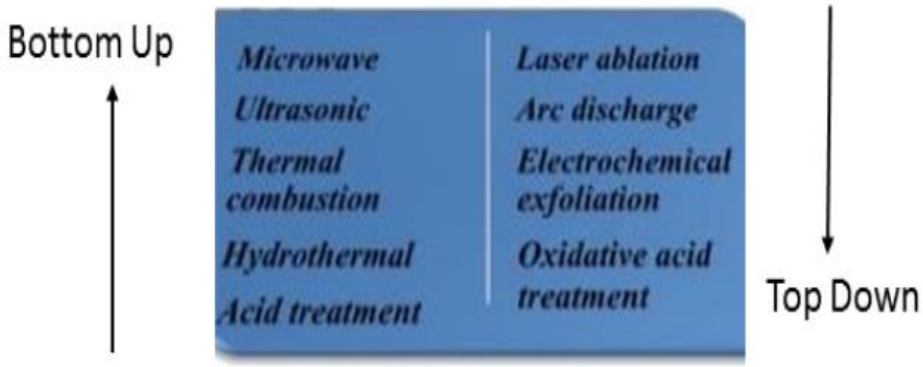


Figure 5: Schematic depicting both bottom-up and top-down approaches utilized for the synthesis of carbon dots. Adapted with permission from Ref: 38 [38].

2.3. Carbon dots and Green chemistry – Feasibility in terms of synthesis

"Top-down" synthesis methods prove beneficial in terms of sustainability and additionally comply with green chemistry principles [55]. Kołodziejczak-Radzimska *et al.*, and Djurisic *et al.* reported that zinc oxide (ZnO) is a vital group II-VI semiconductor and is a beneficial precursor for carbon dots owing to its low cost, abundance of components, ease of preparation in bulk or nanostructured forms and good photocatalytic activity. The researchers utilized a simple, one-pot (solution phase) synthesis technique, which involved carbon dots synthesis through the chemical reaction of D-fructose and NaOH, followed by the addition of zinc salt at pH 10. This method was cost-effective and conformed to "green chemistry principles" in that it is carried out in aqueous solution [56, 57].

Dehvari *et al.* illustrated the use of waste crab shells, which constitute nitrogen elements as a form of chitin, poly-b (1/4)-N- acetyl-D-glucosamine polysaccharides and proteins. These can be utilized as a precursor source for carbon dot synthesis. The researchers doped these carbon dots with transition metal ions, resulting in theranostic carbon nanodots. These carbon dots were synthesized via a one-pot microwave-assisted, sonochemical, pyrolysis method.

The crab shells provided a cheap carbon source as well as presenting itself as a chelating agent able to form metal ions complexes. The researchers were also able to functionalize the surface with folic acid, which enabled these carbon dots to serve as an efficient fluorescent, bioimaging nanoprobe for targeting cancer cells [58].

In support of the yielding nature of carbon dot synthesis to green chemistry principles, a wide variety of precursors were reported; low-cost organic chemicals [59, 60], orange juice [61], dried shrimp [62], *Syzygium cumini* [63], pure milk [64], orange waste peels [65], cornflour [66] and *Pyrus pyrifolia* [63]. All these precursors successfully produced ultra-small fluorescent carbon dots.

Ansi *et al*., reported the design of a cost-effective and simple synthetic technique for the synthesis of carbon dots utilizing table sugar as a precursor [67]. Yang *et al.,* used fungus as a precursor for carbon dots in the application of hyaluronic acid and hyaluronidase detection [68]. Ensafi *et al.,* synthesized carbon dots from saffron, which acted as bio-imaging probes for the detection of prilocaine with high sensitivity and selectivity [69]. Liu *et al*., reported a facile and cost-effective synthesis method for carbon dots utilizing rose-heart radish as a precursor [70]. The advantages versus the disadvantages of all the synthetic methods are illustrated in Table 1 below.

Table 1: Comparison of “Top-down” and “Bottom-up” approaches for the synthesis of carbon dots. Adapted with permission from Ref: 56 [56].

Strategies	Methods	Advantages	Disadvantages	Refs
Bottom-up	**Microwave synthesis**	Easily controllable size, uniform size distribution, short reaction time	High energy cost	[57-60]
	Thermal decomposition	Large-scale generation, low cost, easy operation	Broad size distribution	[60, 61]
	Hydrothermal treatment	Lack of toxicity, low cost, superior quantum efficiency	Low yield	[62, 63]
Top-down	**Laser ablation**	Morphology and size control	High cost, sophisticated process	[64]
	Electrochemical oxidation	High purity and yield, size control	Sophisticated process	[65, 66]
	Chemical oxidation	Large-scale generation, easy process with simple tools	Broad size distribution	[61]

Ultrasonic treatment	Easy process	High energy cost	[67]

2.4. The difference between Nano-Carbon/Carbon Nanotubes (CNTs) and Carbon dots

A carbon nanotube (CNT) is a semi-open structure, which is a single layer of graphene rolled up into a hollow hole, which is seamless [82]. CNTs are, therefore, cylindrical in shape. These CNTs can either be classified as single-walled carbon nanotubes (SWCNTs) or multi-walled carbon nanotubes (MWCNTs), indicative of SWCNTs being comprised of one layer/wall and MWCNTs are composed of more than one layer/wall [83]. The simplest of the CNTs are the SWCNTs, which typically have a diameter within the range of 0.8-1nm, while MWCNTs fall within the range of 5-20nm. MWCNTs can, however, exceed a diameter of 100nm [82]. With regard to length, CNTs can range from >100nm-0.5m [82]. CNTs form part of the carbon family and are 1D in shape. They were first discovered by Ijama in 1991 [84].

CNTs have been utilized in various fields of drug delivery, which include but not limited to chemotherapy [85, 86] and haematological malignancies [87]. The cellular uptake of CNTs are dependent on their surface chemistry and dimension. For example, Kang *et al.,* tested the cellular uptake of CNTs of diameters 1-3 nm, in different lengths; >50nm, 50-100nm and 100-200nm. The results concluded that the CNTs 50nm in length were uptaken by cells via energy-independent insertion and diffusion. The cellular uptake of the CNTs of length 50-100nm and 100-200nm entered the cells via the endocytic pathway [88]. Carbon dots, on the other hand, are deliberately synthesized from a precursor that can permeate a specific region of the cell, to enable optimal cellular uptake as well as efficient, targeted cell delivery. There is deliberate chemical functionalization of the carbon dot surface with selected molecules or precursors [89]. Exemplary of this is a study by Shaung *et al*. who demonstrated carbon dots exhibiting subcellular targeting features. The carbon dots had surface amine moieties and others with lauryl amine, targeting the lysosome and endoplasmic reticulum, respectively [90].

3. Surface functionalization of Carbon dots for biomedical application

Carbon dots are versatile due to their various applications. However, carbon dots which are not functionalized consist of carbon and oxygen elements [91]. The problem presented by “bare” carbon dots is that they exhibit low quantum yield (QY) <5%, which is also a low luminescent efficiency. This is due to specific functional groups, i.e. carboxylic and epoxy groups, which induce the recombination of localized electron-pairs, which are nonradioactive, thus, resulting in the suppression of fluorescence emission [91]. The non-functionalized carbon dots ordinarily emit blue fluorescence as well as exhibit a deficiency of active sites on the carbon dot surface. This ultimately results in the limitation of their application. Therefore, the functionalization of carbon dot surfaces is imperative to the enhancement of the photochemical, photophysical, photoluminescent and drug-delivering properties of carbon dots.

Carbon dots can either undergo surface passivation or functionalization of the CDot surface. This permits the regulation of their properties and dramatically broadens the scope of their application [92]. The original synthesis of carbon dots was based on surface functionalization of small carbon nanoparticles, with polymeric and organic particles. This pre-selection of carbon nanoparticles leads to the deliberate surface functionalization of these carbon dots. The resultant CDots were found to be some of the best in performance in reference to their fluorescence. This improved fluorescence allows for the easy and effective live-tracking of CDots *in vitro* or *in vivo*, as well as cell uptake monitoring [93]. The deliberate pre-selection of precursors allows for specific surface passivation and functionalization of CDots, which improves their cellular uptake, intracellular trafficking and cytotoxicity [94]. CDots can be functionalized with various substrates, depending on the purpose they are intended to be used for. These include but are not limited to; peptides [95], organic molecules [96], polymers [97], ligands [98], a plethora of therapeutic drugs [99] and several others. This surface functionalization enable CDots to be vehicles of targeted drug delivery. Thus far, strategies for functionalization are comprised of surface modification and heteroatom doping [100].

3.1. Surface modification

The surface engineering of carbon dots involves the surface passivation by active functional molecules by means of various chemical bonds i.e. hydrogen, covalent and ionic bonds. This surface modification enhances the properties of carbon dots and allows for the aid in precise drug delivery, target-modulated sensing and diagnostic imaging [101].

Yang *et al.,* proved diagnostic imaging in mice by the utilization of carbon dots functionalized with PEG 1500N. The research team compared the luminous efficacy of the green carbon dots and that of quantum dots and found the green carbon dots to emit brighter light than that of the quantum dots [102].

Zhu *et al.,* demonstrated dual-fluorescent sensing of copper ions. They synergized N-(2-aminoethyl)-N,N,N'-tris(pyridin-2-ylmethyl)ethane-1,2-diamine carbon dots (AE-TPEA-C- DOTS) and cadmium selenide (CdSe)/Zinc sulphide quantum dots (Zns)-QDots. They then observed particle residues in numerous intracellular spaces, at physiological pH [103]. Kong *et al.,* demonstrated that surface functionalized carbon dots can be utilized for the diagnostic imaging of living cells and tissues, at a physiological pH. The researchers conducted an *in vivo* pH alteration sensing test, which illustrated good linearity of the intensity of fluorescence between a pH range of 6.0-8.5. The researchers were also able to prove that based on Na+-K+ exchange, LCC tumour cells and A549 lung cancer cells showed pH variation [104]. Li *et al.,* were able to control the excitation-dependant luminescence of carbon dots by the functionalization of the carbon dot surface utilizing a simple thermal treatment. This resulted in excitation-dependant and excitation independent carbon dots [105].

4. Carbon dots in theranostic biomedical applications

Carbon dots are predominantly composed of sp2 –hybridized carbon, oxygen, nitrogen as well as other doped heteroatoms. Carbon dots have proven beneficial to various biomedical applications.

These biomedical applications are further explained below.

4.1. Carbon dots in Bio-Sensing and Bio-Imaging

Carbon dots are innately advantageous in biosensing and bioimaging due to their excellent resistance to photobleaching and biocompatibility. Carbon dots biosensing can be applied in the selective detection of nucleic acids, fluorometric assays of enzymatic activity and complex discrimination and identification of cancer cells and bacteria [15].

4.2. Selective detection of Nucleic Acids

Nucleic acids are comprised of two large classes of biomolecules: deoxyribonucleic acid (DNA) and ribonucleic acid (RNA), and are imperative to all known life forms. Huang *et al.,* developed a quantitative detection method based on functionalized carbon dot nanoprobes which is based on competitive interactions between molecular quenchers, carbon dots and double-strand DNA
[106]. This method employs a molecular quencher methylene blue or ethidium bromide. They first quench the fluorescence of carbon dots through an electron-transfer process. Fluorescence recovery takes place after the addition of double-stranded DNA, whereby the molecular quenchers selectively imbed themselves in the dsDNA [106].

Godavarthi *et al.* made an attempt to prove the non-specific detection of dsDNA based on the enhancement of the fluorescence of N-doped carbon dots by dsDNA via weak interactions [13]. Quantification of single-strand DNA is more important in areas like gene analysis and disease diagnosis. Li *et al*., demonstrated the tuning of gold nanoparticles via DNA and carbon dots for the purpose of nucleic acid and protein detection [107]. Pierrat *et al*., illustrated the efficient *in vitro* and *in vivo* pulmonary delivery of nucleic acids via carbon dots [108].

4.3. Carbon dots and Chemo-sensing

Carbon dots that are functionalized have been vastly utilized in chemo-sensing applied in biological sciences especially, for the detection of highly polluting biologically active small molecules [15]. In this particular application, carbon dots enjoy a great

advantage over other fluorescent materials owing to their exceptional aqueous solubility, low cost and good stability [15].

4.4. Heavy metal cation detection by carbon dot fluorescent detection

Feng *et al.,* found that the employment of ferric and cupric cations has paramagnetic nature as well as are efficacious quenchers, in comparison to most fluorophores. They found that this strong quenching effect can be exploited by carbon dots, provided that the carbon dots and the ions are in close proximity. This will enable proficient fluorescence quenching in sensitive detection. They found that ferric ions are able to efficaciously quench the fluorescence of N- doped carbon dots. This results from the interaction between the ferric ions and the doping of nitrogen on the surface of the carbon dots [15, 109].

Dong *et al*., found that quantification of the Fe^{3+} and Cu^{2+} ions is based on the coordination-induced efficient fluorescence quenching which is widely employed. They also uncovered the underlying nature of non-fluorescent complex formation
[110]. This is beneficial to iron poison detection in patients. Plácido *et al.,* synthesized carbon dots from microalgae bio-char for the heavy metal detection in aqueous systems [14]. Pang *et al.,* utilized co-doped nitrogen and sulfur carbon dots for the selective fluorescence detection of heavy metal ions [111].

4.5. Bio-active molecule detection by fluorescent sensing

Heteroatom-doped carbon dots exude several active sites on the surface of the carbon dots to enable the interaction between carbon dots and external quenchers, like hydrogen peroxide. This is beneficial to the detection of bioactive molecules such as glucose, which is one of the most widely spread bioactive molecules in the animal body, and is imperative as an energy source.

Shan *et al*., and Qiao *et al.,* found that glucose detection can be based on boron-doped carbon dots. This was established due to the combination of the quenching effect of hydrogen peroxide and the enzymatic reaction of glucose oxidase [112, 113]. Zhang *et al.,* found that an additional popularized detection method for glucose is the

covalent- binding of boronic acid-modified carbon dots and glucose [114]. Qian *et al.,* proved that there is a selective response between silicon-doped carbon dots and hydrogen peroxide. The fluorescence of the Si-doped carbon dots was significantly quenched by the hydrogen peroxide via efficient electron transfer from carbon dots to the hydrogen peroxide. This was due to the strong affinity of hydrogen peroxide to silicone atoms [115].

Glutathione is a bioactive molecule that primarily occurs in living cells and maintains oxidation levels. Huang *et al.,* discovered its discriminative determination over other biothols by means of a dual-channel mode. They functionalized carbon dots with bis(3-pyridylmethyl)amine). Glutathione reacted specifically with the metal complexes of the carbon dots and resulted in a change in the fluorescence [116]. Cholesterol is vital in animals and is an essential component of all animal cell membranes. It plays a primary and fundamental role in the maintenance of the structural integrity and fluidity of the cell membrane. Inclusively, involving the biosynthesis of steroid hormones and bile acid. Sun *et al.,* and Feng *et al*., developed a selective and sensitive fluorescent method for cholesterol detection based on carbon dot nanoprobes functionalized with β-cyclodextrin via competitive host-guest recognition [117, 15].

5. Carbon dots for targeted drug delivery

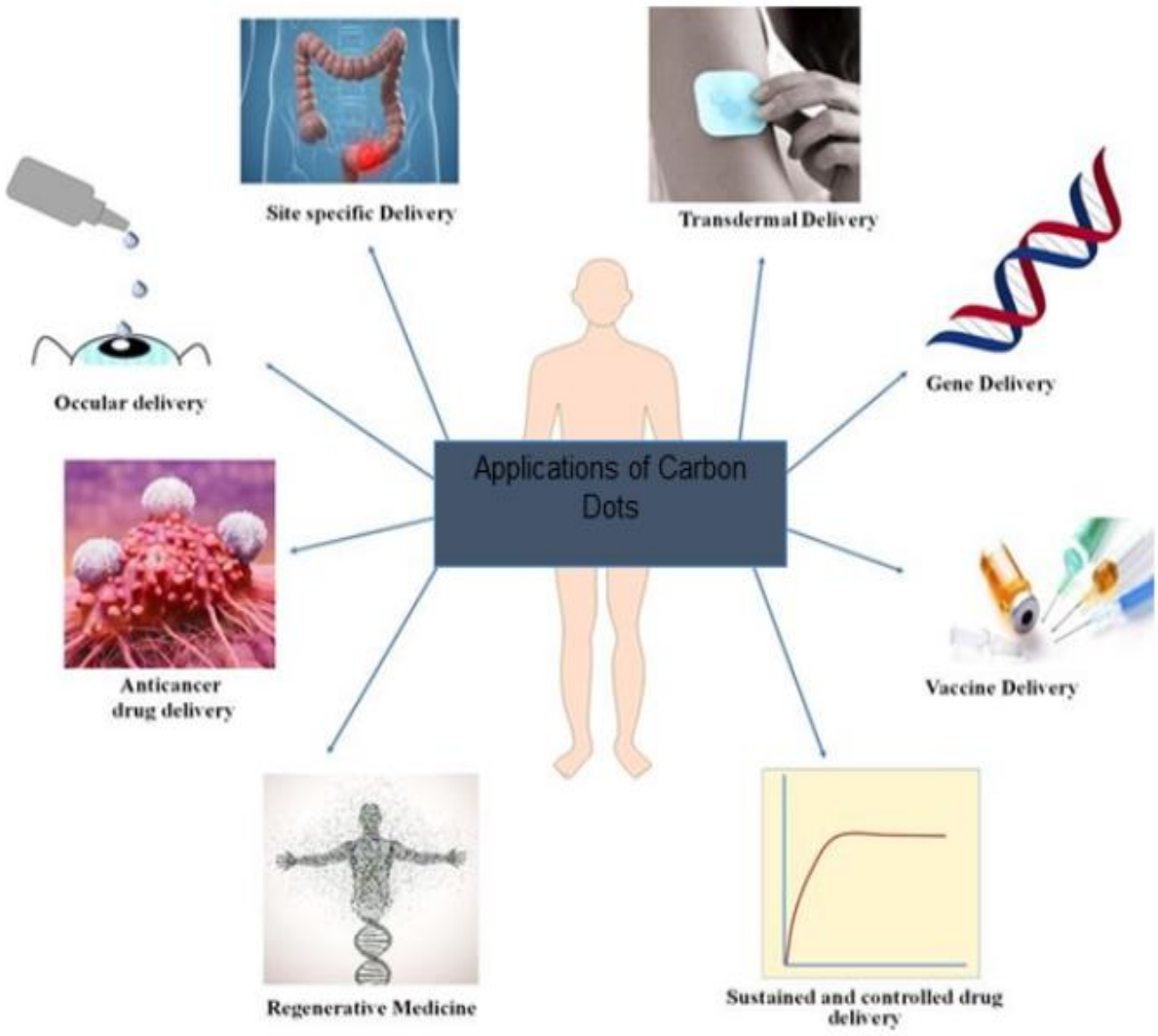


Figure 6: Schematic depicting various applications for carbon dots. Adapted with permission from Ref: 103 [103].

5.1. Carbon dots traversing the Blood-Brain Barrier

Neurodegenerative diseases pose a threat to the health and wellbeing of future generations in that the neurotherapeutics currently available, are unable to effectively cross the BBB [119]. This results in increased dosages being administrated to patients over prolonged periods of time. This ultimately results in increased frequencies of side effects suffered by patients and ultimately results in decreased patient compliance long term.

Carbon dots show promise as vehicle transporters for neurotherapeutics across the BBB effectively and efficiently. Mintz *et al.,* showed that tryptophan can be utilized to synthesize carbon dots which are able to effectively cross the BBB, due to the fact that tryptophan itself is readily able to cross the BBB. Tryptophan was utilized as an amino acid to cross the BBB via LAT1 transporter-mediated endocytosis. The researchers doped carbon dots with nitrogen from two different sources i.e. urea and 1,2-ethylenediamine. These carbon dots were observed crossing the BBB of zebrafish [119]. It has been reported by Wiley *et al.,* that transferrin-containing gold nanoparticles were able to reach the parenchyma of the brain when administered systemically [120].

Dixit *et al.,* performed an *in vitro* study and proved that the utilization of human brain cancer lines (LN229 and U87) showed that transferrin receptor- targeted gold nanoparticles were able to deliver the pro-drug into the mitochondria of the glioma cells [121]. Jiang *et al.,* proved that in addition to the ability of these transferrin conjugates to traverse the BBB effectively, transferrin-conjugated superparamagnetic iron oxide nanoparticles were able to be internalized by C6 glioma cells and detection was enabled via magnetic resonance imaging (MRI) [122].

5.2. Carbon dots and their application in CNS drug delivery.

Alzheimer's disease is a result of amyloidogenesis, which occurs due to the conversion of proteins or peptides from a soluble state to insoluble amyloid fibrils with rich ß-sheet structures. In Alzheimer's disease patients, the major component of amyloid plaques is amyloid ß (A ß). The production of A ß is due to the proteolytic cleavage of the amyloid precursor protein to form peptides of 40-42 amino acids in length [123]. Huang *et al.,* demonstrated the use of carbon dots for the successful detection of monomeric A ß peptides. In addition to this, they proved the feasibility of utilizing carbon dots for the monitoring of A ß fibrillar process. In comparison to the conventional Thioflavin T (ThT) detection process, carbon dots illustrated comparable detection due to monomer binding mechanism, which the conventional ThT detection method lacks. Carbon dots can thus be utilized in the early detection of Alzheimer's disease [124].

A myriad of studies has indicated that the APO *e4* allele could be the major risk factor for several diseases such as Parkinson's, Alzheimer's and Huntington's disease. The APO *e4* allele is one of the three common alleles, apolipoprotein E. Apolipoprotein E is recognized as a lipid transport protein. Mars *et al.*, reported the use of carbon dots, electropolymerized with curcumin as a dual fluorometric and electrochemical platform to sense the APO *e4* allele. The analytic performance illustrated a high efficacy, selectivity and stability. The platform showcased its applicability as a dual DNA sensor in the clinical fluid where it illustrated a high sensitivity response toward DNA targets even in human plasma [125]. Tisch *et al.,* reported a proof-of-concept for the feasibility of the novel diagnostic tool for the early detection of neurodegenerative diseases, utilizing carbon nanomaterials as a sensor- array biomarker test, with Parkinson's and Alzheimer diseases as examples for illustration. The carbon nanomaterials function to detect patterns of volatile organic compounds (VOCs) in exhaled breath. Disease specific breath prints prove advantageous as easily accessible biomarkers. These researchers proved that the carbon nanomaterial biosensors were able to clearly distinguish between Parkinson's and Alzheimer's patients due to the significantly different chemical composition of the exhaled breath [126].

Liu *et al.,* demonstrated that carbon nanowires and nanotubes can be utilized in neural repair and the regeneration process of neuronal cells. These carbon nanomaterials can be utilized as precursors for carbon dots and exude an effect on cellular signal transmission. These carbon nanomaterials show promising results for the improvement of cerebrovascular dysfunction after brain tumours, the augmentation of neuronal cell function within brain tissues and the diagnosis and treatment of brain diseases [127]. Diseases of the CNS are augmented by an increased level of reactive oxygen species (ROS). Fullerenes can be utilized as a precursor for carbon dots, and have been proved by Ali *et al.* to act as a radical "sponge". They are able to incorporate multiple radicals per molecule and remove superoxide radicals via a dismutation catalytic mechanism [128]. Another study proved that a fullerene C60 loaded with tris-malonic acid derivative resulted in the life span increase of mice lacking mitochondrial superoxide dismutase by 300%. Das *et al.,* proposed another class of compounds, cerium oxide nanoparticles (nanoceria) as neuroprotective agents. They performed *in vitro* experiments on isolated rat spinal cord neurons and proved that nanoceria protected cells from cell death due to oxidative stress [129].

5.3. Carbon dots in Chemo-therapeutic applications

Cancer has been a grave challenge to overcome due to the fact that it possesses unpredictable bio-physiological as well as molecular biological alterations which occur during the progression of the cancers and these factors ultimately lead to making its diagnosis as well as its treatment a daunting task [130]. The challenge posed by chemotherapy is the limited delivery of active therapeutics to the microenvironment of tumours. This is due to the aberrated surroundings of tumours, which is a result of the structural and metabolic alterations that occur during the cancerous transformation of cells [130]. Pandey *et al.,* proved that carbon dots are a powerful vehicle for the transport of therapeutics to the solid tumours [131]. Wang *et al.* [132] showed that photothermal therapy (PTT) is able to eliminate tumour cells via the conversion of near-infrared light (NIR) into cytotoxic heat. They were able to prove that the NIR light of wavelengths 700-1100 nm has an ability to trigger efficient cancer therapy. This is due to the characteristics of this light, which include good tissue transparency, accuracy, precision and non-invasive application. They utilized carbon dots as NIR-triggered systems to trigger cancer therapy and for the delivery of doxorubicin to tumor sites [132].

Zheng *et al.,* [133] functionalized an amino group onto the surface of carbon dots with oxaliplatin (oxa-C-dots) via a coupling reaction. This combined the optical properties of the carbon dots and the chemotherapeutic nature of oxaliplatin. This proved to have anticancer as well as bio-imaging properties and the Oxa-C-dots altered the internal environment of cancer cells and entered the cells via endocytosis. Oxaliplatin could be monitored *in vivo* due to the fluorescent nature of carbon dots [133]. Lai *et al.,* [134] embarked on proving that carbon dots conjugated to mSiO2-PEG were able to serve as vehicles for Doxorubicin in HeLa cells [134]. Wang *et al.,* [135] also reported the advantages of utilizing hollow carbon dots as a drug delivery vehicle for the delivery of Doxorubicin. The monitoring of chemotherapy was simplified due to the fluorescent nature of carbon dots and the delivery of the drug to the tumour sites was efficacious due to the biocompatible nature of carbon dots [135]. Figure 7 below depicts the chemotherapeutic drug loading of carbon dots as well as the mechanism of action in tumour cells.

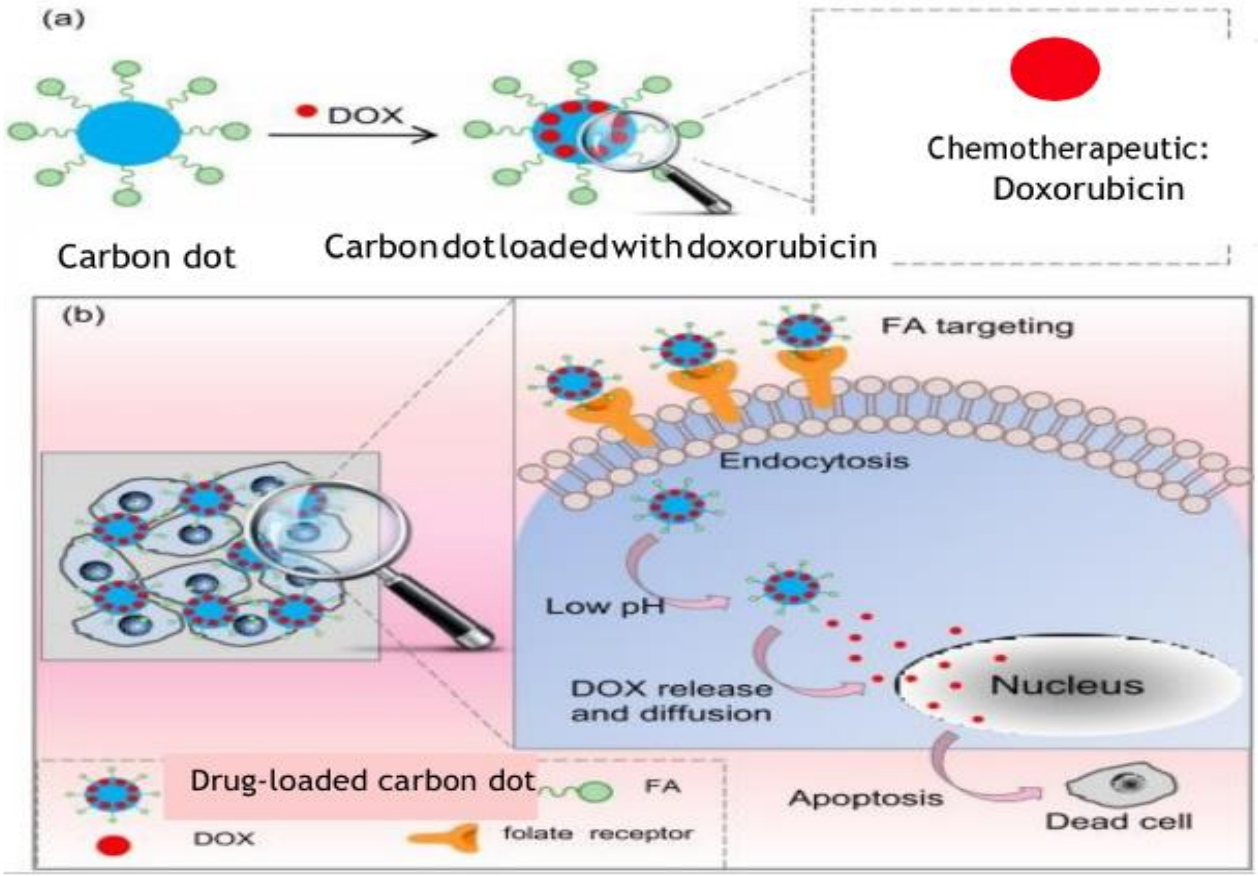


Figure 7: Schematic demonstrating the chemotherapeutic drug-loading of carbon dots as well as the mechanism of action within tumour cells. Adapted with permission from [121].

5.4. Carbon dots in Gene therapy

In order for gene therapy to have promising results, the vehicles utilized for carrying therapeutics must possess inherent safety and efficient drug-carrying abilities. Carbon dots possess abundant fluorescent and biocompatible properties, which make them best suited for this field of therapeutics. Liu *et al.,* [137] utilized carbon dots which had polyethylenimine (PEI)-branched PEI 25 kDa (BPEI-25K)] functionalized to the surface for the transfection of DNA. These PEI functionalized carbon dots functioned as transfection agents and they illustrated low cytotoxicity and excellent water solubility [137]. Kim *et al.,* [138] worked on the *in vitro* transfection of DNA. They monitored cellular plasmid trafficking as well. The researchers compared carbon dots functionalized with PEI (PEI-C-dots), carbon dots functionalized with PEI-AU (gold colloids) and carbon dots functionalized with plasmid DNA (pDNA) for gene delivery.

The researchers found that the initial connection between PEI-C-dots and PEI-AU showed weak fluorescence during transfection but, at a high concentration, pDNA and high fluorescence were recorded due to the dissociation of PEI-C-dots from PEI-AU, which ultimately allowed successful gene delivery [138].

Zhang *et al.,* [139] developed carbon dots functionalized with hyaluronic acid and PEI for gene therapy. The researchers found that these carbon dots had excellent gene condensation capacity, good biocompatibility and good water dispersibility [139]. Han *et al.,* [140] developed a novel gene delivery strategy by the utilization of carbon dots functionalized with Bpei25k, which acted as tumor necrosis factor-Related Apoptosis Inducing Ligand (TRAIL) agents. These TRAIL agents are efficacious against tumorous cells and are gaining growing interest from the oncology community. These functionalized carbon dots illustrated enhanced gene transfection efficiency in human mesenchymal stem cells (hMSCs) [140].

Jaleel *et al.,* [47] found that the protein, tissue-necrosis factor (TNF-α), possesses anti-tumor activity and is a promising candidate for gene therapy. The researchers found that utilizing carbon dots synthesized from chitosan increased the transfection efficiency of the TNF-α gene in tumor cells. They also found that the conjugation of this protein to carbon dots enabled favourable stability and efficient gene delivery [47]. Figure 8 below demonstrates the mode of action of carbon dots in gene therapy.

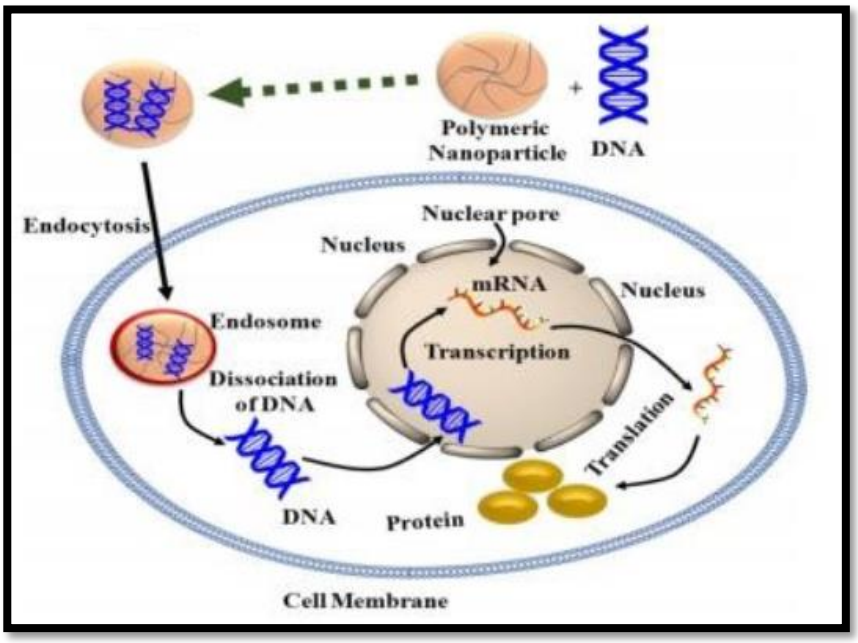


Figure 8: Schematic portraying mode of action of carbon dots in gene therapy. Adapted with permission from [103].

5.5. Carbon dots in Antimicrobial therapy.

Thakur *et al.,* [141] reported a novel microwave-assisted synthesis of carbon dots utilizing Gum Arabic (GA), as a molecular vehicle to ferry ciprofloxacin hydrochloride, in which ciprofloxacin is a broad-spectrum antibiotic. They found that carbon dots can act as an effective nano-sink for ciprofloxacin delivery. Ciprofloxacin was easily anchored to the self-functionalized carbon dots without the need for stringent protocols. They found that these ciprofloxacin carbon dot conjugates exuded potent antimicrobial activity against both gram-positive (*Bacillus subtilis* and *Staphylococcus aureus*) and gram-negative (*Escherichia coli* and *Pseudomonas aeruginosa*) bacteria [141]. Ardekani *et al.,* [142] functionalized carbon dots with metronidazole to combat periodontal disease caused by the gram-negative bacteria *Porphyromonas gingivalis.* The carbon dots were derived from chlorophyll. The researchers found that these carbon dots enhanced the penetration of metronidazole through the cell cytoplasm into the epithelial cells, hereby significantly increasing the local concentration of metronidazole inside the epithelial cells. This ultimately decreased the number of colonies by 99%. It was found that such formulations can be utilized to eliminate *Porphyromonas gingivalis* from the oral cavity [142].

Sattarahmady *et al.,* [53] demonstrated the bactericidal effects of carbon dots on the gram-positive bacterium *Staphylococcus aureus.* They found that the primary reason for the bactericidal effect of carbon dots was their light-absorbing and cell capturing abilities. The researchers employed near-infrared (NIR) irradiation to increase the solution temperature, which resulted in the induction of reactive oxygen species (ROS) production and damage to the bacterial cell walls. These processes stimulated the destruction of protein function, enzymes and lipids in the bacteria; ultimately inducing bacterial death. They were also able to prove that the photothermal treatment (PTT) effect of carbon dots exuded toxic effects in *S. Aureus* and *Methicillin-resistant S. Aureus (MRSA),* which were concentration-dependant and resulted in higher content diffusion, higher membrane permeability, cell wall disruption and oxidative stress [53].

Dong *et al.,* [143] reported the antiviral effect of carbon dots on the Norovirus (NoV) strains causing human infection i.e. GI.1 and GII.4 virus-like particles (VLPs). The carbon dots were functionalized with either 2,2'-(ethylenedioxy)bis(ethylamine) (EDA-CDots) or 3- ethoxypropylamine (EPA-CDots). The researchers found that carbon dots induced efficient inhibition of VLPs' binding to saliva human blood group antigen (HBGA) receptors in the gastrointestinal tract. Between the two types of carbon dots, the positively-charged EDA-CDots proved much more effective than the negatively charged EPA-CDots as compared to the inhibition of VLPs binding to HBGA receptors. This was due to the EDA-CDots binding being much more favourable to the negatively-charged VLPs. The researchers found that these carbon dots also exuded inhibitory effects on the binding of VLPs to their respective antibodies. However, this measured significantly less to the inhibition of VLPs binding to HBGA receptors. Dong *et al.,* [143] demonstrated proof-of-concept of the antiviral activity of carbon dots via the inhibition of virus binding to HBGA receptors. This looks promising for the inhibition of human NoV (HuNoV) infection due to the disabling of HuNoV, recognizing their binding sites on host cells [143].

Abu Rabe *et al.,* [144] proved through their findings that carbon dots are emerging as a new class of photo-activated effective antibacterial agents. The researchers synthesized carbon dots with various surface passivations. Firstly, carbon dots with small passivation molecules of different groups/charges were synthesized by functionalizing the carbon dot surface with 2,2- (ethylenedioxy)bis (ethylamine) (EDA)

and 3-ethoxypropylamine (EPA). Secondly, carbon dots with passivation polymers of tunable surface charges and sizes were synthesized by functionalizing the carbon dot surface with oligomeric polyethyleneimine of different molecular weights; PEI, Mw= ~1,20034 g/mol and PEI, Mw= ~600 g/mol [144]. These carbon dots were tested against gram-positive *Bacillus Subtilis* and the study elucidated to the fact that the surface charge on the carbon dots dominated carbon dot and bacterial cell interaction. The carbon dots illustrated effective photo-activated antimicrobial activity against the *Bacillus subtilis* bacterium [144]. Figure 6 above summarises some biomedical applications of carbon dots.

6. Conclusions

CDots provide a safer, more selective and sensitive, cheaper and time-efficient alternative to conventional drug delivery systems. Due to the large surface area, high drug-loading capacity and easily functionalized surfaces of these nanomaterials, carbon dots are ideal for the delivery of drugs to specific target sites. Their easily functionalized surfaces allow for attachment of site-specific ligands enabling the delivery of drugs to specific receptors on specific target organs in the body, decreasing the side-effects that patients experience and increasing the overall patient compliance and quality of life. This property is subjecting chemotherapy to major improvements as these CDots are able to deliver chemotherapeutic drugs to cancerous tumor cells, and leave the healthy cells unharmed. CDots are also very effective in gene therapy. In order for gene therapy to be efficacious and successful, the delivery of the system has to be safe and specific. CDots provide both safe and target-specific drug delivery, making them ideal for gene therapy. CDots have proven efficacious in neurological diseases such as, but not limited to, Alzheimer's and Parkinson's disease. Owing to the fact that carbon dots can be synthesized from various biodegradable polymers, they exude controlled drug release properties. These carbonaceous nanodots have proved extensively beneficial in additional biomedical fields, including, but not limited to, chemo-sensing, bio-sensing, bio-imaging, and antimicrobial therapy. However, the application of CDots in tissue regeneration, sexually transmitted diseases (STDs) and sexually transmitted illnesses (STIs) has hardly been documented. CDots show much promise for future advancement and applications in pulmonary diseases and cell labelling.

7. References

1. Zhou A, Song F, Yao W, *et al.* Efficient solid-state and dual-mode photoluminescence of carbon-dots/NaLuF4 microcrystals for multifunctional applications. *J Alloys* Compd 2019; 775: 457-65. http://dx.doi.org/10.1016/j.jallcom.2018.10.125.

2. Xiao C, Lai L, Zhang L, *et al.* Spectroscopic and Isothermal Titration Calorimetry Studies of Binding Interactions Between Carbon Nanodots and Serum Albumins. *J Solution Chem* 2018; 47(9): 1438-48. http://dx.doi.org/10.1007/s10953-018-0792-2

3. Sharma S, Singh N, Nepovimova E, *et al.* Interaction of synthesized nitrogen enriched graphene quantum dots with novel anti-Alzheimer's drugs: spectroscopic insights. *J Biomol Struct Dyn* 2019; •••: 1-16. http://dx.doi.org/10.1080/07391102.2019.1619625 PMID: 31096863

6. Mishra V, Patil A, Thakur S, Kesharwani P. Carbon dots: emerging theranostic nanoarchitectures. *Drug Discov Today* 2018; 23(6):1219-32. http://dx.doi.org/10.1016/j.drudis.2018.01.006 PMID: 29366761

5. Boakye-Yiadom KO, Kesse S, Opoku-Damoah Y, *et al.* Carbon dots: Applications in bioimaging and theranostics. *Int J Pharm* 2019; 564: 308-17. http://dx.doi.org/10.1016/j.ijpharm.2019.04.055 PMID: 31015004

6. Atchudan R, Edison T, Perumal S, Vinodh R, Lee Y. Betel-derived nitrogen-doped multicolour carbon dots for environmental and biological applications. *J Mol Liq* 2019; 296111817 http://dx.doi.org/10.1016/j.molliq.2019.111817

7. Devi P, Saini S, Kim KH. The advanced role of carbon quantum dots in nanomedical applications. *Biosens Bioelectron* 2019; 141111158 http://dx.doi.org/10.1016/j.bios.2019.02.059 PMID: 31323605

8. Su Q, Wei X, Mao J, Yang X. Carbon nanopowder directed synthesis of carbon dots for sensing multiple targets. *Colloids Surf A Physicochem Eng Asp* 2019; 562: 86-92. http://dx.doi.org/10.1016/j.colsurfa.2018.11.015

9. Wang Y, Li Y, Xu Y. Synthesis of mechanical responsive carbon dots with fluorescence enhancement. *J Colloid Interface Sci* 2020; 560: 85-90. http://dx.doi.org/10.1016/j.jcis.2019.10.039 PMID: 31654898

10. Xiong Y, Schneider J, Ushakova E, Rogach A. Influence of molecular fluorophores on the research field of chemically synthesized carbon dots. *Nano Today* 2018; 23: 124-39. http://dx.doi.org/10.1016/j.nantod.2018.10.010

11. Zhang S, Zhang L, Huang L, *et al.* Study on the fluorescence properties of carbon dots prepared via combustion process. *J Lumin* 2019; 206: 608-12. http://dx.doi.org/10.1016/j.jlumin.2018.10.086

12. Parvin N, Mandal T. Dually emissive P,N-co-doped carbon dots for fluorescent and photoacoustic tissue imaging in living mice. *Mikrochim Acta* 2017; 184(4): 1117-25. http://dx.doi.org/10.1007/s00604-017-2108-4

13. Godavarthi S, Mohan Kumar K, Vázquez Vélez E, *et al.* Nitrogen-doped carbon dots derived from Sargassum fluitans as fluorophore for DNA detection. *J Photochem Photobiol B* 2017; 172: 36-41. http://dx.doi.org/10.1016/j.jphotobiol.2017.05.014 PMID: 28514712

14. Plácido J, Bustamante-López S, Meissner KE, Kelly DE, Kelly SL. Microalgae biochar-derived carbon dots and their application in heavy metal sensing in aqueous systems. *Sci Total Environ* 2019; 656: 531-9. http://dx.doi.org/10.1016/j.scitotenv.2018.11.393 PMID: 30529956

15. Feng H, Qian Z. Functional Carbon Quantum Dots: A Versatile Platform for Chemosensing and Biosensing. Chem Rec 2018;18(5): 491-505. http://dx.doi.org/10.1002/tcr.201700055 PMID: 29171708

16. Le Joncour V, Laakkonen P. Seek & Destroy, use of targeting peptides for cancer detection and drug delivery. *Bioorg Med Chem* 2018; 26(10): 2797-806. http://dx.doi.org/10.1016/j.bmc.2017.08.052 PMID: 28893601

17. Das R, Bandyopadhyay R, Pramanik P. Carbon quantum dots from natural resource: A review. *Materials Today Chemistry* 2018; 8: 96- 109.

18. Niidome T, Huang L. Gene therapy progress and prospects: nonviral vectors. *Gene Ther* 2002; 9(24): 1647-52. http://dx.doi.org/10.1038/sj.gt.3301923 PMID: 12457277

19. Mohammadinejad R, Dadashzadeh A, Moghassemi S, *et al.* Shedding light on gene therapy: Carbon dots for the minimally invasive image-guided delivery of plasmids and noncoding RNAs - A review. *J Adv Res* 2019; 18: 81-93. http://dx.doi.org/10.1016/j.jare.2019.01.004 PMID: 30828478

20. Gong J, Chen X, Tang T. Recent progress in controlled carbonization of (waste) polymers. *Prog Polym Sci* 2019; 94: 1-32. http://dx.doi.org/10.1016/j.progpolymsci.2019.04.001

21. Cai T, Zhang Y, Liu D, Tong D, Liu S. Nanostructured molybdenum/heteroatom-doped carbon dots nanohybrids for lubrication by direct carbonization route. *Mater Lett* 2019; 250: 20-4. http://dx.doi.org/10.1016/j.matlet.2019.04.107

22. Knop K, Hoogenboom R, Fischer D, Schubert US. Poly(ethylene glycol) in drug delivery: pros and cons as well as potential alternatives. *Angew Chem Int Ed Engl* 2010; 49(36): 6288-308. http://dx.doi.org/10.1002/anie.200902672 PMID: 20648499

23. Naik V, Gunjal D, Gore A, *et al.* Quick and low-cost synthesis of sulphur doped carbon dots by simple acidic carbonization of sucrose for the detection of Fe3+ ions in highly acidic environment. *Diamond Related Materials* 2018; 88: 262-8. http://dx.doi.org/10.1016/j.diamond.2018.07.018

24. Cheng C, Shi Y, Li M, Xing M, Wu Q. Carbon quantum dots from carbonized walnut shells: Structural evolution, fluorescence characteristics, and intracellular bioimaging. *Mater Sci Eng C* 2017; 79:473-80. http://dx.doi.org/10.1016/j.msec.2017.05.094 PMID: 28629043

25. Hong Y, Uhm H. Production of carbon nanotubes by microwave plasma torch at atmospheric pressure. Phys Plasmas 2005;12(5)053504 http://dx.doi.org/10.1063/1.1914805

26. Ma X, Li S, Hessel V, Lin L, Meskers S, Gallucci F. 2019; Synthesis of luminescent carbon quantum dots by microplasma process. *Chemical Engineering and Processing - Process Intensification* 140:29-35. http://dx.doi.org/10.1016/j.cep.2019.04.017

27. Henam SD, Ahmad F, Shah MA, Parveen S, Wani AH. Microwave synthesis of nanoparticles and their antifungal activities. *Spectrochim Acta A Mol Biomol Spectrosc* 2019; 213: 337-41. http://dx.doi.org/10.1016/j.saa.2019.01.071 PMID: 30711904

28. Yang P, Zhu Z, Chen M, Chen W, Zhou X. Microwave-assisted synthesis of xylan-derived carbon quantum dots for tetracycline sensing. Opt Mater 2018; 85: 329-36. http://dx.doi.org/10.1016/j.optmat.2018.06.034

29. Choi Y, Thongsai N, Chae A, *et al.* Microwave-assisted synthesis of luminescent and biocompatible lysine-base carbon quantum dots. *J Ind Eng Chem* 2017; 47: 329-35. http://dx.doi.org/10.1016/j.jiec.2016.12.002

30. Hou J, Li H, Wang L, *et al.* Rapid microwave-assisted synthesis of molecularly imprinted polymers on carbon quantum dots for fluorescent sensing of tetracycline in milk. Talanta 2016; 146: 34-40. http://dx.doi.org/10.1016/j.talanta.2015.08.024 PMID: 26695231

31. Liu S, Cui J, Huang J, Tian B, Jia F, Wang Z. Facile one-pot synthesis of highly fluorescent nitrogen-doped carbon dots by mild hydrothermal method and their applications in detection of Cr(VI) ions. *Spectrochim Acta A Mol Biomol Spectrosc* 2019; 206: 65-71. http://dx.doi.org/10.1016/j.saa.2018.07.082 PMID: 30081269

32. Huang Q, Hu S, Zhang H, *et al.* Carbon dots and chitosan composite film based biosensor for the sensitive and selective determination of dopamine. *Analyst (Lond)* 2013; 138(18): 5417-23. http://dx.doi.org/10.1039/c3an00510k PMID: 23833763

33. Huang H, Xu Y, Tang C, Chen J, Wang A, Feng J. Facile and green synthesis of photoluminescent carbon nanoparticles for cellular imaging. *New J Chem* 2014; 38(2): 784. http://dx.doi.org/10.1039/c3nj01185b

34. Sarkar T, Bohidar HB, Solanki PR. Carbon dots-modified chitosan based electrochemical biosensing platform for detection of vitamin D. *Int J Biol Macromol* 2018; 109: 687-97. http://dx.doi.org/10.1016/j.ijbiomac.2017.12.122 PMID: 29275197

35. Jia X, Han Y, Pei M, *et al.* Multi-functionalized hyaluronic acid nanogels crosslinked with carbon dots as dual receptor-mediated targeting tumor theranostics. *Carbohydr Polym* 2016; 152: 391-7. http://dx.doi.org/10.1016/j.carbpol.2016.06.109 PMID: 27516286

36. Stern R, Jedrzejas MJ. Hyaluronidases: their genomics, structures, and mechanisms of action. *Chem Rev* 2006; 106(3): 818-39. http://dx.doi.org/10.1021/cr050247k PMID: 16522010

37. Choi KY, Yoon HY, Kim JH, *et al.* Smart nanocarrier based on PEGylated hyaluronic acid for cancer therapy. ACS Nano 2011;5(11): 8591-9. http://dx.doi.org/10.1021/nn202070n PMID: 21967065

38. Liu Y, *et al.* One-step microwave-assisted polyol synthesis of green luminescent carbon dots as http://dx.doi.org/10.1016/j.carbon.2013.10.086

39. Cermelj K, Ruengkajorn K, Buffet J, O'Hare D. Layered double hydroxide nanosheets via solvothermal delamination. *Journal of Energy Chemistry* 2019; 35: 88-94. http://dx.doi.org/10.1016/j.jechem.2018.11.008

40. Mamaghani AH, Haghighat F, Lee CS. Hydrothermal/solvothermal synthesis and treatment of TiO2 for photocatalytic degradation of air pollutants: Preparation, characterization, properties, and performance. *Chemosphere* 2019; 219: 804-25. http://dx.doi.org/10.1016/j.chemosphere.2018.12.029 PMID: 30572234

41. Yang J, *et al.* One-step synthesized carbon dots with bacterial contact-enhanced fluorescence emission property: Fast Gram-type identification and selective Gram-positive bacterial inactivation. *Carbon Elsevier Ltd* 2019; 146: 827-39.

42. Liu Y, Duan W, Song W, *et al.* Red Emission B, N, S-co-Doped Carbon Dots for Colorimetric and Fluorescent Dual Mode Detection of Fe3+ Ions in Complex Biological Fluids and Living Cells. *ACS Appl Mater Interfaces* 2017; 9(14): 12663-72. http://dx.doi.org/10.1021/acsami.6b15746 PMID: 28339185

43. Khan ZMSH, *et al.* 'Hydrothermal treatment of red lentils for the synthesis of fluorescent carbon quantum dots and its application for sensing Fe3+', Optical Materials. *Elsevier B* 2019; 91: 386-95.

44. Guo L, Li L, Liu M, *et al.* Bottom-up preparation of nitrogen doped carbon quantum dots with green emission under microwave-assisted hydrothermal treatment and their biological imaging. *Mater Sci Eng C* 2018; 84: 60-6. http://dx.doi.org/10.1016/j.msec.2017.11.034 PMID: 29519444

45. Yuan M, *et al.* 'One-step, green, and economic synthesis of watersoluble photoluminescent carbon dots by hydrothermal treatment of wheat straw, and their bio-applications in labeling, imaging, and sensing, Applied Surface Science. Elsevier B 2015; 355: 1136-44. http://dx.doi.org/10.1016/j.apsusc.2015.07.095

46. Ding X, Liu Y, Li J, *et al.* Hydrazone-bearing PMMA-functionalized magnetic nanocubes as pH-responsive drug carriers for remotely targeted cancer therapy in vitro and in vivo. *ACS Appl Mater Interfaces* 2014; 6(10): 7395-407. http://dx.doi.org/10.1021/am500818m PMID: 24749476

47. Jaleel JA, Ashraf SM, Rathinasamy K, Pramod K. Carbon dot festooned and surface passivated graphene-reinforced chitosan construct for tumor-targeted delivery of TNF-α gene. *Int J Biol* Macromol 2019; 127: 628-36. http://dx.doi.org/10.1016/j.ijbiomac.2019.01.174 PMID: 30708020

48. Zhao Q, Wang S, Yang Y, *et al.* Hyaluronic acid and carbon dots-gated hollow mesoporous silica for redox and enzyme-triggered targeted drug delivery and bioimaging. Mater Sci Eng C 2017; 78: 475-84. http://dx.doi.org/10.1016/j.msec.2017.04.059 PMID: 28576012

49. Yamina AM, Fizir M, Itatahine A, He H, Dramou P. Preparation of multifunctional PEG-graft-Halloysite Nanotubes for Controlled Drug Release, Tumor Cell Targeting, and Bio-imaging. *Colloids Surf B Biointerfaces* 2018; 170: 322-9. http://dx.doi.org/10.1016/j.colsurfb.2018.06.042 PMID: 29936385

50. Shen J, Zhu Y, Yang X, Li C. Graphene quantum dots: emergent nanolights for bioimaging, sensors, catalysis and photovoltaic devices. *Chem Commun (Camb)* 2012; 48(31): 3686-99. http://dx.doi.org/10.1039/c2cc00110a PMID: 22410424

51. Xiao S, Huang C, Li Y. Modern Inorganic Synthetic Chemistry. Beijing: *Elsevier* 2017; pp. 431- 55.

52. Calabro R L, Yang D S, Kim D Y. Academic Press Inc. 2018; 527: pp. Liquid-phase laser ablation synthesis of graphene quantum dots from carbon nano-onions: Comparison with chemical oxidation In: *Journal of Colloid and Interface Science*. 132-40. http://dx.doi.org/10.1016/j.jcis.2018.04.113

53. Sattarahmady N, Rezaie-Yazdi M, Tondro GH, Akbari N. Bactericidal laser ablation of carbon dots: An in vitro study on wild-type and antibiotic-resistant Staphylococcus aureus*. J Photochem Photobiol B* 2017; 166: 323-32. http://dx.doi.org/10.1016/j.jphotobiol.2016.12.006 PMID: 28024283

54. Peng Z, Han X, Li S, *et al.* Carbon dots: Biomacromolecule interaction, bioimaging and nanomedicine. *Coord Chem Rev* 2017; 343:256-77. http://dx.doi.org/10.1016/j.ccr.2017.06.001

55. Bozetine H, Wang Q, Barras A, *et al.* Green chemistry approach for the synthesis of ZnO-carbon dots nanocomposites with good photocatalytic properties under visible light. *J Colloid Interface Sci* 2016;465: 286-94. http://dx.doi.org/10.1016/j.jcis.2015.12.001 PMID: 26674245

56. Kołodziejczak-Radzimska A, Jesionowski T. Zinc oxide-From synthesis to application: A review. *Materials (Basel)* 2014; 7(4):2833-81. http://dx.doi.org/10.3390/ma7042833 PMID: 28788596

57. Djurišić A, Chen X, Leung Y, Man Ching Ng A. ZnO nanostructures: growth, properties and applications. *J Mater Chem* 2012; 22(14): 6526. http://dx.doi.org/10.1039/c2jm15548f

58. Dehvari K, Liu K, Tseng P, Gedda G, Girma W, Chang J. Sonochemical-assisted green synthesis of nitrogen-doped carbon dots from crab shell as targeted nanoprobes for cell imaging. *Journal of the Taiwan Institute of Chemical Engineers* 2019; 95: 495-503. http://dx.doi.org/10.1016/j.jtice.2018.08.037

59. Li X, Wang H, Shimizu Y, Pyatenko A, Kawaguchi K, Koshizaki N. Preparation of carbon quantum dots with tunable photoluminescence by rapid laser passivation in ordinary organic solvents. *Chem Commun (Camb)* 2011; 47(3): 932-4. http://dx.doi.org/10.1039/C0CC03552A PMID: 21079826

60. Hsu PC, Chang HT. Synthesis of high-quality carbon nanodots from hydrophilic compounds: role of functional groups. *Chem Commun (Camb)* 2012; 48(33): 3984-6. http://dx.doi.org/10.1039/c2cc30188a PMID: 22422194

61. Sahu S, Behera B, Maiti TK, Mohapatra S. Simple one-step synthesis of highly luminescent carbon dots from orange juice: application as excellent bio-imaging agents. *Chem Commun (Camb)* 2012;48(70): 8835-7. http://dx.doi.org/10.1039/c2cc33796g PMID: 22836910

62. D'souza SL, Deshmukh B, Bhamore JR, Rawat KA, Lenka N, Kailasa SK. Synthesis of fluorescent nitrogen-doped carbon dots from dried shrimps for cell imaging and boldine drug delivery system. *RSC Advances* 2016; 6: 12169-79. http://dx.doi.org/10.1039/C5RA24621K

63. Bhamore JR, Jha S, Singhal RK, Park TJ, Kailasa SK. Facile green synthesis of carbon dots from Pyrus pyrifolia fruit for assaying of Al3+ ion via chelation enhanced fluorescence mechanism. *J Mol Liq* 2018; •••: 2649-16. http://dx.doi.org/10.1016/j.molliq.2018.05.041

64. Wang D, Wang X, Guo Y, Liu W, Qin W. Luminescent properties of milk carbon dots and their sulphur and nitrogen doped analogues. *RSC Advances* 2014; 4: 51658-65. http://dx.doi.org/10.1039/C4RA11158C

65. Prasannan A, Imae T. One-pot synthesis of fluorescent carbon dots from orange waste peels. *Ind Eng Chem Res* 2013; 52: 15673-8. http://dx.doi.org/10.1021/ie402421s

66. Wei J, Zhang X, Sheng Y, *et al.* Dual functional carbon dots derived from cornflour via a simple one-pot hydrothermal route. Mater Lett 2014; 123: 107-11. http://dx.doi.org/10.1016/j.matlet.2014.02.090

67. Ansi VA, Renuka NK. Table sugar derived Carbon dot – a naked eye sensor for toxic Pb2+ ions. *Sens Actuators B Chem* 2018; 264: 67-75. http://dx.doi.org/10.1016/j.snb.2018.02.167

68. Yang K, Liu M, Wang Y, *et al.* Carbon dots derived from fungus for sensing hyaluronic acid and hyaluronidase. *Sens Actuators B Chem* 2017; 251: 503-8. http://dx.doi.org/10.1016/j.snb.2017.05.086

69. Ensafi AA, Hghighat Sefat S, Kazemifard N, Rezaei B, Moradi F. A novel one-step and green synthesis of highly fluorescent carbon dots from saffron for cell imaging and sensing of prilocaine. *Sens Actuators B Chem* 2017; 253: 451-60. http://dx.doi.org/10.1016/j.snb.2017.06.163

70. Liu W, Diao H, Chang H, Wang H, Li T, Wei W. Green synthesis of carbon dots from rose-heart radish and application for Fe3+ detection and cell imaging. *Sens Actuators B Chem* 2017; 241: 190-8. http://dx.doi.org/10.1016/j.snb.2016.10.068

71. Wang Q, Liu X, Zhang L, Lv Y. Microwave-assisted synthesis of carbon nanodots through an eggshell membrane and their fluorescent application. *Analyst (Lond)* 2012; 137(22): 5392-7. http://dx.doi.org/10.1039/c2an36059d PMID: 23037913

72. Zhu H, Wang X, Li Y, Wang Z, Yang F, Yang X. Microwave synthesis of fluorescent carbon nanoparticles with electrochemiluminescence properties. *Chem Commun (Camb)* 2009; (34): 5118-20. http://dx.doi.org/10.1039/b907612c PMID: 20448965

73. Tang L, Ji R, Cao X, *et al.* Deep ultraviolet photoluminescence of water-soluble self-passivated graphene quantum dots. *ACS Nano* 2012; 6(6): 5102-10. http://dx.doi.org/10.1021/nn300760g PMID: 22559247

74. Zhai X, Zhang P, Liu C, *et al.* Highly luminescent carbon nanodots by microwave-assisted pyrolysis. *Chem Commun (Camb)* 2012; 48(64): 7955-7. http://dx.doi.org/10.1039/c2cc33869f PMID: 22763501

75. Ma CB, Zhu ZT, Wang HX, *et al.* A general solid-state synthesis of chemically-doped fluorescent graphene quantum dots for bioimaging and optoelectronic applications. *Nanoscale* 2015; 7(22): 10162-9. http://dx.doi.org/10.1039/C5NR01757B PMID: 25985855

76. Chen B, Li F, Li S, *et al.* Large scale synthesis of photoluminescent carbon nanodots and their application for bioimaging. *Nanoscale* 2013; 5(5): 1967-71. http://dx.doi.org/10.1039/c2nr32675b PMID: 23361842

77. Mehta VN, Jha S, Kailasa SK. One-pot green synthesis of carbon dots by using Saccharum officinarum juice for fluorescent imaging of bacteria (Escherichia coli) and yeast (Saccharomyces cerevisiae) cells. *Mater Sci Eng C* 2014; 38: 20-7. http://dx.doi.org/10.1016/j.msec.2014.01.038 PMID: 24656348

78. Qu D, Zheng M, Du P, *et al.* Highly luminescent S, N co-doped graphene quantum dots with broad visible absorption bands for visible light photocatalysts. *Nanoscale* 2013; 5(24): 12272-7. http://dx.doi.org/10.1039/c3nr04402e PMID: 24150696

79. Wang L, Wang X, Bhirde A, *et al.* Carbon-dot-based two-photon visible nanocarriers for safe and highly efficient delivery of siRNA and DNA. *Adv Healthc Mater* 2014; 3(8): 1203-9. http://dx.doi.org/10.1002/adhm.201300611 PMID: 24692418.

80. Zhou J, Booker C, Li R, *et al.* An electrochemical avenue to blue luminescent nanocrystals from multiwalled carbon nanotubes (MWCNTs). *J Am Chem Soc* 2007; 129(4): 744-5. http://dx.doi.org/10.1021/ja0669070 PMID: 17243794.

81. Lu J, Yang JX, Wang J, Lim A, Wang S, Loh KP. One-pot synthesis of fluorescent carbon nanoribbons, nanoparticles, and graphene by the exfoliation of graphite in ionic liquids. *ACS Nano* 2009;3(8): 2367-75. http://dx.doi.org/10.1021/nn900546b PMID: 19702326.

82. Nanocarbon. Fundamentals and Applications of Nano Silicon in Plasmonics and Fullerines 2008; pp. 287-309.

83. Zawadzka A, Płóciennik P, Korcala A, Szroeder P. Optical properties of chiral single-walled carbon nanotubes thin films. *Opt Mater* 2019; 96109295 http://dx.doi.org/10.1016/j.optmat.2019.109295

84. Zhang D, Yang H. Formation of carbon nanoscrolls from graphene sheet: A molecular dynamics study. *J Mol Struct* 2016; 1125: 282-7. http://dx.doi.org/10.1016/j.molstruc.2016.06.083

85. Maleki R, Afrouzi HH, Hosseini M, Toghraie D, Rostami S. Molecular dynamics simulation of Doxorubicin loading with Nisopropyl acrylamide carbon nanotube in a drug delivery system. *Comput Methods Programs Biomed* 2020; 184105303

86. Kamel M, Raissi H, Morsali A, Shahabi M. Assessment of the adsorption mechanism of Flutamide anticancer drug on the functionalized single-walled carbon nanotube surface as a drug delivery vehicle: An alternative theoretical approach based on DFT and MD. *Appl Surf Sci* 2018; 434: 492-503. http://dx.doi.org/10.1016/j.apsusc.2017.10.165

87. Falank C, Tasset AW, Farrell M, *et al.* Development of medicalgrade, discrete, multi-walled carbon nanotubes as drug delivery molecules to enhance the treatment of hematological malignancies. *Nanomedicine (Lond)* 2019; 20102025

http://dx.doi.org/10.1016/j.nano.2019.102025 PMID: 31170511

88. Li Z, de Barros ALB, Soares DCF, Moss SN, Alisaraie L. Functionalized single-walled carbon nanotubes: cellular uptake, biodistribution and applications in drug delivery. *Int J Pharm* 2017; 524(1-2): 41-54. http://dx.doi.org/10.1016/j.ijpharm.2017.03.017 PMID: 28300630

89. Yan GH, Song ZM, Liu YY, *et al.* Effects of carbon dots surface functionalities on cellular behaviors - Mechanistic exploration for opportunities in manipulating uptake and translocation. *Colloids Surf B Biointerfaces* 2019; 181: 48-57.

http://dx.doi.org/10.1016/j.colsurfb.2019.05.027 PMID: 31121381

90. S, Mao Q-X, Yuan X-L, Kong X-L, Chen X-W, Wang J-H. Targeted imaging of the lysosome and endoplasmic reticulum and their pH monitoring with surface regulated carbon dots. *Nanoscale* 2018; 10(26): 12788-96.

http://dx.doi.org/10.1039/C8NR03453B PMID: 29947397

91. Zhu S, Zhang J, Tang S, *et al.* Surface Chemistry Routes to Modulate the Photoluminescence of Graphene Quantum Dots: From Fluorescence Mechanism to Up-Conversion Bioimaging Applications. *Adv Funct Mater* 2012; 22(22): 4732-40.

http://dx.doi.org/10.1002/adfm.201201499

92. Kundu A, Lee J, Park B, *et al.* Facile approach to synthesize highly fluorescent multicolor emissive carbon dots via surface functionalization for cellular imaging. *J Colloid Interface Sci* 2018; 513: 505-14.

http://dx.doi.org/10.1016/j.jcis.2017.10.095 PMID: 29179091

93. LeCroy G, Yang S, Yang F, *et al.* Functionalized carbon nanoparticles: Syntheses and applications in optical bioimaging and energy conversion. *Coord Chem Rev* 2016; 320-321: 66-81. http://dx.doi.org/10.1016/j.ccr.2016.02.017

94. Havrdova M, Hola K, Skopalik J, *et al.* Toxicity of carbon dots – Effect of surface functionalization on the cell viability, reactiveoxygen species generation and cell cycle. *Carbon* 2016; 99: 238-48. http://dx.doi.org/10.1016/j.carbon.2015.12.027

95. Roy E, Patra S, Madhuri R, Sharma P. RETRACTED: Carbon dot/TAT peptide co-conjugated bubble nanoliposome for multicolour cell imaging, nuclear-targeted

delivery, and chemo/photothermal synergistic therapy. *Chem Eng J* 2017; 312: 144-57. http://dx.doi.org/10.1016/j.cej.2016.11.122

96. Hu Y, Gao Z. Hot-injection strategy for 1-min synthesis of carbon dots from oxygen-containing organic solvents: Toward fluorescence sensing of hemoglobin. *Dyes Pigments* 2019; 165: 429-35. http://dx.doi.org/10.1016/j.dyepig.2019.03.001

97. Liu H, Ding J, Zhang K, Ding L. Fabrication of carbon dots@restricted access molecularly imprinted polymers for selective detection of metronidazole in serum. *Talanta* 2020; 209120508 http://dx.doi.org/10.1016/j.talanta.2019.120508 PMID: 31892057

98. Amer Ridha A, Pakravan P, Hemati Azandaryani A, Zhaleh H. Carbon dots; the smallest photoresponsive structure of carbon in advanced drug targeting. *J Drug Deliv Sci Technol* 2020; 55101408 http://dx.doi.org/10.1016/j.jddst.2019.101408

99. Lu L, Ma M, Tan T, *et al.* Novel dual ligands capped perovskite quantum dots for fluoride detection. *Sens Actuators B Chem* 2018; 270: 291-7. http://dx.doi.org/10.1016/j.snb.2018.05.038

100. Dong Y, Pang H, Yang HB, *et al.* Carbon-based dots co-doped with nitrogen and sulfur for high quantum yield and excitation-independent emission. *Angew Chem Int Ed Engl* 2013; 52(30):7800-4. http://dx.doi.org/10.1002/anie.201301114 PMID: 23761198

101. Liu T, Li N, Dong J, Luo H, Li N. Fluorescence detection of mercury ions and cysteine based on magnesium and nitrogen co-doped carbon quantum dots and IMPLICATION logic gate operation. *Sens Actuators B Chem* 2016; 231: 147-53. http://dx.doi.org/10.1016/j.snb.2016.02.141

102. Yang ST, Wang X, Wang H, *et al.* Carbon Dots as Nontoxic and High-Performance Fluorescence Imaging Agents. *J Phys Chem C Nanomater Interfaces* 2009; 113(42): 18110-4. http://dx.doi.org/10.1021/jp9085969 PMID: 20357893

103. Zhu C, Zhai J, Dong S. Bifunctional fluorescent carbon nanodots: green synthesis via soy milk and application as metal-free electrocatalysts for oxygen reduction. *Chem Commun (Camb)* 2012; 48(75): 9367-9. http://dx.doi.org/10.1039/c2cc33844k PMID: 22911246

104. Kong B, Zhu A, Ding C, Zhao X, Li B, Tian Y. Carbon dot-based inorganic-organic nanosystem for two-photon imaging and biosensing of pH variation in living cells and tissues. *Adv Mater* 2012;24(43): 5844-8. http://dx.doi.org/10.1002/adma.201202599 PMID: 22933395

105. Li F, Liu C, Yang J, Wang Z, Liu W, Tian F. Mg/N double doping strategy to fabricate extremely high luminescent carbon dots for bioimaging. *RSC Advances* 2014; 4(7): 3201-5. http://dx.doi.org/10.1039/C3RA43826K

106. Huang S, Wang L, Zhu F, *et al.* A ratiometric nanosensor based on fluorescent carbon dots for label-free and highly selective recognition of DNA. *RSC Advances* 2015; 5(55): 44587-97. http://dx.doi.org/10.1039/C5RA05519A

107. Han Y, Tang D, Yang Y, *et al.* Non-metal single/dual doped carbon quantum dots: a general flame synthetic method and electrocatalytic properties. *Nanoscale* 2015; 7(14): 5955-62. http://dx.doi.org/10.1039/C4NR07116F PMID: 25771786

108. Li N, Liu S, Zhu Y, *et al.* Tuning gold nanoparticles growth via DNA and carbon dots for nucleic acid and protein detection. *Sens Actuators B Chem* 2017; 251: 455 61. http://dx.doi.org/10.1016/j.snb.2017.05.071

109. Pierrat P, Wang R, Kereselidze D, *et al.* Efficient in vitro and in vivo pulmonary delivery of nucleic acid by carbon dot-based nanocarriers. *Biomaterials* 2015; 51: 290-302. http://dx.doi.org/10.1016/j.biomaterials.2015.02.017 PMID: 25771019

110. Liu F, *et al.* 'One-pot synthesis of NiFe2O4 integrated with EDTA-derived carbon dots for enhanced removal of tetracycline', *Chemical Engineering Journal. Elsevier B* 2017; 310: 187-96.

111. Pang Y, Gao H, Wu S, Li X. Facile synthesis the nitrogen and sulfur co-doped carbon dots for selective fluorescence detection of heavy metal ions. *Mater Lett* 2017; 193: 236-9. http://dx.doi.org/10.1016/j.matlet.2017.01.149

112. Shan X, Chai L, Ma J, Qian Z, Chen J, Feng H. B-doped carbon quantum dots as a sensitive fluorescence probe for hydrogen peroxide and glucose detection. *Analyst (Lond)* 2014; 139(10): 2322-5. http://dx.doi.org/10.1039/C3AN02222F PMID: 24695439

113. Qiao S, Li H, Li H, *et al.* Label-free carbon quantum dots as photoluminescence probes for ultrasensitive detection of glucose. *RSC Advances* 2015; 5(84): 69042-6. http://dx.doi.org/10.1039/C5RA12829C

114. Zhang R, Chen W. Nitrogen-doped carbon quantum dots: facile synthesis and application as a “turn-off” fluorescent probe for detection of Hg2+ ions. *Biosens Bioelectron* 2014; 55: 83-90. http://dx.doi.org/10.1016/j.bios.2013.11.074 PMID: 24365697

115. Qian Z, Shan X, Chai L, Ma J, Chen J, Feng H. Si-doped carbon quantum dots: a facile and general preparation strategy, bioimaging application, and multifunctional sensor. *ACS Appl Mater Interfaces* 2014; 6(9): 6797-805. http://dx.doi.org/10.1021/am500403n PMID: 24707855

116. Huang Y, Zhou J, Feng H, *et al.* A dual-channel fluorescent chemosensor for discriminative detection of glutathione based on functionalized carbon quantum dots. *Biosens Bioelectron* 2016; 86: 748-55. http://dx.doi.org/10.1016/j.bios.2016.07.081 PMID: 27476056

117. Sun Q, Fang S, Fang Y, Qian Z, Feng H. Fluorometric detection of cholesterol based on β-cyclodextrin functionalized carbon quantum dots via competitive host-guest recognition. *Talanta* 2017; 167:513-9. http://dx.doi.org/10.1016/j.talanta.2017.02.060 PMID: 28340753

118. Prajapati S, Jain A, Jain A, Jain S. Biodegradable polymers and constructs: A novel approach in drug delivery. *Eur Polym J* 2019; 120109191 http://dx.doi.org/10.1016/j.eurpolymj.2019.08.018

119. Mintz KJ, Mercado G, Zhou Y, *et al.* Tryptophan carbon dots and their ability to cross the blood-brain barrier. *Colloids Surf B Biointerfaces* 2019; 176: 488-93. http://dx.doi.org/10.1016/j.colsurfb.2019.01.031 PMID: 30690384

120. Wiley DT, Webster P, Gale A, Davis ME. Transcytosis and brain uptake of transferrin-containing nanoparticles by tuning avidity to transferrin receptor. *Proc Natl Acad Sci USA* 2013; 110(21): 8662- 7. http://dx.doi.org/10.1073/pnas.1307152110 PMID: 23650374

121. Dixit S, Novak T, Miller K, Zhu Y, Kenney ME, Broome AM. Transferrin receptor-targeted theranostic gold nanoparticles for photosensitizer delivery in brain tumors.

Nanoscale 2015; 7(5): 1782-90. http://dx.doi.org/10.1039/C4NR04853A PMID: 25519743

122. Jiang W, Xie H, Ghoorah D, *et al.* Conjugation of functionalized SPIONs with transferrin for targeting and imaging brain glial tumors in rat model. *PLoS One* 2012; 7(5)e37376 http://dx.doi.org/10.1371/journal.pone.0037376 PMID: 22615995

123. Roberson ED, Mucke L. 100 years and counting: prospects for defeating Alzheimer's disease. *Science* 2006; 314(5800): 781-4. http://dx.doi.org/10.1126/science.1132813 PMID: 17082448

124. Huang H, Li P, Zhang M, *et al.* Graphene quantum dots for detecting monomeric amyloid peptides. *Nanoscale* 2017; 9(16): 5044-8. http://dx.doi.org/10.1039/C6NR10017A PMID: 28397888

125. Mars A, Hamami M, Bechnak L, Patra D, Raouafi N. Curcumingraphene quantum dots for dual mode sensing platform: Electrochemical and fluorescence detection of APOe4, responsible of Alzheimer's disease. *Anal Chim Acta* 2018; 1036: 141-6. http://dx.doi.org/10.1016/j.aca.2018.06.075 PMID: 30253824

126. Tisch U, Schlesinger I, Ionescu R, *et al.* Detection of Alzheimer's and Parkinson's disease from exhaled breath using nanomaterialbased sensors. *Nanomedicine (Lond)* 2013; 8(1): 43-56. http://dx.doi.org/10.2217/nnm.12.105 PMID: 23067372

127. Liu JJ, Wang CY, Wang JG, Ruan HJ, Fan CY. Peripheral nerve regeneration using composite poly(lactic acid-caprolactone)/nerve growth factor conduits prepared by coaxial electrospinning. *J Biomed Mater Res A* 2011; 96(1): 13-20. http://dx.doi.org/10.1002/jbm.a.32946 PMID: 20949481

128. Ali SS, Hardt JI, Quick KL, *et al.* A biologically effective fullerene (C60) derivative with superoxide dismutase mimetic properties. *Free Radic Biol Med* 2004; 37(8): 1191-202. http://dx.doi.org/10.1016/j.freeradbiomed.2004.07.002 PMID: 15451059

129. Das M, Patil S, Bhargava N, *et al.* Auto-catalytic ceria nanoparticles offer neuroprotection to adult rat spinal cord neurons. *Biomaterials* 2007; 28(10): 1918-25. http://dx.doi.org/10.1016/j.biomaterials.2006.11.036 PMID: 17222903

130. Pandey S, Gedda G, Thakur M, *et al.* Theranostic carbon dots 'clathrate-like' nanostructures for targeted photo-chemotherapy and bioimaging of cancer. *J Ind Eng Chem* 2017; 56: 62-73. http://dx.doi.org/10.1016/j.jiec.2017.06.008

131. Pandey S, Mewada A, Thakur M, Tank A, Sharon M. Cysteamine hydrochloride protected carbon dots as a vehicle for the efficient release release of the anti-schizophrenic drug haloperidol. *RSC Advances* 2013; 3(48): 26290.

http://dx.doi.org/10.1039/c3ra42139b

132. Wang X, Li X, Mao Y, Wang D, Zhao Q, Wang S. Multi-stimuli responsive nanosystem modified by tumor-targeted carbon dots for chemophototherapy synergistic therapy. *J Colloid Interface Sci* 2019; 552: 639-50. http://dx.doi.org/10.1016/j.jcis.2019.05.085 PMID: 31173992

133. Zheng M, Liu S, Li J, *et al.* Integrating oxaliplatin with highly luminescent carbon dots: an unprecedented theranostic agent for personalized medicine. *Adv Mater* 2014; 26(21): 3554-60. http://dx.doi.org/10.1002/adma.201306192 PMID: 24634004

134. Lai C, Hsiao Y, Peng Y, Chou P. Facile synthesis of highly emissive carbon dots from pyrolysis of glycerol; gram scale production of carbon dots/mSiO2 for cell imaging and drug release. *J Mater Chem* 2012; 22(29): 14403. http://dx.doi.org/10.1039/c2jm32206d

135. Wang K, Gao Z, Gao G, *et al.* Systematic safety evaluation on photoluminescent carbon dots. *Nanoscale Res Lett* 2013; 8(1): 122. http://dx.doi.org/10.1186/1556-276X-8-122 PMID: 23497260

136. Chiu SH, Gedda G, Girma WM, *et al.* Rapid fabrication of carbon quantum dots as multifunctional nanovehicles for dual-modal targeted imaging and chemotherapy. *Acta Biomater* 2016; 46: 151-64. http://dx.doi.org/10.1016/j.actbio.2016.09.027 PMID: 27662808

137. Liu C, Zhang P, Zhai X, *et al.* Nano-carrier for gene delivery and bioimaging based on carbon dots with PEI-passivation enhanced fluorescence. *Biomaterials* 2012; 33(13): 3604-13. http://dx.doi.org/10.1016/j.biomaterials.2012.01.052 PMID: 22341214

138. Kim J, Park J, Kim H, Singha K, Kim WJ. Transfection and intracellular trafficking properties of carbon dot-gold nanoparticle molecular assembly conjugated with PEI-pDNA. *Biomaterials* 2013;34(29): 7168-80. http://dx.doi.org/10.1016/j.biomaterials.2013.05.072 PMID: 23790437

139. Zhang M, Zhao X, Fang Z, *et al.* Fabrication of HA/PEIfunctionalized carbon dots for tumor targeting, intracellular imaging and gene delivery. *RSC Advances* 2017; 7(6): 3369-75. http://dx.doi.org/10.1039/C6RA26048A

140. Han J, Na K. Transfection of the TRAIL gene into human mesenchymal stem cells using biocompatible polyethyleneimine carbon dots for cancer gene therapy. *J Ind Eng Chem* 2019. http://dx.doi.org/10.1016/j.jiec.2019.02.015

141. Thakur M, Pandey S, Mewada A, *et al.* Antibiotic Conjugated Fluorescent Carbon Dots as a Theranostic Agent for Controlled Drug Release. Bioimaging, and Enhanced Antimicrobial Activity 2019.

142. Ardekani SM, Dehghani A, Ye P, Nguyen KA, Gomes VG. Conjugated carbon quantum dots: Potent nano-antibiotic for intracellular pathogens. *J Colloid Interface Sci* 2019; 552: 378-87. http://dx.doi.org/10.1016/j.jcis.2019.05.067 PMID: 31136856

143. Dong X, Moyer MM, Yang F, Sun YP, Yang L. Carbon Dots' Antiviral Functions Against Noroviruses. *Sci Rep* 2017; 7(1): 519. http://dx.doi.org/10.1038/s41598-017-00675-x PMID: 28364126

144. Abu Rabe DI, Al Awak MM, Yang F, *et al.* The dominant role of surface functionalization in carbon dots' photo-activated antibacterial activity. *Int J Nanomedicine* 2019; 14: 2655-65. http://dx.doi.org/10.2147/IJN.S200493 PMID: 31118606

CHAPTER 3: CRITICAL EVALUATION OF THE PHYSICOCHEMICAL AND PHYSICOMECHANICAL PROPERTIES OF A NOVEL LOADED AND UNLOADED CARBON DOT SYSTEM

3.1. INTRODUCTION

Carbon dots have emerged as a fascinating new carbonaceous nanomaterial which can be applied in various fields of drug delivery [1]. These nanomaterials pose an alternative to the semi-conductor quantum dot which possesses limitations such as high toxicity [2]. Carbon dots however have been classified as a new class of the smallest, biocompatible nanomaterial [1] and have been shown to have a higher drug-loaded capacity as opposed to quantum dots which are larger [1]. One of the most prominent properties of this nanomaterial is the allowance for targeted drug delivery [3]. In addition to the site specificity of carbon dots, they are also able to be synthesized from precursors which enhance the penetration of the target organ in question [1] or can even have the surface passivated with target specific ligands or precursors in order to facilitate the target specific delivery of drugs to specific sites [3,4]. This ultimately increases bioavailability of the drug as well as decreases systemic side effects suffered by patients [3,4]. This is all due to the easy surface passivation of carbon dots [3,4].

Carbon dots have thus been selected as the drug delivery vehicle for dopamine to the brain via the intranasal route for the treatment of Parkinson's' Disease (PD). The gold standard at the moment is Levodopa. The challenge presented here is that it is an oral formulation and dopamine is readily metabolized in the gastrointestinal tract (GIT) [5]. This results in low concentrations of dopamine actually reaching the brain. This concentration is lowered further by the strict protective mechanisms of the Blood-Brain Barrier (BBB) [1]. This results in higher dosages of drug required in an attempt to circumvent these obstacles [1]. As this project endeavours to present a solution to overcome the obstacles mentioned above, the physicochemical and morphological properties and characteristics are detailed below. The physicochemical characteristics of the carbon dot system was analysed by Fourier Transform Infrared Spectroscopy (FTIR), Differential Scanning Calorimetry (DSC), X-ray Diffraction (XRD), Zeta

potential and Rheology. The morphological properties of the system were analysed by Zeta size and TEM. *In vitro* drug entrapment and drug release studies was also carried out and is explicated below. Cytotoxicity studies were conducted in order to determine the toxicity of the system and is further described below.

3.2. Methods and materials

3.2.1. Materials

Chitosan (CHT) (medium molecular weight), Sodium Alginate, Dopamine Hydrochloride, Tween 80, Phosphate buffered saline tablets (pH 7.4), Glacial acetic acid, Cellulose dialysis tubing (MWCO= 14KDa) were purchased from Sigma-Aldrich (St. Louis, MO, USA). Sodium Hydroxide pellets were purchased from Merck (Pty) Ltd (Estate South, Modderfontein, Gauteng, South Africa,). Sodium citrate was purchased from Associated Chemical Enterprises (Theta, Johannesburg south, South Africa), Urea was purchased from Rochelle Chemicals (Electron, Johannesburg, South Africa). PC12 cell line was purchased from Cellonex (Separations, South Africa). The MTT assay and Ham's F12 medium was purchased from Roche & Gibco Thermoscientific (East Rand, Gauteng, South Africa) and MilliQ deionized water.

3.2.2. Synthesis of carbon dots

The synthesis method was modified from Hou *et al*., [22]. Sodium citrate (486mg) and urea (1330mg) were weighed out and transferred into a 100mL glass beaker. Tween 80 (0.5mL) and MilliQ (10mL) deionised water was then added to the beaker. The mouth of the beaker was secured with aluminium foil. The beaker was then placed on a magnetic stirrer and then left under constant magnetic stirring at 150rpm, at 160°C. The reaction proceeded for half an hour. The resultant solution was then dialysed against MilliQ deionised water for 6 hours to remove residual sodium citrate, urea and surfactant. The carbon dots were then lyophilized utilizing a Freezone 12 freeze drier (Labconco, Kansas City, USA). The carbon dots were left to lyopholize for 12 hours at -80°C. Caution was exercised to not over-lyopholize as this would extract the molecular water from the carbon dots and destroy the sample. The product was then stored at room temperature for further use.

3.2.3 Surface passivation of carbon dots by attachment of dopamine to the carbon dot surface

A 1mg/mL stock solution of dopamine was prepared by dissolving 100mg dopamine hydrochloride solution in 100mL MilliQ deionised water. Attachment of dopamine was performed simultaneously during the carbon dot synthesis. 1mL of the dopamine stock solution was added to the 100mL beaker before it was placed onto the magnetic stirrer.

3.2.4. Nanogel synthesis

The Chitosan-Alginate nanogel was synthesised according to the method by Park *et al*. [6] with modifications. A 3% w/v solution of Chitosan was prepared by dissolving 300mg Chitosan in 100mL of 0.2M glacial acetic acid and stirring overnight to ensure complete homogeneity. Once the solution was completely dissolved, 0.1M NaOH was added slowly to the solution to neutralize the pH. The neutralization of the pH allows a gel-like precipitate to form [6]. The precipitate was then washed twice with MilliQ deionised water. A 3% w/v solution of sodium alginate was prepared by dissolving 300mg sodium alginate in 100mL deionised water. The solution was left to stir until completely dissolved. The chitosan and sodium alginate solution were mixed in a 1:1 ratio and then treated at 50W for 60s using a sonicator (Sonics vibra cell, Newtown, 7CT, USA) [6]. The nanogel was then stored between 4-8°C for further use.

3.2.5. Box Benkhen design study for optimization of the carbon dot formulation

A Box-Benkhen 2 factor experimental design was generated to determine an optimized carbon dot formulation. Minitab® V15 statistical software (Minitab® Inc., PA, USA) was utilized. The employed variables were the duration of reaction, the volume of the surfactant and the concentration of the reagents. These variables were evaluated for their effect on zeta size and zeta potential. The independent and dependant variables are listed in Table 2. The design template generated 15 formulations as depicted in Table 3.

Table 2: The independent and dependant variables generated by the experimental design.

Response	Goal	Lower	Target	Upper	Weight	Importance
Zeta potential (mV)	Minimum		-2	-1	1	1
Size (nm)	Target	10	15	50	1	1

Table 3: Formulations generated by the experimental design.

Formulation	Reaction time (min)	Surfactant	Total Polymer (mg) in 1:3 ratio	Mass (mg) in 1:3 ratio	
				Sodium Citrate	Urea
1	16	12.5%	200	50	150
2	38	12.5%	1100	275	825
3	38	50%	2000	500	1500
4	60	50%	1100	275	825
5	38	50%	200	50	150
6	60	12.5%	2000	500	1500
7	38	20%	2000	500	1500
8	16	50%	1100	275	825
9	60	20%	1100	275	825
10	38	12.5%	1100	275	825
11	60	12.5%	200	50	150
12	38	20%	200	50	150
13	16	12.5%	2000	500	1500
14	38	12.5%	1100	275	825
15	16	20%	1100	275	825

Following extensive preformulation studies, these variables were found to have a direct impact on the particle size and Polydispersity index (PDI) of the carbon dots. As the reaction time increased, this resulted in an increase in size and PDI. A decrease in surfactant concentration lead to an increase in particle size and PDI. It was determined that as the concentration of sodium citrate and urea increased, the particle

size and PDI increased as well. As the focus was to synthesize a formulation with the smallest possible size and PDI, these variables played a pertinent role in constructing the optimized formulation with these desirable properties.

3.2.6. Fourier Transform Infrared Spectroscopy (FTIR)

Every molecule has a vibrational spectrum which is considered to be a unique physical property of that molecule and is characteristic of that specific molecule [7]. Hence, Fourier Transform Infrared Spectroscopy (FTIR) was utilized to evaluate the vibrational changes in chemical structures of compounds utilized in this project. The FTIR spectra of the pristine polymers, reagents, pure drug, loaded- and unloaded carbon dot systems was detected using a PerkinElmer Spectrum 2000 ATR-FTIR Spectrometer. The instrument employed a single-reflection diamond MIRTGS detector (PerkinElmer Spectrum 100, Wales, UK). Each sample was carefully placed on the single bounce diamond crystal and the analysis was carried out by the universal ATR polarization accessory. The parameters set are outlined in table 4 below.

Table 4: Parameters set for FTIR analysis.

Wave range	4000-650 cm^{-1}
Resolution	4 cm^{-1}
Number of scans	20
Constant pressure	110 psi

3.2.7. Thermal properties of the pristine reagents, pure drug, loaded and unloaded carbon dot systems using Differential Scanning Calorimetry (DSC) analysis

This is a thermo-analytical technique which functions to determine the difference in the amount of heat required to elicit an increase in temperature of a sample and reference. This is measured as a function of temperature [8]. The thermal properties of the pristine reagents, pure drug, loaded- and unloaded carbon dot systems were

determined utilizing a Mettler Toledo DSC-1 STAR^e system (Mettler Toledo, DSC1, STARe System, Swchwerzenback, Switzerland). Samples ranging between 3-10mg were weighed into a 40µL aluminium crucible pan and sealed. A small hole was pierced into the lid of the pan to allow for dissipation of pressure. Samples were analysed from 30-300°C, with a temperature ramp of 10°C/min. All analysis was carried out under inert atmospheric conditions with a flow rate of 50ml/min of N_2 gas.

3.2.8. X-Ray Diffraction (XRD) analysis of the carbon dot

This is a technique that uses the X-ray scattering phenomenon to explicate the crystal structure of materials which are crystalline or semicrystalline [9]. It employs scattering of x-rays by periodic array of atoms which gives rise to definite diffraction patterns and this in turn confers a qualitative image of atomic arrangements within the crystal lattice [4]. The carbon dot system was analysed utilizing a Rigaku MiniFlex600 Benchtop X-ray Diffractometer (Rigaku Corporation, Tokyo, Japan) with CuKα radiation at 15 mA and 40 kV. The sample was fixed to the sample holder using double-sided tape. The parameters employed were: 2θ range set: 2-90° and a scan rate set: 10°/min. Samples were run on the Rigaku MiniFlex Guidance version 1.2.0 software and evaluation of the data was carried out on Rigaku PDXL Basis software.

3.2.9. Rheological analysis of the nanogel

Rheology refers to the science of studying flow and deformation of materials [10]. It is concerned with the relationship between shear strains, sheer stress and time [11]. It is also used to determine the viscosity of a material. Viscosity is the resistance of a liquid to flow [10]. The viscoelastic behaviour of the nanogel was evaluated by using 0.2mL of the synthesized chitosan-alginate (CHT-ALG) nanogel which was incubated for half an hour. The instrument employed was a Modular Advanced Rheometer (ThermoHaake MARS Modular Advanced Rheometer, Thermo Electron, Karlsruhe, Germany). This instrument determined the G’ (dynamic storage modulus), G’’ (loss modulus) and viscosity of the nanogel. The parameters set are outlined in Table 5.

Table 5: Parameters set for Rheological analysis of CHT-ALG nanogel.

Damping	30.00
Cone and plate gap	0.0051m
Temperature	37°C
Driver version	0.29
M-factor	57.010 rad/s
A-factor	89051.00 Pa
Inertia	1.721 X 10^{-6} kg m^2

3.2.10. Particle size and zeta potential analysis of carbon dot formulations

Determination of the zeta potential is a vital step as it is one of the key properties of a particle that affects the stability of the particle as well as its cell adhesion [12]. The zeta potential values can be positive or negative and affect the stability of the formulation. This is due to electrostatic repulsion between particles of like charges which leads to particle segregation [12]. All Box-Benkhen formulations (0.5mL for zeta size and 1mL for zeta potential) were placed into a cuvette and analysed using a ZetaSizer Nano ZS instrument (Malvern Instruments Ltd. UK).

3.2.11. Morphological characteristics of the system using Transmission electron microscopy (TEM)

The use of Transmission electron microscopy (TEM) is considered to be the most popular technique for analysing nanoparticles due to the TEM providing chemical information and images at a spatial resolution equal to that of atomic dimensions [13]. The structural morphology of the carbon dot system was evaluated utilizing TEM (Jeol 1200 EX, Japan). The lyophilized carbon dot sample was redispersed in distilled water and allowed to completely dissolve. A drop was then placed onto the 200-mesh thick formvar copper grid (TABB Laboratories Equipment, Berks, UK), by use of a pipette. The grid was left on filter paper for a while, at room temperature, to allow the distilled water to completely evaporate before analysis.

3.2.12. Drug loading and drug release analysis

Drug loading of the carbon dot system was undertaken by adding 1mL of the 1mg/mL stock solution of dopamine to the reagents while synthesizing the carbon dots. This approach was selected to ensure maximum drug entrapment. The loaded carbon dot system was then dialyzed against MilliQ deionized water for 6 hours to remove residual drug. The dialysis tubing was then placed in fresh MilliQ deionized water and left to dialyze for a set period. The drug entrapment was calculated as follows:

$$\%Entrapment\ Efficieny = \frac{\text{Theoretical amount of drug loaded} - \text{Free drug}}{Theoretical\ amount\ of\ drug\ loaded}\ X\ 100$$

(Equation 1)

The concentration of the free drug was evaluated utilizing a UV spectrophotometer, at wavelength 280 nm (IMPLEN NanophotometerTM, Implen GmbH, München Germany).

In vitro drug release studies were carried out by placing the loaded carbon dot solution in dialysis tubing and then in a beaker containing MilliQ deionized water. The drug release was carried out in Phosphate Buffer Saline (PBS) buffer at two pH values i.e. 5.5 for nasal pH and 7.4 for blood pH. The beakers were placed in an orbital shaker incubator (LM-530-2, MRC Laboratory Instruments Ltd, Hahistadrut, Holon, Israel) at 37 ± 0.5°C, with 50 rpm, for incubation. At every time point, 2mL of solution was withdrawn from each beaker and replaced with 2mL of fresh PBS buffer to maintain sink physiological conditions throughout the entire study. The data was analysed using a UV spectrophotometer, at wavelength 280 nm (IMPLEN NanophotometerTM, Implen GmbH, München Germany).

3.2.13. Cytotoxicity studies

In vitro cell studies were undertaken to determine the cytotoxicity of the carbon dot systems. A rat adrenal pheochromocytoma PC12 cell line was used for the analysis.

The cell line was cultured in Ham's F12 medium supplemented with 15% Donor Equine Serum (DES), 2.5% Foetal Bovine Serum (FBS) and 1% Penicillin/Streptomycin. The cell line was cultured in a humidified 5% CO_2 atmosphere at 37°C.

To determine cytotoxicity, a 3-(4, 5-dimethylthiazolyl-2)-2, 5-diphenyltetrazolium bromide (MTT) assay was performed [9]. This assay is a sensitive and reliable indicator of cellular metabolic activity. This assay functions on the reduction of MTT, a yellow tetrazolium dye which was water-soluble [14]. The reduction of the MTT happens primarily by the mitochondrial dehydrogenases in the cells. The tetrazolium dye is transformed into purple formazan crystals [14]. The formazan crystals are then dissolved in Dimethyl Sulfoxide (DMSO) and then analyzed spectrophotometrically. The spectra of treated and untreated cells give an estimate of cytotoxicity [14].

PC12 cells were seeded into the 96-well plate at a density of 5 x 10^4 cells/mL. Ninety (90) µL of PC12 cell suspension was added into each well of a 96-well plate. This was then incubated for 24 hours. The cells were then treated with the pure drug, loaded carbon dots and unloaded carbon dots. This was incubated for 48 and 72 hours. After 48 hours, 10µL of MTT solution was added and the well plate was then incubated for 4 hours. After 4 hours 100µL of solubilizing agent, i.e. Dimethyl Sulfoxide (DMSO), was added. The well plate was then read the next day using a multiplatereader (BioTek, USA). The Relative cell viability was then calculate using the formula below:

$$Cell\ viability\ \% = \frac{Asample}{\text{Apositive control}}\ X\ 100$$

(Equation 2)

Here, A_{sample} is representative of the absorbance of the treated cells and $A_{positive\ control,}$ i.e. 5-fluorouracil, is representative of the positive control, in the absence of treatment.

3.3. RESULTS AND DISCUSSION

3.3.1. Evaluation of the unloaded- and dopamine-loaded carbon dot systems.

3.3.1.1. Evaluation of Box-Benkhen optimization

Each formulation, from Table 2, was synthesized and the data and responses obtained after analysis was then run by the mathematical design in order to attain the optimized

formulation. This was carried out to determine the greatest possible correlation for the optimized formulation [15]. The formulations were then analysed to evaluate the zeta size and potential of the formulations and to optimize the carbon dots for the smallest size, PDI and best zeta potential. The results are illustrated in Table 6 below.

Table 6: Zeta size and zeta potential results of the Box-Benkhen design formulations.

Formulation	Particle size Average	Zeta potential Average
1	12.69	-0.399
2	13.47	0.313
3	22.28	1.865
4	16.67	-0.682
5	10.40	-2.61
6	21.70	1.757
7	27.41	0.014
8	11.54	-0.692
9	15.87	0.385
10	13.43	0.373
11	39.24	-0.173
12	13.22	-0.675
13	14.27	0.786
14	88.67	-0.384
15	17.75	0.356

The results were subsequently analyzed and the optimized formulation and predicted responses were generated, as illustrated by Tables 7-9 respectively, below.

Table 7: Optimized formulation generated by Box-Benkhen design.

Solution	Time (min)	Surfactant (mL)	Total Polymer (mg)	Zeta potential (mV) Fit	Size (nm) Fit	Composite Desirability
1	29.9	0.5	486	-2	15	1

Table 8: Multipurpose prediction table illustrating the optimal variables generated by the Box-Behnken design.

Variable	Setting
Time (min)	29.9372
Surfactant (mL)	0.5000
Total Polymer (mg)	4861330

The design of experiments generated Solution 1 as the optimized (unloaded) formulation. As shown in Tables 7 and 8, the optimal reaction time was 30 minutes, the optimal surfactant volume was 0.5mL and the optimal mass of sodium citrate and urea was 486mg and 1330mg, respectively. The optimal responses are also depicted in Table 7. The design set a minimum zeta potential value at -2mV and a particle size of 15nm that was achievable within the formulation parameters for the optimal formulation. Reaction time was a factor that affected the size of the carbon dots in that as the reaction time increased, the size would increase [22]. The reaction time for the optimized formulation thus needed to allow for a small particle size to form, as further described in this chapter. The concentration of surfactant also affected the particle size in that as it increased, the particle size too would increase. The amount of reagent in the solution impacted the particle size by virtue of the fact that as the masses of sodium citrate and urea increase, the particle size increased accordingly. The design focused on identifying a formulation that would present the smallest size and most stable zeta potential. This is evident in Tables 7-9 above. The optimized formulation

presented carbon dots with an actual particle size of 10.34 nm therefore conforming to the very definition of a carbon dot [1].

3.3.1.2. *Particle size and zeta potential analysis of the unloaded- and dopamine-loaded carbon dot optimized formulations.*

Determination of the particle size of these formulations was imperative as the particles had to fall within a certain size range to be classified as carbon dots, as well as for effectively cross the BBB to enable increased and efficient neuroavailability of dopamine in the brain. Carbon dots generally have a size of less than or equal to 10nm [1, 16]. The zeta size analyses are illustrated in Figures 10 and 11 below.

		Size (d.nm):	% Intensity:	St Dev (d.nm):
Z-Average (d.nm): 10.82	Peak 1:	9.850	85.3	2.789
PdI: 0.308	Peak 2:	1046	14.7	428.2
Intercept: 0.942	Peak 3:	0.000	0.0	0.000
Result quality : Good				

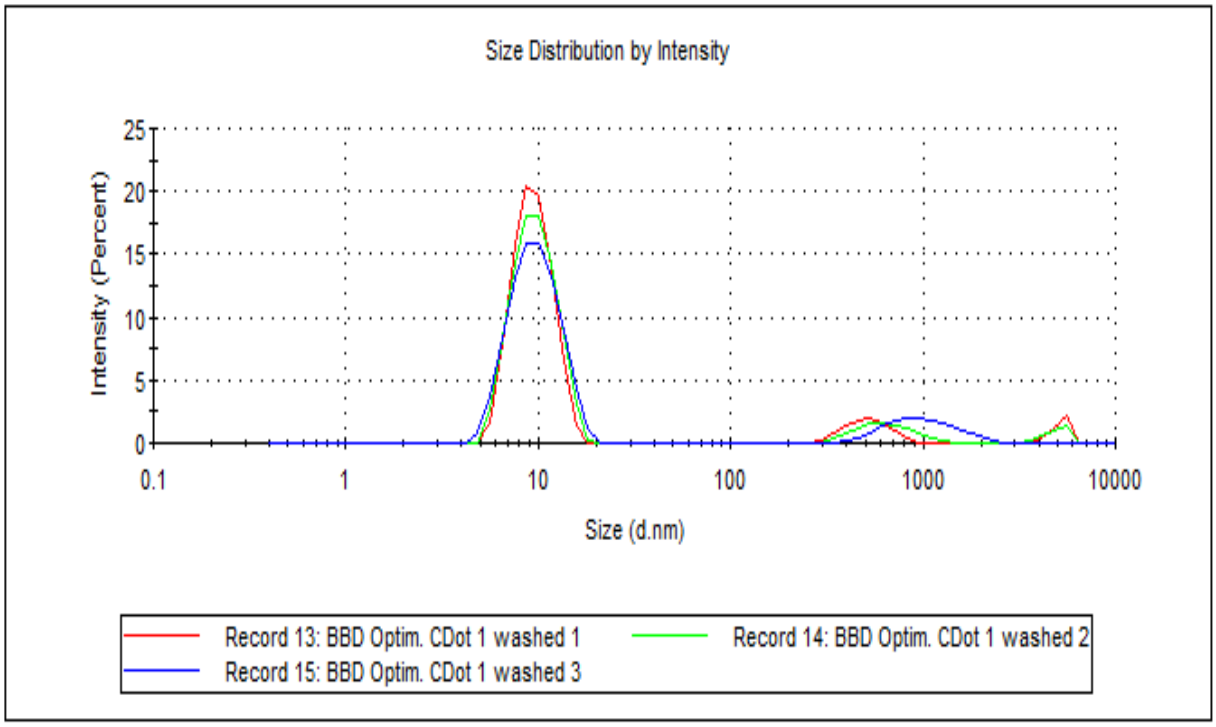


Figure 10: Zeta size analysis of the unloaded carbon dot optimized formulation

		Size (d.nm):	% Intensity:	St Dev (d.nm):
Z-Average (d.nm): 10.34	Peak 1:	10.01	96.5	2.679
PdI: 0.259	Peak 2:	5085	3.5	560.8
Intercept: 0.924	Peak 3:	0.000	0.0	0.000
Result quality : Good				

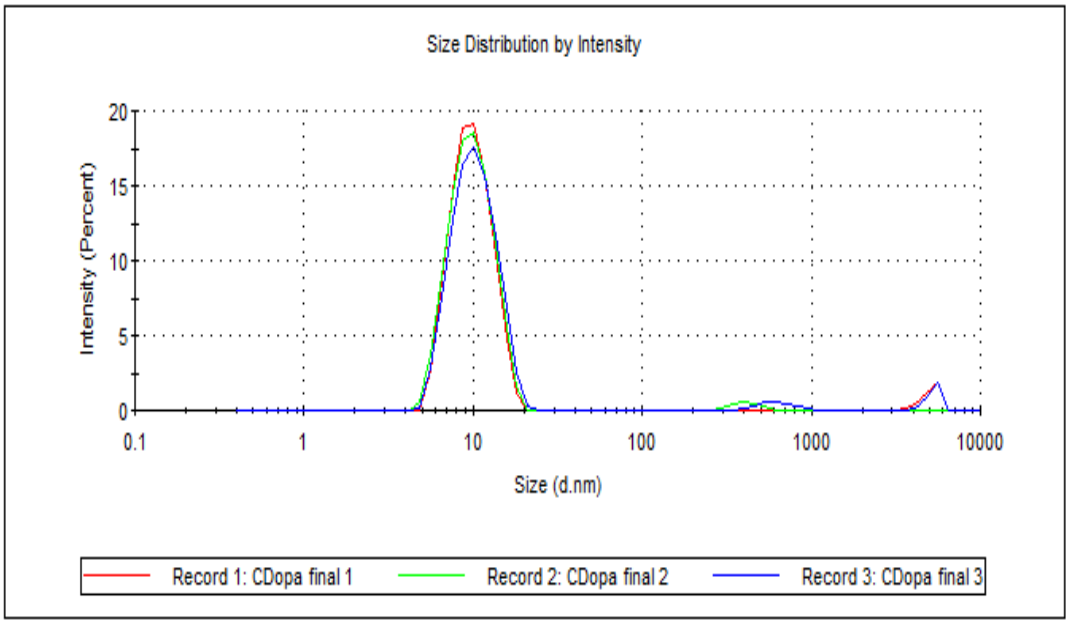


Figure 11: Zeta size analysis of the dopamine-loaded carbon dot optimized formulation.

The unloaded and dopamine-loaded carbon dot formulations were analysed for particle size was found to be 10.82nm and 10.34nm, respectively. The overall size of the carbon dot adjusted very slightly before and after the addition of dopamine.

The polydispersity index (PDI) of a sample is indicative of the heterogeneity of said sample on the basis of size and uniformity of particles [17,18]. This polydispersity can occur due to the aggregation or agglomeration of a sample during isolation or analysis, as well as due to the size of a sample [17]. The PDI of the unloaded and dopamine-loaded carbon dot samples was 0.308 and 0.259, respectively. This clarifies that the samples had a fairly narrow size distribution and were well-dispersed.

A formulation which has a zeta potential value falling in a range of $-30 \leq x \geq +30$ (mV) is indicative of having sufficient repulsive forces between the particles to enable the formulation to have optimal stability [19]. The zeta potential of the unloaded and dopamine-loaded carbon dot formulations was analysed and are illustrated in Figures 11 and 12. The zeta potential value of the unloaded carbon dot formulation was -

9.62mV and increased to -4.63mV for the dopamine-loaded carbon dot sample. The increase is due to the $(NH_2)^+$ Amine group provided by dopamine and therefore proves the surface passivation of dopamine onto the carbon dot surface. These zeta potential values were indicative of the tendency of carbon dots to layer. The solutions were well-dispersed as proven by the PDI values, but carbon dots have an inherent characteristic of layering which gave rise to the zeta potential values [1].

		Mean (mV)	Area (%)	St Dev (mV)
Zeta Potential (mV): -9.62	Peak 1:	-6.62	71.5	4.31
Zeta Deviation (mV): 6.88	Peak 2:	-18.5	28.5	3.33
Conductivity (mS/cm): 2.50	Peak 3:	0.00	0.0	0.00

Result quality : Good

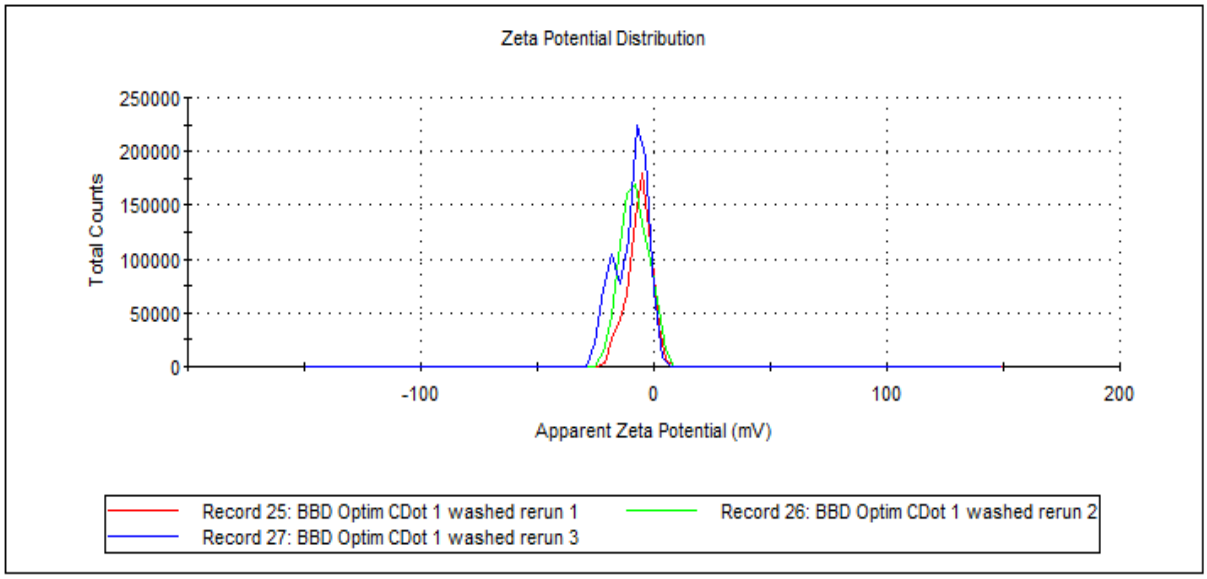


Figure 12: Graph depicting the zeta potential analysis of the unloaded carbon dot optimized formulation.

		Mean (mV)	Area (%)	St Dev (mV)
Zeta Potential (mV): -4.63	Peak 1:	-9.54	55.1	3.28
Zeta Deviation (mV): 6.88	Peak 2:	1.46	44.9	4.03
Conductivity (mS/cm): 1.68	Peak 3:	0.00	0.0	0.00

Result quality : Good

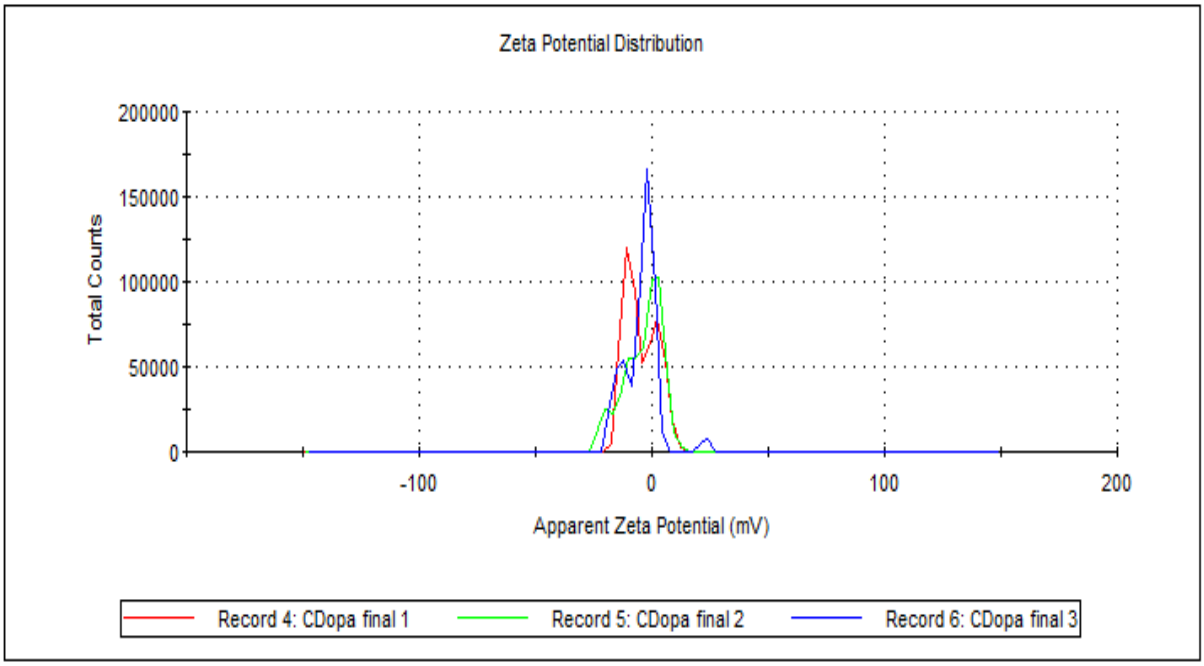


Figure 13: Graph illustrating the zeta potential analysis of the dopamine-loaded carbon dot optimized formulation.

The particle sizes of both the unloaded- and loaded carbon dot optimized formulations proved to fall within the range of identification as carbon dots. This was imperative so as to allow the easy and efficient traversal of the particles across the BBB. Carbon dots have a large surface area due to their small size and this favours the surface passivation of the carbon dots with dopamine in this research.

3.3.1.3. FTIR Spectroscopy

The FTIR spectra of the pristine reagents (urea and sodium citrate), pristine polymers (chitosan, sodium alginate), pure drug (dopamine), loaded- and unloaded carbon dot systems and the chitosan-alginate nanogel were detected and are depicted in Figures 14 A-H below. Figure 14A shows the FTIR spectrum of urea. The sharp peak at 3328.03cm^{-1} correlates to the N-H stretch of the amide functional group [20]. The

broad peak 2802.43cm^{-1} correlates to the C-H stretch of the carbonyl group [20]. Figure 14B depicts sodium citrate. The peak at 3445.43cm^{-1} correlates to an O-H stretch indicative of a hydroxyl functional group [21]. The peak at 1579.04cm^{-1} correlates to a C-O stretch relating to a carbonyl group [21]. Figure 14C illustrates the FTIR spectrum of the unloaded carbon dot system. The sharp peak at 3423.02 cm^{-1} correlates to an O-H stretch and the peak at 1676.06cm^{-1} correlates to a C=O group, both originating from sodium citrate [22]. The other sharp peaks at 3337.39cm^{-1} and 1586.44cm^{-1} correlates to the N-H stretch and C-O stretch respectively, which both originate from urea [22]. Figure 14D demonstrates the FTIR spectrum of dopamine. The peak at 3333.21cm^{-1} correlates to the ArO-H H-bonded phenol functional group [23]. The sharp peaks at 1600.11cm^{-1} and 1616.09cm^{-1} correlate to the NH_2 in plane bend of the amine groups on dopamine [23]. Figure 14E depicts the dopamine-loaded carbon dot. The broad peak at 3337.42cm^{-1} correlates to the ArO-H H-bonded phenolic functional group from dopamine [23]. The peak at 1634.61cm^{-1} correlates to the NH_2 in plane bend of the amine groups on dopamine [23]. This further proves the surface passivation of the carbon dot with dopamine. Figure 14F shows the FTIR spectrum of chitosan. The broad peak at 3358.27cm^{-1} correlates to the O-H stretch indicative of a hydroxyl group [24]. The peaks at 1588.11cm^{-1} and 1148.51cm^{-1} correlates to the NH_2 in plane bend and the C-N stretch of the amine group on chitosan [24]. Figure 14G depicts sodium alginate. The broad peak at 3239.83cm^{-1} correlates to the O-H stretch of the hydroxyl group on sodium alginate [24]. Figure 14H illustrates the nanogel. The broad peak at 3281.85cm^{-1} correlates to the O=H stretch of the hydroxyl group donated by sodium alginate [24]. The peak at 1633.51cm^{-1} correlates to the NH_2 in-plane bend of the amine group on chitosan [24]. This further proves the synthesis of the chitosan-alginate nanogel.

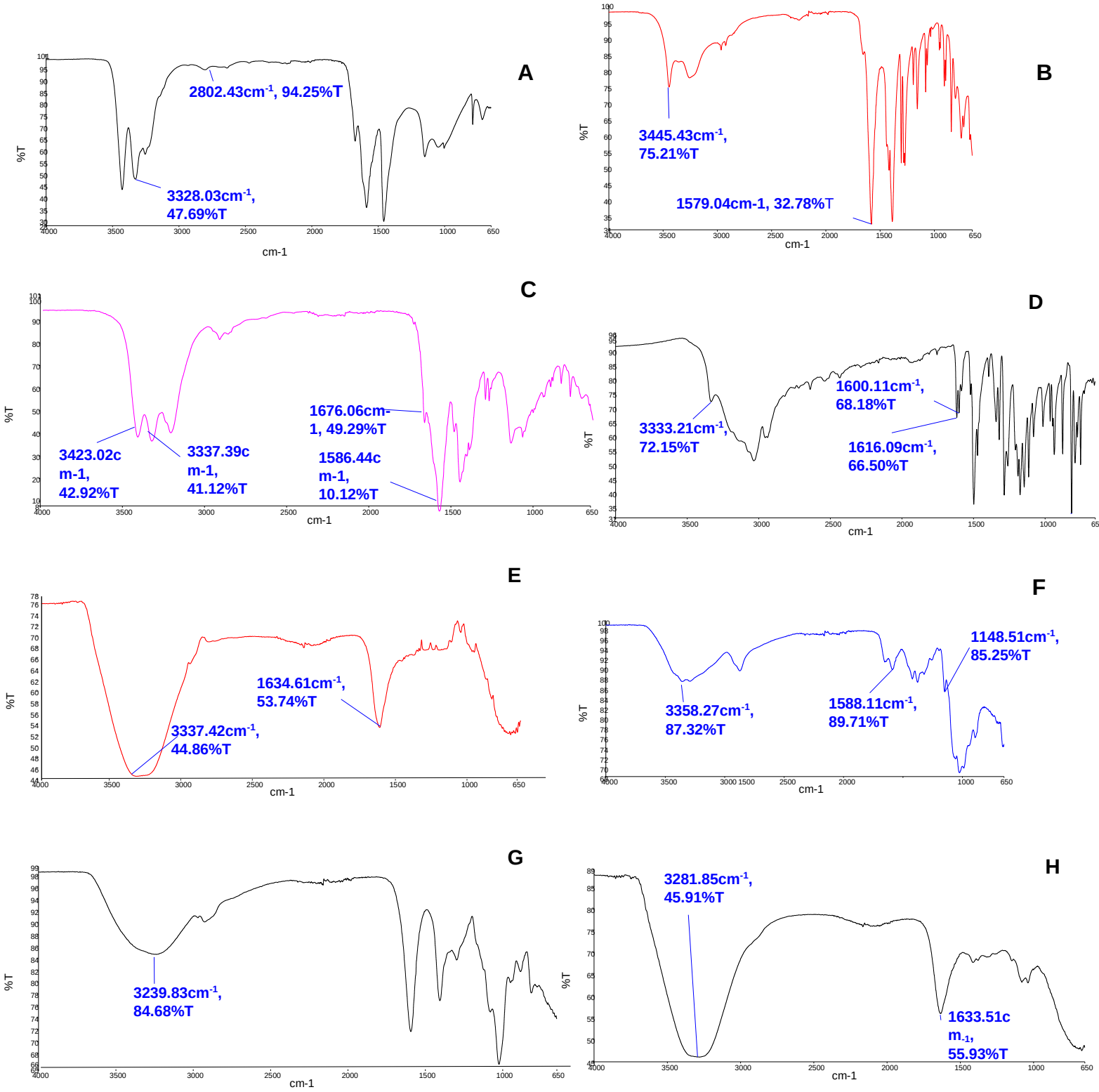


Figure 14 A-H: FTIR spectra of a) Urea, b) Sodium Citrate, c) unloaded carbon dot system, d) Dopamine, e) Dopamine-loaded carbon dot system, f) Chitosan, g) Sodium Alginate, h) Chitosan-Alginate Nanogel.

3.3.1.4. Thermal evaluation utilizing Differential Scanning Calorimetry (DSC) analysis

DSC thermograms were evaluated for the thermal properties of the pristine reagents (urea and sodium citrate), pure drug (dopamine), loaded- and unloaded carbon dot systems to determine the melting points of each of them. Urea (Figure 15A) had two endothermic peaks at 134.25°C and 237.46°C. Sodium Citrate (Figure 15B) illustrated one endothermic peak at 161.48°C. There was a shift in the thermogram for the carbon dot after synthesis with urea and sodium citrate. Figure 15C represents the thermogram for the unloaded carbon dot where there were two endothermic peaks at 67.93°C and 113.66°C. The shift in degradation temperatures further proves the synthesis of the carbon dots. Dopamine (Figure 15D) demonstrated one endothermic peak at 248.31°C. The dopamine-loaded carbon dot (Figure 15E) explicates two endothermic peaks at 120.65°C and 200.77°C. The shift in degradation temperature clarified in the thermograms of dopamine and the dopamine-loaded carbon dots further substantiates the successful surface passivation of dopamine on the carbon dot.

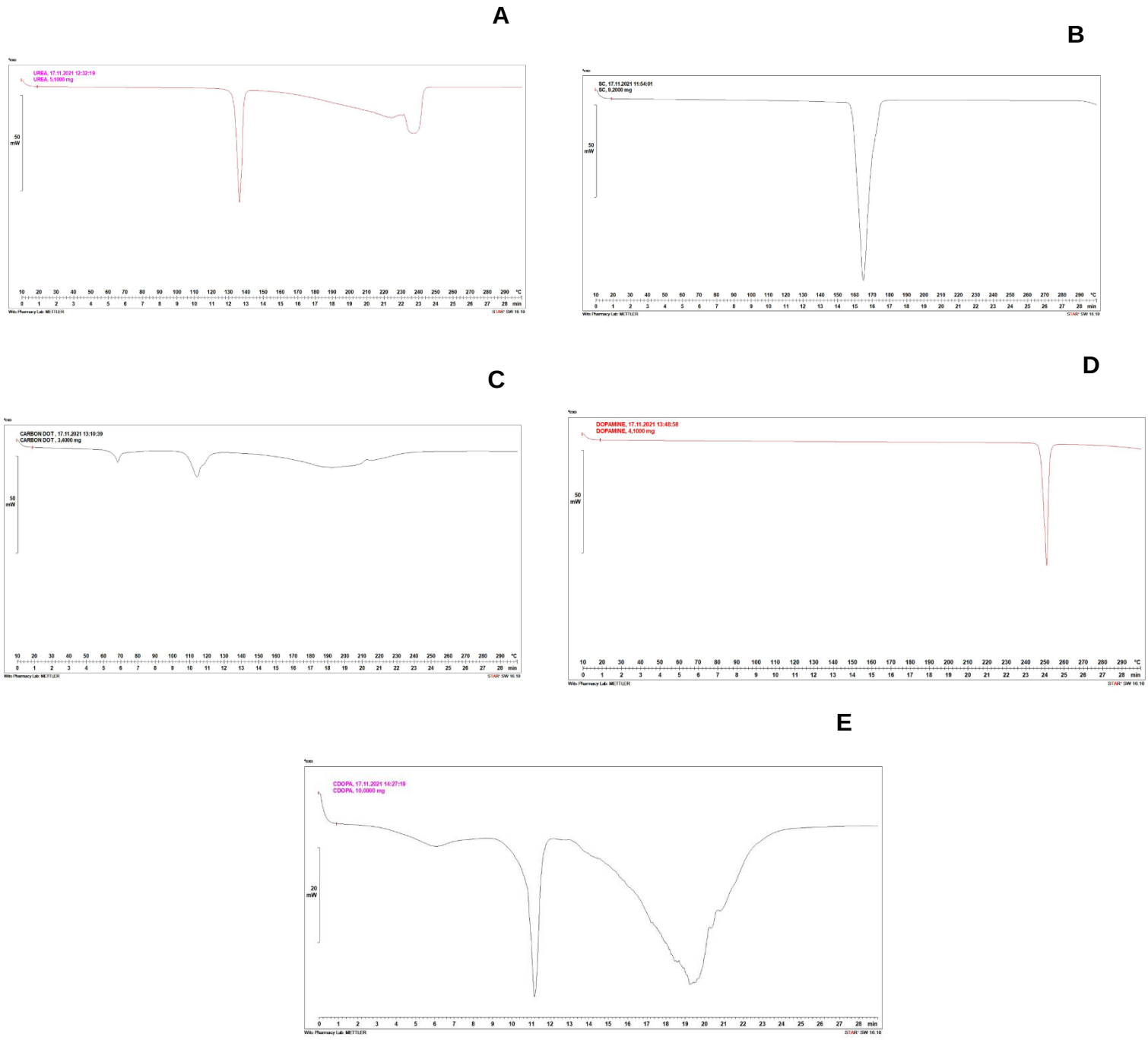


Figure 15A-E: Thermograms depicting a) Urea, b) Sodium citrate, c) Unloaded carbon dot system, d) Dopamine, e) Dopamine-loaded carbon dot system.

3.3.1.5. X-Ray Diffraction (XRD) analysis

This analytical technique is non-destructive and was employed to determine the degree of phases in the unloaded carbon dot system. According to Braggs Law, Equation 3 below, in a crystalline sample, a lattice vector is correlated to each ring diffraction. The angle between the beam axis and the ring is the scattering angle. The analysis of the unloaded sample thus generates a diffractogram which is representative of the diffraction intensity to the scattering angle. Narrower peaks are produced by samples of greater crystalline nature and following this, broader peaks are produced by samples that are of a lower crystalline nature.

$$n\,\gamma = 2dsin\theta$$

(Equation 3)

Where *n* is the integer, *γ* is the wavelength of the x-ray beam, *d* is the lattice planes distance and *θ* is Braggs angle.

With reference to the diffractogram of the unloaded carbon dot system illustrated in Figure 16 below, it is clearly evident that the unloaded carbon dot system is significantly crystalline in nature. Hence, the molecular order in the crystal lattice is enhanced.

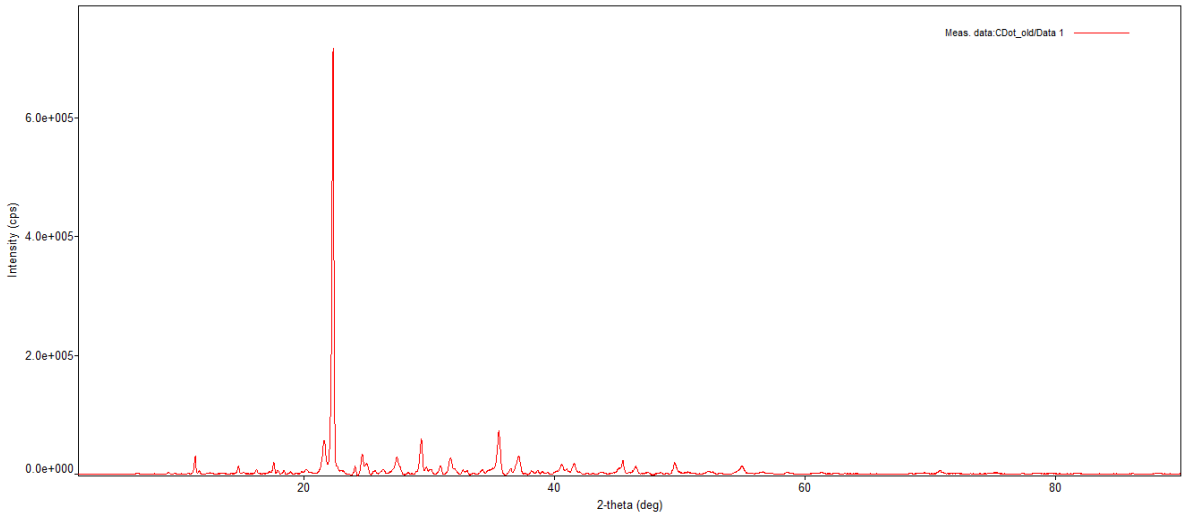
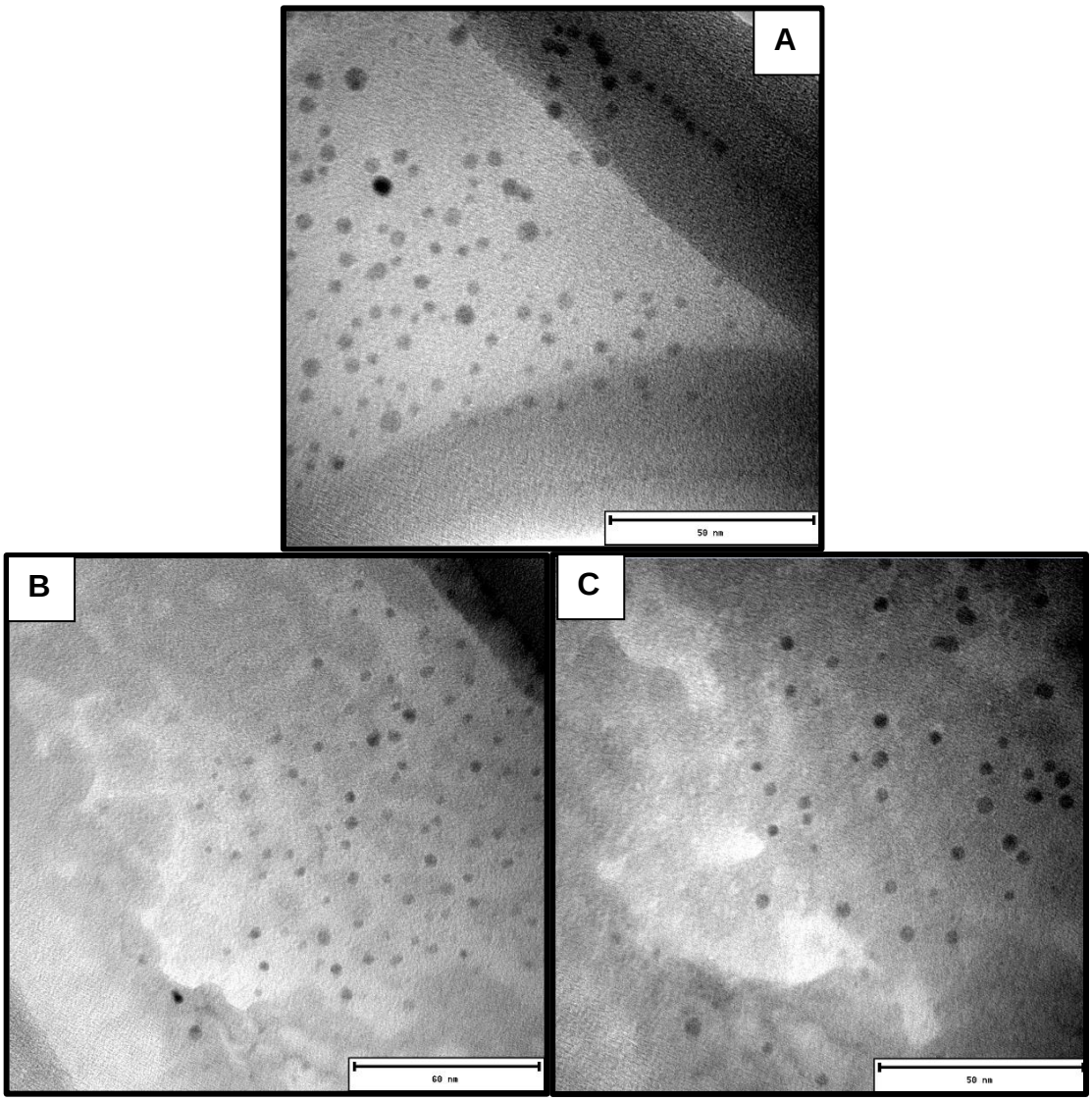


Figure 16: Diffractogram depicting the unloaded carbon dot system.

3.3.1.6. Morphological characteristics of the optimized loaded carbon dot system using Transmission electron microscopy (TEM)

The successful synthesis of the carbon dots was further substantiated by the TEM microscopy technique. Microscopy was able to readily detect several images of the carbon dots due to their photoluminescent properties. The carbon dots presented themselves as dark, circular dots. Each carbon dot had a distinctive boundary and they were circular in shape. The arrangement of the carbon dots showed spacing between the dots and there were no agglomerates or bunches of carbon dots. They were all positioned individually and not packed on top of one another. The small surface area of the carbon dots was present in the images, and this was instrumental in the impressive drug loading capacity of the carbon dots. Very little sample was utilized for TEM analysis and a myriad of carbon dots could be seen. Hereby proving the absolute efficiency in synthesis and cost-effectiveness. There were no residual substrates around or on the carbon dots. There were no extra layers on top of or below the carbon dots. The perfect arrangement and presentation of the carbon dots served as a confirmation that the synthesis process was not invasive and that the lyophilization process only preserved the carbo dots for further use but did not interfere with the overall structure and physical characteristics of the carbon dots. The structural template of the carbon dots was provided by urea and sodium citrate [22]. By utilization of the scale bar, the carbon dots were found to be ~10nm in size which further confirmed the zeta size analysis undertaken. The well-defined spherical carbon dots also confirmed that the synthesis process as well as lyophilization did not have a negative impact on formation of particles. Figures 17A-C below depict the TEM imaging of the carbon dots.



Figures 17A-C: TEM images of carbon dots.

3.3.1.7. Rheological evaluation of nanogel

The viscosity of the Chitosan-Alginate nanogel was evaluated at a temperature of 0-50°C, at a rate of 1°C/min and employing a shear rate of $100s^{-1}$. Figure 18 clearly depicts that the nanogel was viscous in nature and that the viscosity increased with an increase in temperature. This is the ideal requirements for this system because when the nanogel is applied into the patient's nasal cavity, the nanogel is required to be mucoadhesive so as to attach to the nasal mucosa and allow for optimal absorption of drug through the nose-to-brain barrier. The gel needs to be viscous in order to be retained in the nasal cavity and not run out of the nose. The nanogel has to however not become too viscous so as to cause discomfort to the patient, Figure 19 depicts the

gradual increase in viscosity, which indicates that the nanogel would not become uncomfortably viscous in the nasal cavity of the patient. This graph also substantiates the mucoadhesive properties of chitosan and sodium alginate [27,28]. Temperature ramp measurements were run at a heating rate of 1°C/min. The temperature range was 0-50°C. The stress and frequency employed was 1Pa and 1Hz, respectively. As demonstrated in figure 50, G' was higher than G''. G' and G'' increase gradual as the temperature increased, this was indicative of this nanogel being thermoresponsive because the gel was becoming more viscous as the temperature increased. The chitosan and sodium alginate reacted in response to an increase in temperature, therefore his nanogel was proven to be a thermoresponsive gel system. The gradual increase in G' and G'' was also indicative of the nanogel being a strong nanogel. This is ideal as the nanogel has to be durable in order to survive the cleansing mechanisms of the nasal cavity. This graph also clearly shows that the nanogel is stable due to G' being higher than G'' [30].

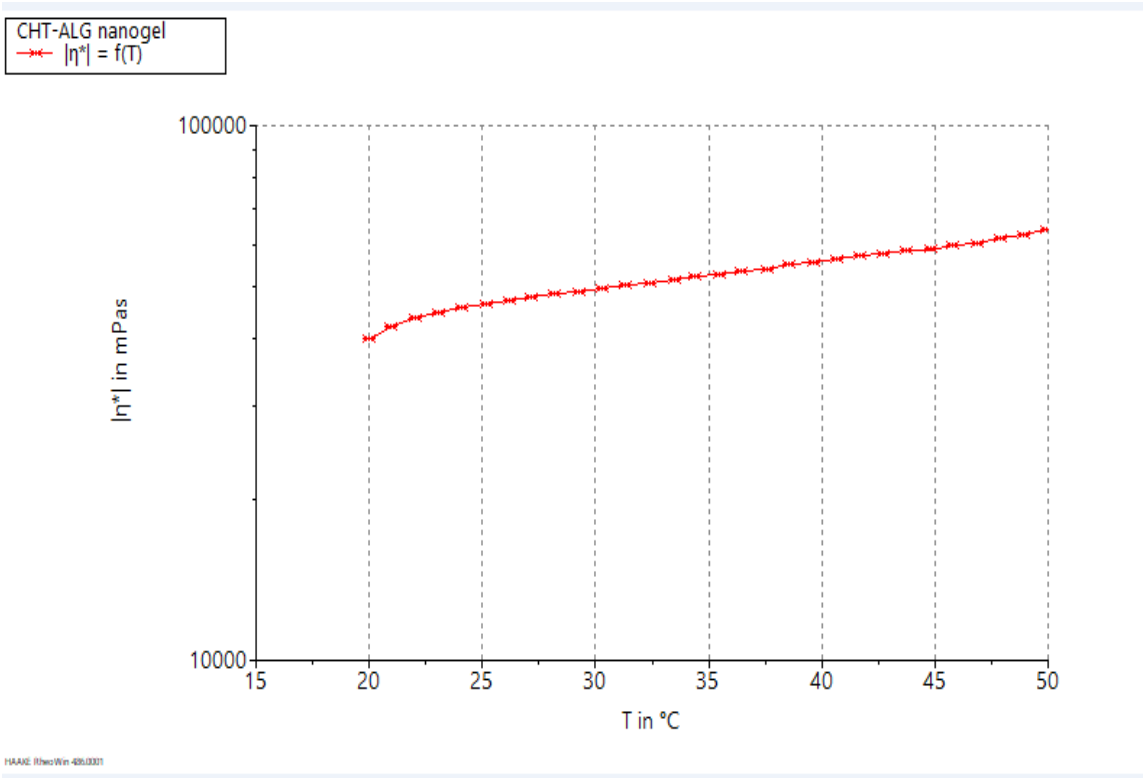


Figure 18: Graph depicting the viscosity of the nanogel.

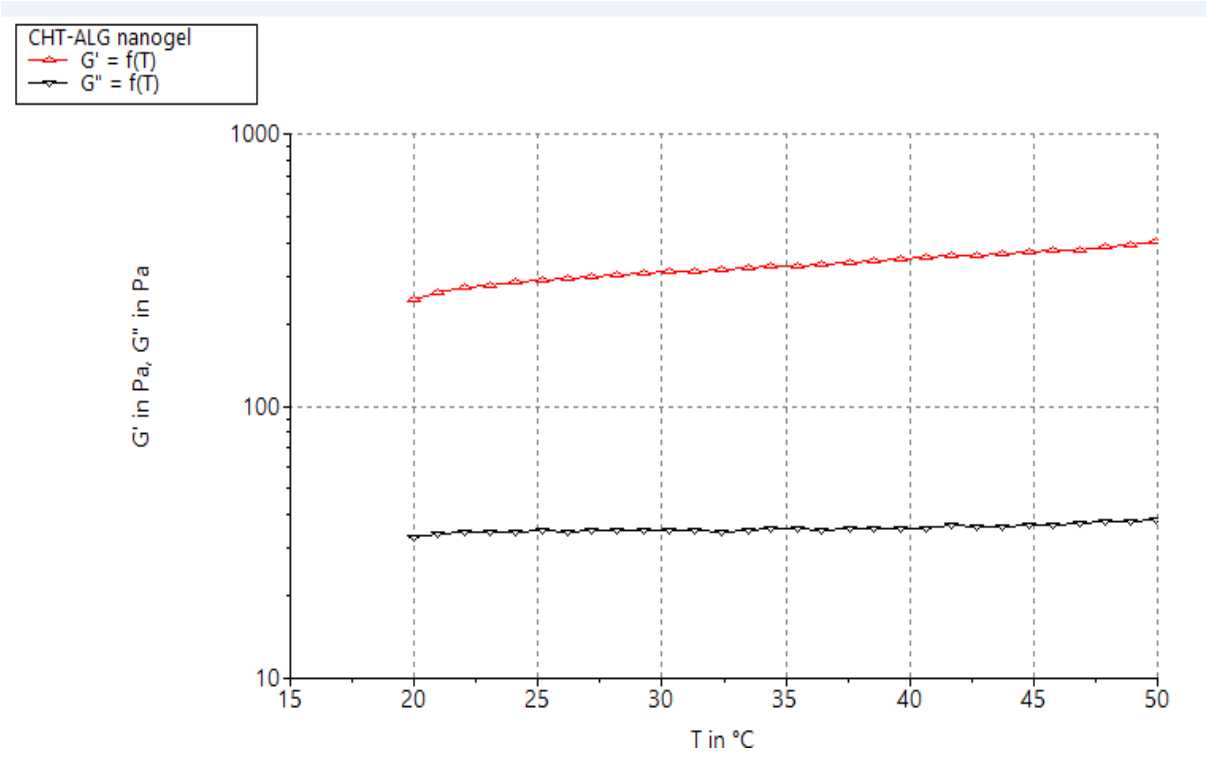


Figure 19: Graph demonstrating the temperature ramp of the nanogel.

3.3.1.8 Drug loading and drug release

3.3.1.8a. Encapsulation of dopamine in both the unloaded- and loaded carbon dot systems.

As previously discussed, dopamine was loaded onto the carbon dot during the synthetic process. The small size of the carbon dot highly influenced the maximum loading of drug due to the large surface area of the carbon dot [25]. As discussed in Chapter 2, the reagents used to synthesize the carbon dots provide the structural template for the carbon dot. As described under FTIR analysis, there were carbonyl, hydroxyl and amide functional groups on the surface of the carbon dot. This encouraged successful and efficient surface passivation of the carbon dot surface with dopamine. The calibration curve was utilized to determine the %entrapment efficiency of the formulation. The calculated value of %entrapment efficiency was thus calculated to be 98.67%.

3.3.1.8b. In vitro drug release study

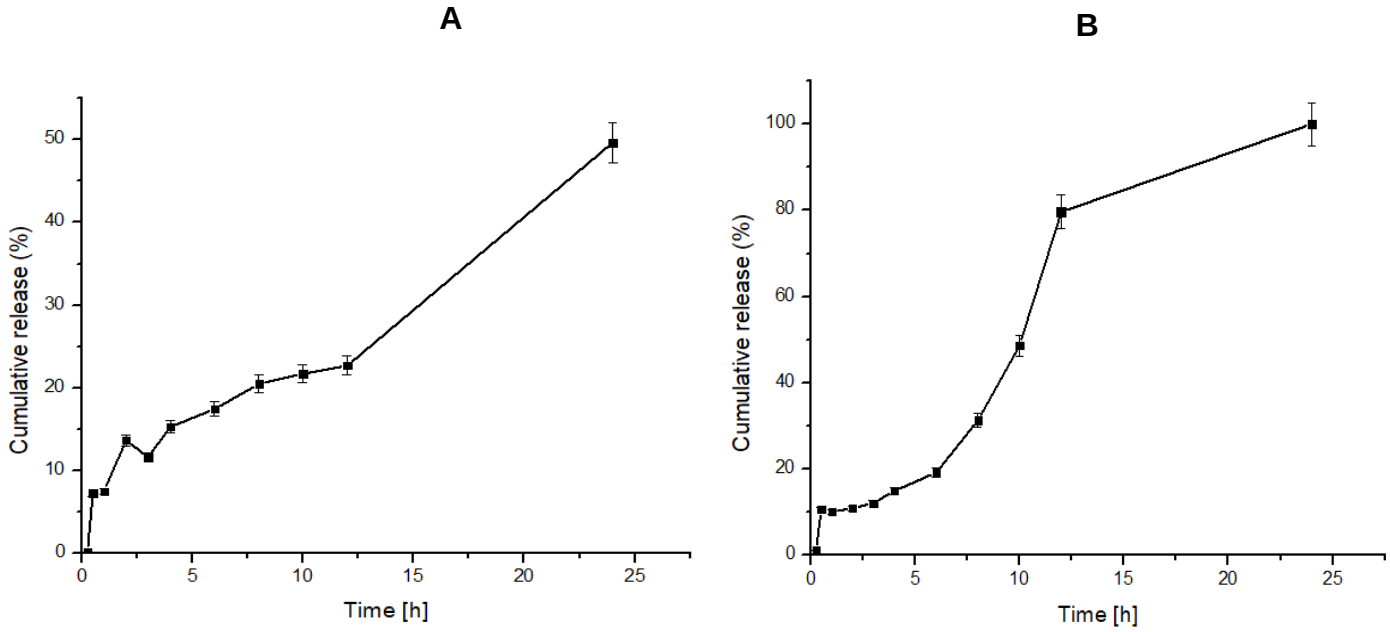
The drug release profile of the dopamine-loaded carbon dot systems was tested under various conditions as summarised in Table 10.:

Table 10: Conditions for analysis of drug release

Variable	**Formulation**
pH 7.4	Dopamine-loaded carbon dot system
pH 7.4	Dopamine-loaded carbon dot system in the nanogel
pH 5.5	Dopamine-loaded carbon dot system
pH 5.5	Dopamine-loaded carbon dot system in the nanogel

The drug release study was conducted at two different pH values, i.e. 7.4 and 5.5. A pH of 7.4 was utilized to mimic the blood pH and a pH of 5.5 represents the pH of the nasal cavity [26]. The carbon dot system loaded with dopamine was tested with and without the nanogel so as to ascertain what effect the nanogel had on the release of dopamine. Figure 20A displays the drug release from the dopamine-loaded carbon dot system without the nanogel (CDopa) in pH 7.4. There was a gradual release of dopamine between 15 minutes to 30 minutes. From 30 minutes up until 24 hours there was a sharp increase in the release of dopamine. The maximum cumulative release was 49.61%. The %standard deviation was between 0 and 0.005. Figure 20B depicts the dopamine-loaded carbon dot system in the nanogel (Cgel) at pH 7.4. There is a marked difference in the shape of the curve, this curve is much smoother and depicts a more gradual release of dopamine between times 15 minutes to 6 hours. Between 6 and 8 hours the rate of drug release increased. This formulation released a maximum of 100% after 24 hours. In comparison to the dopamine-loaded carbon dot system without the nanogel, this formulation was able to release more than 50% more drug. The nanogel allowed for effective leaching out of the dopamine and would perform the same in the body due to the mucoadhesive nature of chitosan and sodium alginate [27,28]. The %standard deviation was between 0.005 and 0.03. Figure 20C is

representative of the drug release from the dopamine-loaded carbon dot system without the nanogel at pH 5.5. A burst release was observed between 15 minutes and half an hour. The drug release then decreased between half an hour and 1 hour which could be due to the light in the orbital shaker as dopamine is light-sensitive [29]. Thereafter there was a gradual drug release between 1 hour and 12 hours. Between 12 and 24 hours there was a sharp release of drug. This formulation displayed a Cumulative release of 23.63% after 24 hours. This value is significantly lower than the same formulation in pH 7.4, indicating that the release of this formulation is pH-sensitive. The %standard deviation was between 0 and 0.005. Figure 20D demonstrates the dopamine-loaded carbon dot system within the nanogel at pH 5.5. This formulation also displayed a smooth release curve. There was a gradual release of dopamine with an enhanced slow-release characteristic enabled by the nanogel, where the gradual release of dopamine lasted from 15 minutes to 12 hours. There was then a burst release of dopamine between 12 and 24 hours. This formulation had a maximum %Cumulative release of 100% after 24 hours. The %standard deviation for this formulation 0 and 0.03.



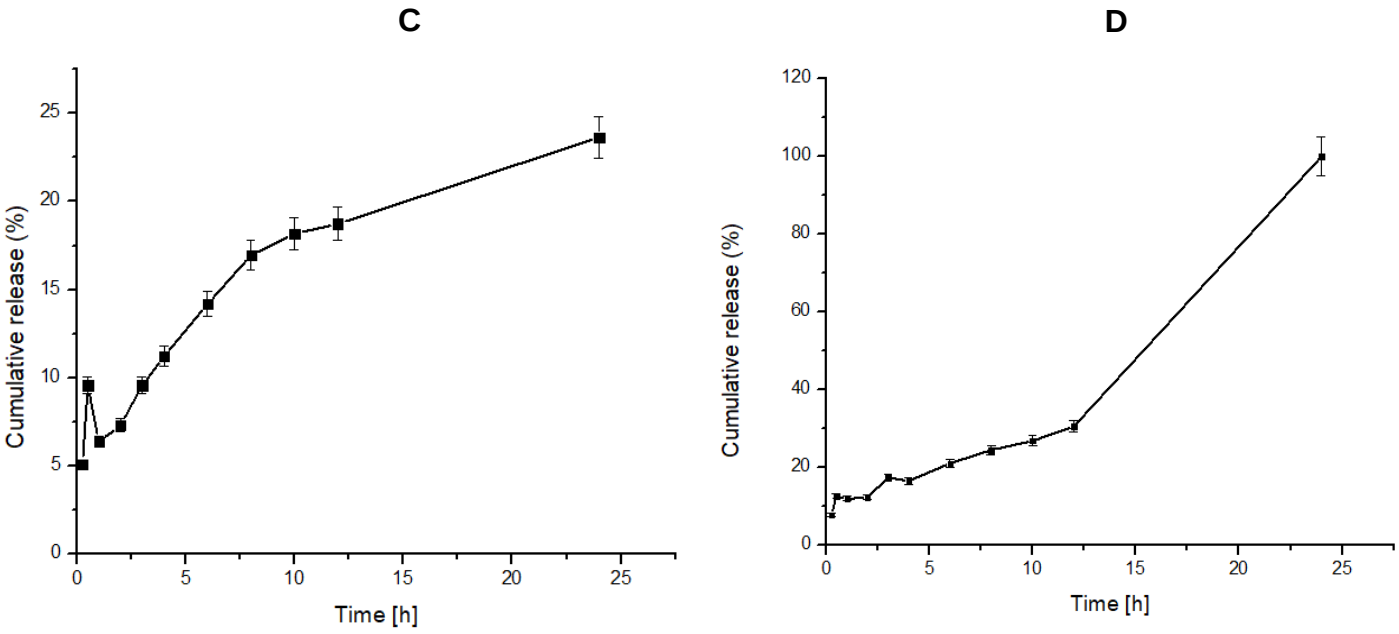


Figure 20A-D: Graphs illustrating the A) Drug release curve for the dopamine-loaded carbon dot without the nanogel at pH 7.4. B) Drug release curve for the dopamine-loaded carbon dot in the nanogel at pH 7.4. C) Drug release curve for the dopamine-loaded carbon dot without the nanogel at pH 5.5. D) Drug release curve for the dopamine-loaded carbon dot in the nanogel at pH 5.5.

In conclusion, the nanogel allowed for a more controlled and sustained release in pH 7.4 as can be clearly noted from the drug release curves. The dopamine-loaded carbon dots alone also exhibited a sustained release however illustrating a less smoothened curve as it is with the nanogel. In pH 5.5, the nanogel enable a notably enhanced degree of controlled and sustained release of dopamine over time as opposed to the dopamine-loaded carbon dots alone.

3.3.1.9. Cytotoxicity studies

The MTT Assay confirmed that the dopamine, unloaded- and loaded carbon dots are cytocompatible as substantiated by %Relative cell viabilities (%RCV) presented in Figures 21 and 22. After 48 hours, dopamine, the dopamine-loaded carbon dots and the unloaded carbon dots actually promoted cell proliferation as can be seen by %RCV values over 100%. This is due to the fact that dopamine promotes and supports cell

generation [1]. For dopamine, cell proliferation is proved by the %RCV values at 215.90%, 170.36%, 144.31% and 107.38% which correlate to 125µg/mL, 7.81µg/mL, 62.5µg/mL and 31.25µg/mL respectively. The %RCV at a concentration of 15.625µg/mL was 99.79% which also substantiates the bioavailability and nontoxicity of dopamine in the brain. After 72 hours, the concentration which demonstrated the most cell proliferation was 15.625µg/mL with a %RCV of 330.63%. The %RCV values also showed excellent cell proliferation as well as nontoxicity where concentrations of 125µg/mL, 62.5µg/mL and 31.25µg/mL showed cell proliferation at values of 128.84%, 114.22% and 105.93% respectively. The concentration at 7.81µg/mL had a %RCV of 98.70% which also proved a minimal amount of cytotoxicity.

Looking at figure 21 and 22, the dopamine-loaded carbon dots were not significantly cytotoxic and also allowed for cell proliferation. At 48 hours, concentrations 125µg/mL, 7.81µg/mL and 62.5 µg/mL showed cell proliferation with %RCV values at 114.26% 113.85% and 100.51% respectively. The concentrations 31.25µg/mL and 15.625µg/mL showed %RCV values at 94.36% and 95.38% which showed minimal cytotoxicity of this system. At 72 hours, there was cell proliferation present for concentrations 125µg/mL, 15.625µg/mL and 7.81µg/mL at 103.57%, 101.22% and 124.41% respectively. Concentrations 62.5 µg/mL and 31.25µg/mL had values of 94.96% and 91.96% which substantiated the minimal cytotoxicity of the system.

Figures 21 and 22 illustrate that the unloaded carbon dot systems were also minimally cytotoxic and also enabled cell proliferation. At 48 hours, concentrations 125µg/mL and 7.81µg/mL had values of 114.26% and 116.41% respectively. This was indicative of cell proliferation. Concentrations 62.5 µg/mL, 31.25µg/mL and 15.625µg/mL had values at 92.31%, 96% and 96.82%. This showed minimal cytotoxicity of this system. At 72 hours, concentrations 125µg/mL and 7.81µg/mL had values of 102.27% and 120.96% respectively which still showed that there was cell proliferation present. The remaining concentrations 62.5 µg/mL, 31.25µg/mL and 15.625µg/mL had values at 97.73, 95.45% and 96.34% which also illustrated very minimal cytotoxicity for the unloaded carbon dot system. The dopamine-loaded carbon dots also allowed cell

proliferation as can be seen in figure 22 At a concentration of 7.81µg/mL the %RCV was 116.41%.

The error bars on both Figure 21 and 22 are representative of the standard deviation of said vales. For figure 21; the standard deviation for dopamine, CDopa, CDot and the positive control was 42.65, 8.73, 10.08 and 0 respectively. The standard deviation for Figure 22 was as follows; dopamine 88.06, CDopa 11,52, CDot 9.50 and the positive control was 0.

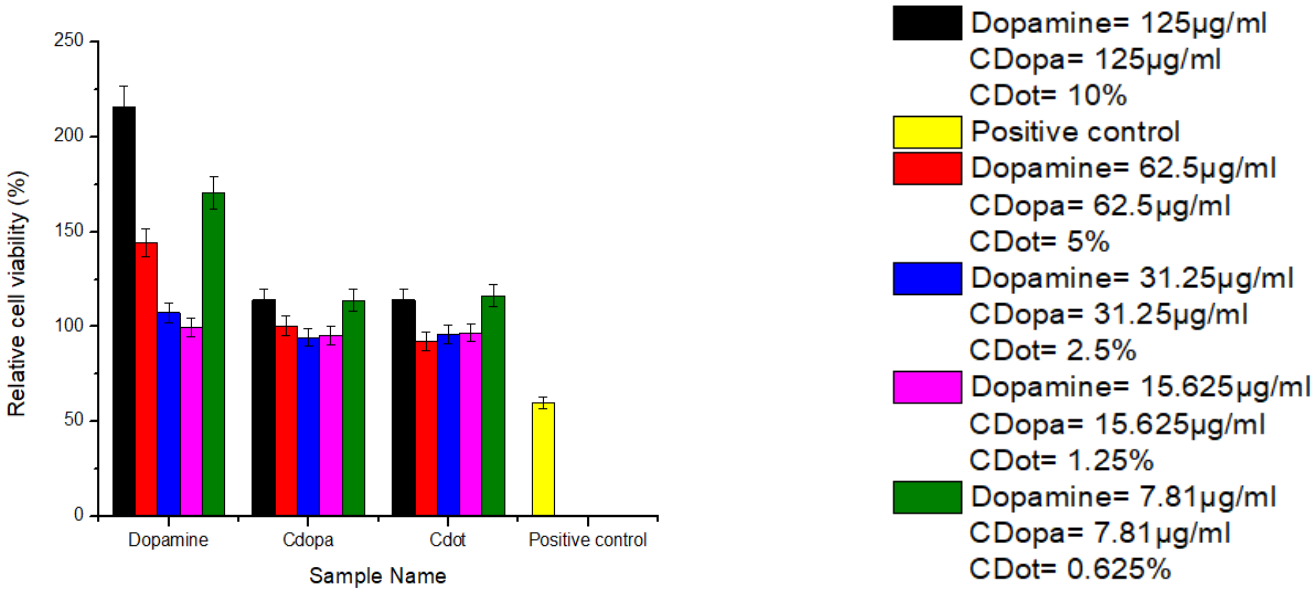


Figure 21: Graph depicting the MTT Assay after 48 hours with error bars indicative of standard deviation.

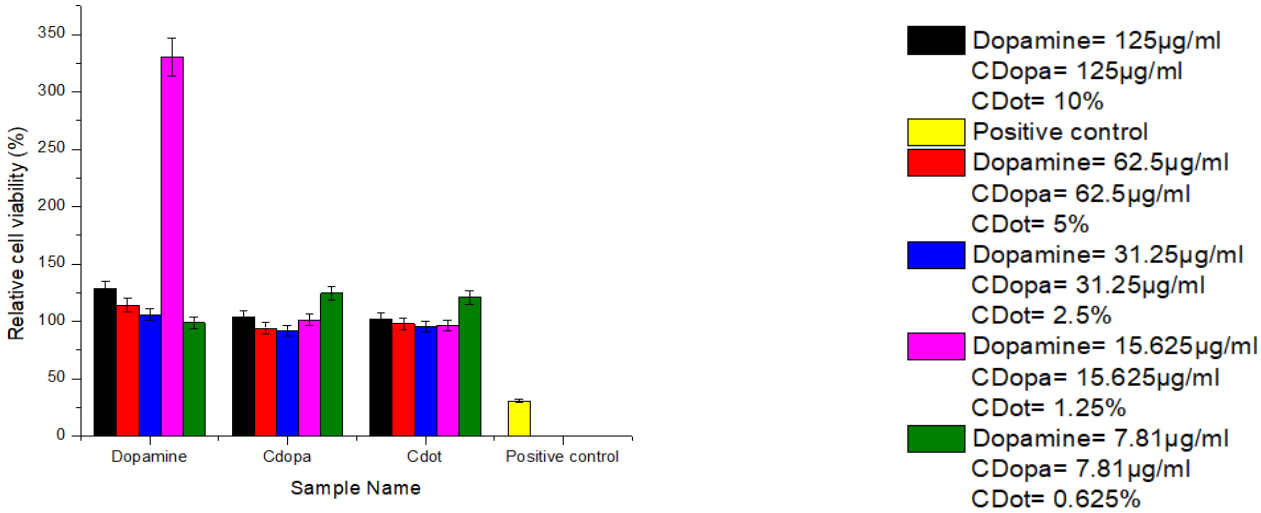
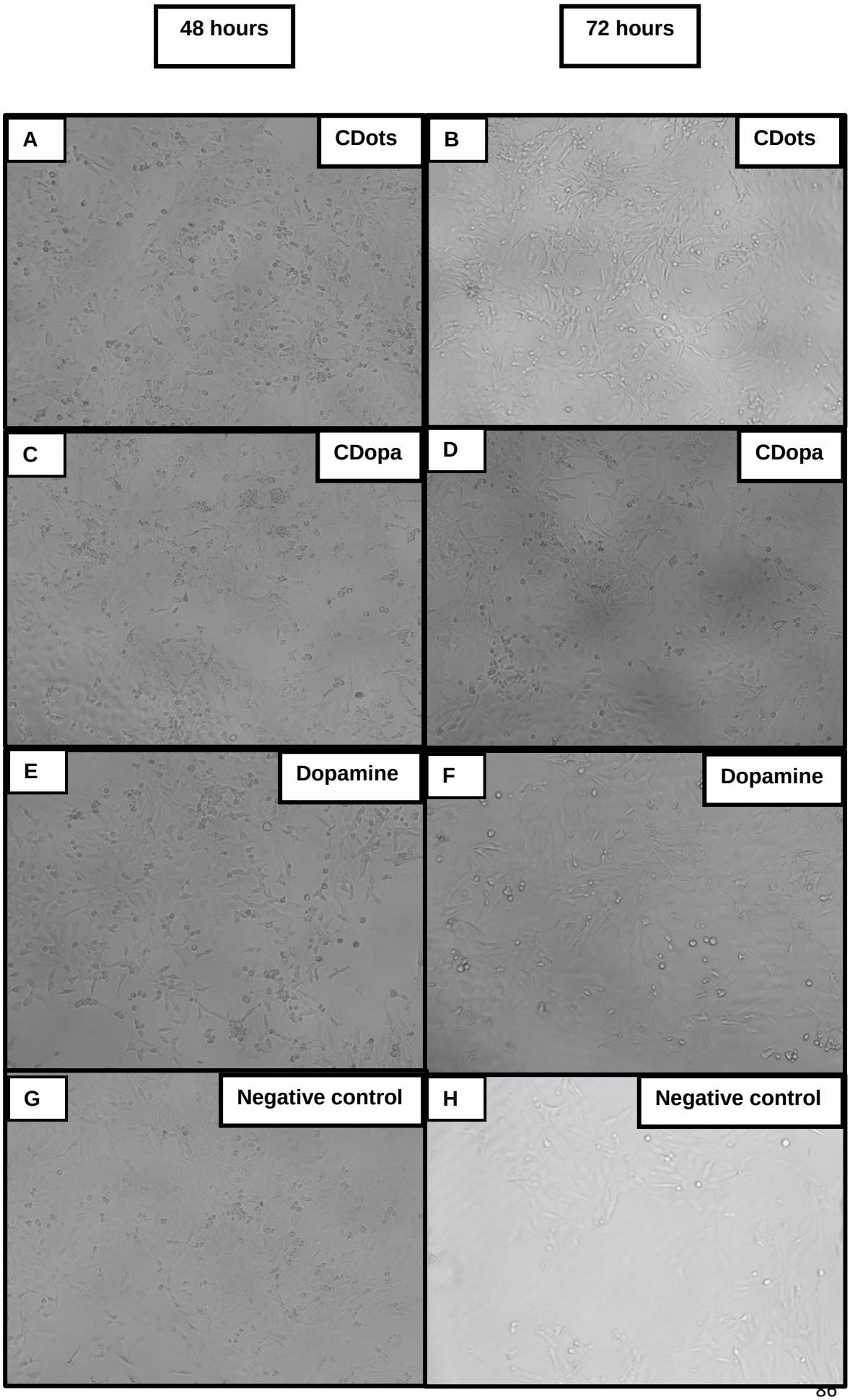
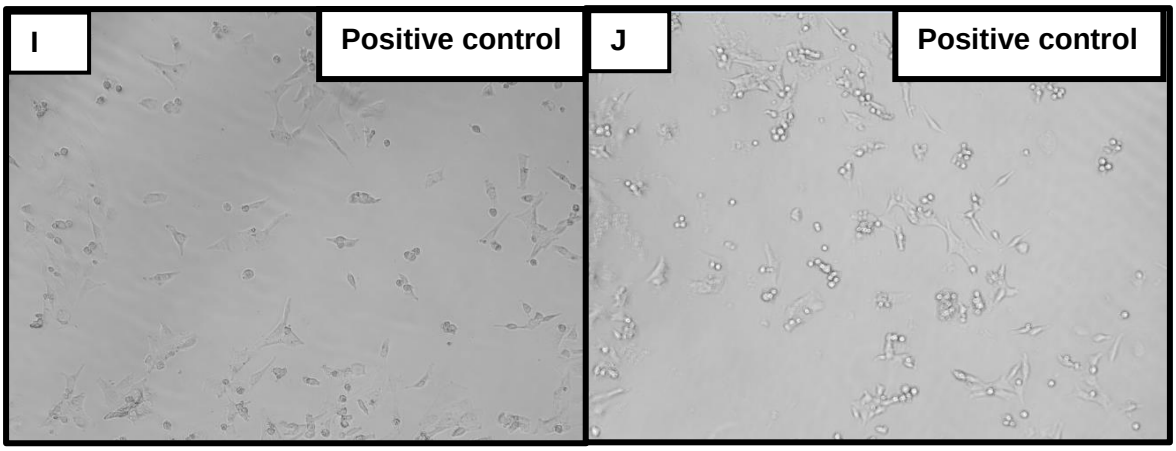


Figure 22: Graph depicting the MTT Assay after 72 hours with error bars indicative of standard deviation


48 hours
72 hours
A
CDots
B
CDots
C
CDopa
D
CDopa
E
Dopamine
F
Dopamine
G
Negative control
H
Negative control



Figures 23 A) Image of PC12 cells treated with CDots at 48 hours. B) Images of PC12 cells treated with CDots at 72 hours. C) Images of PC12 cells treated with CDopa at 48 hours. D) Images of PC12 cells treated with CDopa at 72 hours. E) Images of PC12 cells treated with Dopamine at 48 hours. F) Image of PC12 cells treated with Dopamine at 72 hours. G) Image of Negatvive control at 48 hours. H) Image of Negative control at 72 hours. I) Image of Positive control at 48 hours. J) Image of Positive control at 72 hours.

3.3.1.10. Concluding remarks

The unloaded- and loaded carbon dot systems proved to have been synthesized as well as of good quality due to the substantiations from all the analysis above. FTIR analysis confirmed the successful synthesis of carbon dots from urea and sodium citrate. It also confirmed the surface passivation of dopamine on the carbon dots. DSC analysis also confirmed the successful synthesis of the carbon dots from the individual reagents due to a shift in the thermographic peaks. The DSC analysis also confirmed the surface passivation of dopamine by virtue of another thermographic peak shift. XRD analysis clearly depicted the crystalline nature of the carbon dots. Zeta potential analysis substantiated the surface passivation of dopamine due to the increase in zeta potential. Zeta size analysis and TEM confirmed the morphological characteristics and size of the carbon dot system. *In vitro* drug entrapment and release studies confirmed that carbon dots are able to entrap large amount of drug and release the drug in a slow and sustained release pattern which is ideal for the application in Parkinson's' Disease treatment. Cytotoxicity studies proved these systems to be non-cytotoxic to PC12 cells and actually showed their ability to promote and support cell proliferation.

3.4. REFERENCES

1. Cohen, E., Kondiah, P., Choonara, Y., du Toit, L. and Pillay, V., 2020. Carbon dots as Nanotherapeutics for Biomedical Application. *Current Pharmaceutical Design*, 26(19), pp.2207-2221.

2. Xiao C, Lai L, Zhang L, *et al.* Spectroscopic and Isothermal Titration Calorimetry Studies of Binding Interactions Between Carbon Nanodots and Serum Albumins. *J Solution Chem* 2018; 47(9): 1438-48. http://dx.doi.org/10.1007/s10953-018-0792-2 .

3. Mishra V, Patil A, Thakur S, Kesharwani P. Carbon dots: emerging theranostic nanoarchitectures. *Drug Discov Today* 2018; 23(6):1219-32. http://dx.doi.org/10.1016/j.drudis.2018.01.006 PMID: 29366761

4. Feng H, Qian Z. Functional Carbon Quantum Dots: A Versatile Platform for Chemosensing and Biosensing. Chem Rec 2018;18(5): 491-505. http://dx.doi.org/10.1002/tcr.201700055 PMID: 29171708

5. Oh, T., Daadi, E., Kim, J., Daadi, E., Chen, P., Roy-Choudry, G., Bohmann, J., Blass, B. and Daadi, M., 2022. Dopamine D3 receptor ligand suppresses the expression of levodopa-induced dyskinesia in nonhuman primate model of parkinson's disease. *Experimental Neurology*, 347, p.113920.

6. Park D, Choi B, Zhu S, Huh J, Kim B, Lee S. Injectable bone using chitosan-alginate gel/mesenchymal stem cells/BMP-2 composites. Journal of Cranio-Maxillofacial Surgery. 2005;33(1):50-54.

7. Coates J. Interpretation of Infrared Spectra, A Practical Approach. Encyclopedia of Analytical Chemistry. 2006;.

8. Karoui R. Food Authenticity and Fraud. Chemical Analysis of Food: Techniques and Applications. 2012;:499-517.

9. Rajeswari A, Jackcina Stobel Christy E, Gopi S, Jayaraj K, Pius A. Characterization studies of polymer-based composites related to functionalized filler-matrix interface. Interfaces in Particle and Fibre Reinforced Composites. 2020;:219-250.

10. Ebnesajjad S. Fabrication and Processing of Polytetrafluoroethylene Dispersions. Fluoroplastics. 2015;:278-299.

11. Sonebi M, Yahia A. Mix design procedure, tests, and standards. Self-Compacting Concrete: Materials, Properties and Applications. 2020;:1-30.

12. Gaikwad V, Choudhari P, Bhatia N, Bhatia M. Characterization of pharmaceutical nanocarriers: in vitro and in vivo studies. Nanomaterials for Drug Delivery and Therapy. 2019;:33-58.

13. Kumar P, Pavithra K, Naushad M. Characterization techniques for nanomaterials. Nanomaterials for Solar Cell Applications. 2019;:97-124.

14. Patravale V, Dandekar P, Jain R. Nanotoxicology: evaluating toxicity potential of drug-nanoparticles. Nanoparticulate Drug Delivery. 2012;:123-155.

15. Ait-Amir B, Pougnet P, El Hami A. 6 - Meta-Model Development. Embedded Mechatronic Systems 2 (Second Edition). 2022;(2):157-187.

16. Wang M, Su Y, Liu Y, Liang Y, Wu S, Zhou N et al. Antibacterial fluorescent nano-sized lanthanum-doped carbon quantum dot embedded polyvinyl alcohol for accelerated wound healing. Journal of Colloid and Interface Science. 2022;608:973-983.

17. Mudalige T, Qu H, Van Haute D, Ansar S, Paredes A, Ingle T. Characterization of Nanomaterials. Nanomaterials for Food Applications. 2019;:313-353.

18. Jain R, Savla H, Naik I, Maniar J, Punjabi K, Vaidya S et al. Novel Nanotechnology Based Delivery Systems for Chemotherapy and Prophylaxis of Tuberculosis. Handbook of Nanomaterials for Industrial Applications. 2018;:587-620.

19. Joseph E, Singhvi G. Multifunctional nanocrystals for cancer therapy: a potential nanocarrier. Nanomaterials for Drug Delivery and Therapy. 2019;:91-116.

20. Dong, Y., Hou, L. and Wu, P., 2020. Exploring the diffusion behavior of urea aqueous solution in the viscose film by ATR-FTIR spectroscopy. *Cellulose*, 27(5), pp.2403-2415.

21. Long, R., Wang, G., Hu, Z., Sun, P. and Zhang, L., 2020. Gradually activated lithium uptake in sodium citrate toward high-capacity organic anode for lithium-ion batteries. *Rare Metals*, 40(6), pp.1366-1372.

22. Hou, Y., Lu, Q., Deng, J., Li, H. and Zhang, Y., 2015. One-pot electrochemical synthesis of functionalized fluorescent carbon dots and their selective sensing for mercury ion. *Analytica Chimica Acta*, 866, pp.69-74.

23. Yadav, T. and Mukherjee, V., 2018. Interpretation of IR and Raman spectra of dopamine neurotransmitter and effect of hydrogen bond in HCl. *Journal of Molecular Structure*, 1160, pp.256-270.

24. Park, D., Choi, B., Zhu, S., Huh, J., Kim, B. and Lee, S., 2005. Injectable bone using chitosan-alginate gel/mesenchymal stem cells/BMP-2 composites. *Journal of Cranio-Maxillofacial Surgery*, 33(1), pp.50-54.

25. Li S, Li L, Tu H, Zhang H, Silvester D, Banks C et al. The development of carbon dots: From the perspective of materials chemistry. Materials Today. 2021;51:188-207.

26. Washington N, Steele R, Jackson S, Bush D, Mason J, Gill D et al. Determination of baseline human nasal pH and the effect of intranasally administered buffers. International Journal of Pharmaceutics. 2000;198(2):139-146.

27. Hasnain M, Nayak A. Chitosan as mucoadhesive polymer in drug delivery. Chitosan in Drug Delivery. 2022;:225-246.

28. Khalid S, Abbas G, Hanif M, Shah S, Shah S, Jalil A et al. Thiolated sodium alginate conjugates for mucoadhesive and controlled release behavior of metformin microspheres. International Journal of Biological Macromolecules. 2020;164:2691-2700.

29. El-Zohry A, Hashem E. Environmental Method to Determine Dopamine and Ascorbic Acid Simultaneously via Derivative Spectrophotometry. Journal of Spectroscopy. 2013;2013:1-7.

30. Afzal, S., Maswal, M. and Dar, A., 2018. Rheological behaviour of pH responsive composite hydrogels of chitosan and alginate. Characterization and its use in encapsulation of citral. *Colloids and Surfaces B: Biointerfaces,* 169, pp.99-106.

CHAPTER 4: CONCLUSION AND FUTURE RECOMMENDATIONS

4.1. Conclusion

Parkinson's disease is a debilitating disease whose effects are far reaching and impedes the patient's ability to live a good, wholesome life as there is no cure for the disease. Parkinson's disease is a neurodegenerative disease in which the dopamine receptors in the substantia nigra of the brain perish thus resulting in a decline in dopamine production and provision around the body. The effects of this disease include, and is not limited to, paraesthesias, paralysis and cognitive impairments. Current therapeutic regimens only provide symptomatic relief. The disease progresses as time passes and the effects become more severe. The golden standard for Parkinson's treatment at the moment is Levodopa (L-Dopa). This is a precursor to dopamine and is administered orally. Dopamine is readily metabolized in the gastrointestinal tract (GIT) by the decarboxylase enzyme. Due to this, efforts have been made to administer L-Dopa along with carbidopa – a decarboxylase enzyme inhibitor, in order to curb the metabolism of L-Dopa in the GIT. This however has not completely solved the problem as a minute concentration of Dopamine actually reaches the brain via systemic circulation. Once it reaches the brain, this already reduced concentration faces yet another challenge – the Blood-Brain Barrier (BBB). The BBB provides a very strict barrier between the systemic circulation and the brain and is extremely selective about what it allows into the brain. Modern neurotherapeutic struggle to pass through the BBB. All these factors thus lead toward larger doses of medication to be administered to the patients in order to circumvent these challenges. These larger doses increase the side effect profiles suffered by the patients and ultimately decreases patient compliance as a whole.

There is a dire need for a neurotherapeutic which can evade the GIT, successfully traverse the BBB and also be administered in a low yet effective dosage so as to increase neuroavailability of Dopamine but minimize the side effect profile suffered by patients. Carbon dots have aroused much attention by researchers for application in a myriad of fields including drug delivery. Carbon dots are carbonaceous nanomaterials which can be synthesized from practically any carbon-based material. These nanoparticles are small in size, photoluminescent, non-toxic, water-soluble and biocompatible. The size provides a large surface area, and the surfaces are easily

passivated which ensures an exceptional drug entrapment, as can be seen in this dissertation. The %drug entrapment efficiency in this project was 98.67%. The dopamine-loaded carbon dot systems were formulated in a chitosan-alginate nanogel, for intranasal administration. This was another mechanism put in place to avoid the metabolism of dopamine in the GIT and to ensure the highest possible bioavailability of dopamine in the brain, at the lowest possible dose. The dopamine-loaded carbon dot system demonstrated a slow, sustained, controlled drug release profile which is indicative of minimal dosing required in patients. This drug delivery system proved to be easily synthesized, in just half an hour; cost-effective, nontoxic (as indicated by cytotoxicity studies), and a stable formulation as substantiated by the physicochemical and morphological analyses undertaken in this study. Overall, this formulation shows great promise in the future treatment of Parkinson's disease.

4.2. Future recommendations

In vitro biocompatibility and cytotoxicity studies were undertaken on a PC12 cell line in this project. It would be highly advantageous to perform an *in vivo* study in the future.

The addition of a ligand to the carbon dot which would greatly enhance target specificity.

The scientific literature surrounding carbon dots in neurotherapeutic application is scarce and limited. Carbon dot research regarding neurodegenerative diseases is an area of research which is elusive and made finding guidelines and methods to follow challenging for this project. An intervention which would serve great benefit to the field of Carbon dot therapeutics would be increased research and publication surrounding the biomedical application of carbon dots in neurotherapeutics.

An aspect of great advantage for the future would be a comparative study between dopamine hydrochloride and the conventional golden standard therapy at the moment, Leva-dopa. This would be of extensive advantage in determining the limitations in this project as well as overall Parkinson's Disease treatment regimens to date.

Appendix

2. CHAPTER 2: A Literature Review of Carbon Dots as Nanotherapeutics for Biomedical Application

Current Pharmaceutical Design, 2020, *26*, 1-15 1

REVIEW ARTICLE

Carbon Dots as Nanotherapeutics for Biomedical Application

Eemaan N. Cohen, Pierre P.D. Kondiah, Yahya E. Choonara, Lisa C. du Toit[1] and Viness Pillay*

Wits Advanced Drug Delivery Platform Research Unit, Department of Pharmacy and Pharmacology, School of Therapeutic Sciences, University of the Witwatersrand, Johannesburg, 7 York Road, Parktown, 2193, South Africa

ARTICLE HISTORY

Received: November 5, 2019
Accepted: February 10, 2020

DOI:
10.2174/1381612826666200402102308

Abstract: Carbon nanodots are zero-dimensional spherical allotropes of carbon and are less than 10nm in size (ranging from 2-8nm). Based on their biocompatibility, remarkable water solubility, eco- friendliness, conductivity, desirable optical properties and low toxicity, carbon dots have revolutionized the biomedical field. In addition, they have intrinsic photo-luminesce to facilitate bio-imaging, bio-sensing and theranostics. Carbon dots are also ideal for targeted drug delivery. Through functionalization of their surfaces for attachment of receptor-specific ligands, they ultimately result in improved drug efficacy and a decrease in side-effects. This feature may be ideal for effective chemo-, gene- and antibiotic-therapy. Carbon dots also comply with green chemistry principles with regard to their safe, rapid and eco-friendly synthesis. Carbon dots thus, have significantly enhanced drug delivery and exhibit much promise for future biomedical applications. The purpose of this review is to elucidate the various applications of carbon dots in biomedical fields. In doing so, this review highlights the synthesis, surface functionalization and applicability of biodegradable polymers for the synthesis of carbon dots. It further highlights a myriad of biodegradable, biocompatible and cost-effective polymers that can be utilized for the fabrication of carbon dots. The limitations of these polymers are illustrated as well. Additionally, this review discusses the application of carbon dots in theranostics, chemo-sensing and targeted drug delivery systems. This review also serves to discuss the various properties of carbon dots which allow chemotherapy and gene therapy to be safer and more target-specific, resulting in the reduction of side effects experienced by patients and also the overall increase in patient compliance and quality of life.

Keywords: Carbon dot, Nanomedicine, Bio-imaging, Bio-sensing, Chemotherapy, Gene therapy, Antimicrobial therapy, Neurological diseases.

1. INTRODUCTION

Nanomedicine is a vast field explored by many researchers to design novel, biocompatible and non-toxic platforms that can be applied in various biomedical fields. An emergent nanomaterial of great interest is Carbon Dots (CDots) [1]. CDots form a part of an ingenious series of carbonaceous nanomaterials and are zero-dimensional spherical allotropes of carbon [2, 3]. These nanomaterials (10nm in size; ranging from 2-8nm) are environmentally benign clusters of carbon atoms, with traces of oxygen, hydrogen and nitrogen and have a sp^2 hybridized structure, including various functional groups such as carboxyl (-COOH), aldehyde (-CHO) and hydroxyl (-OH) groups [4, 5, 6]. CDots are also known as Carbon Nano-Dots, graphene quantum dots or carbon quantum dots. CDots were accidentally discovered in 2004 by Xu *et al.* during the processing of single-walled carbon nanotubes (SWCNTs) [1, 7], also known as the arc discharge synthesis of carbon nanotubes [5]. CDots obtained their scientific designation as "carbon quantum dots" in 2006 by Su *et al.*, who worked on their surface passivation in order to enhance the intrinsic quality of fluorescence that CDots possess [1, 7]. These fluorescent nanoparticles serve as an alternative to the orthodox semi-conductor quantum dot, which possesses limitations such as high toxicity, due to the addition of heavy metals during their formulation [2, 8]. CDots are documented to have been synthesized from a myriad of different sources. Some of these sources include, but are not limited to carbon fibre, citric acid, graphite and glucose [9].

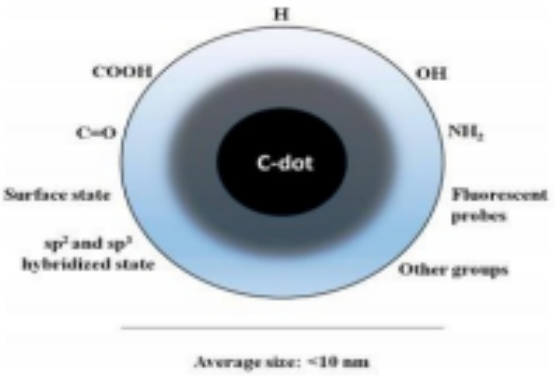


Fig. (1). Schematic depicting carbon dot design with various functional groups on the carbon dot surface. Adapted with permission from Ref: 4 [4]. (*A higher resolution / colour version of this figure is available in the electronic copy of the article*).

Since the discovery of carbon dots, their properties and chemical nature have been extensively researched and they have been designated as a new class of the smallest, biocompatible, viable nanomaterials [7]. Carbon dots can be crystalline or amorphous in nature [10] and have revolutionized chemical, biomedical and nanomedi-

*Address correspondence to this author at the Wits Advanced Drug Delivery Platform Research Unit, Department of Pharmacy and Pharmacology, School of Therapeutic Sciences, University of the Witwatersrand, Johannesburg, 7 York Road, Parktown, 2193, South Africa; Tel: +27-11-717-2274; E-mail: viness.pillay@wits.ac.za

1381-6128/20 $65.00+.00 © 2020 Bentham Science Publishers